

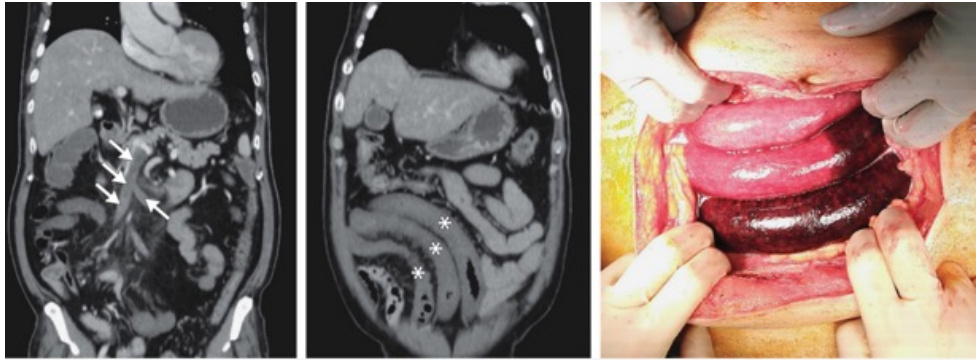
<https://www.mdc-berlin.de/de/veroeffentlichungstypen/clinical-journal-club>

The weekly Clinical Journal Club by Dr. Friedrich C. Luft

Usually every Wednesday 17:00 - 18:00



Als gemeinsame Einrichtung von MDC und Charité fördert das Experimental and Clinical Research Center die Zusammenarbeit zwischen Grundlagenwissenschaftlern und klinischen Forschern. Hier werden neue Ansätze für Diagnose, Prävention und Therapie von Herz-Kreislauf- und Stoffwechselerkrankungen, Krebs sowie neurologischen Erkrankungen entwickelt und zeitnah am Patienten eingesetzt. Sie sind eingeladen, uns beizutreten. [Bewerben Sie sich!](#)



A 68-year-old man with cirrhosis presented to the emergency department with a 2-day history of severe abdominal pain. On physical examination, hypoactive bowel sounds, pain with palpation, and rebound tenderness throughout the abdomen were noted. Computed tomography of the abdomen with administration of contrast material showed thrombosis of the superior mesenteric vein (left, arrows). What complication of superior mesenteric vein thrombosis was also seen on imaging?

Ascites

Ischemic Colitis

Portal hypertension

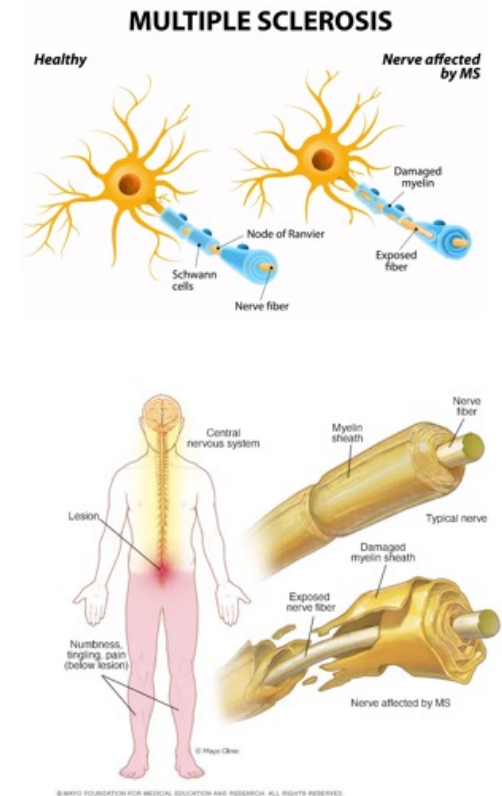
Small-Bowel Perforation

Small-Bowel Infarction

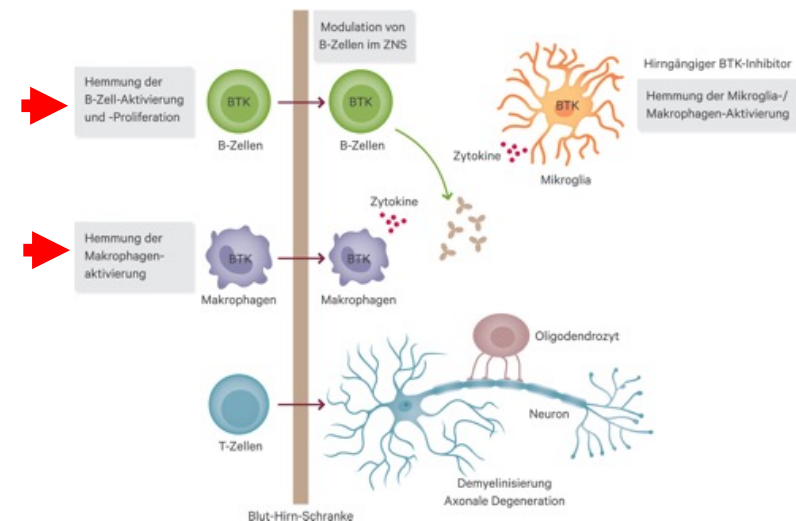
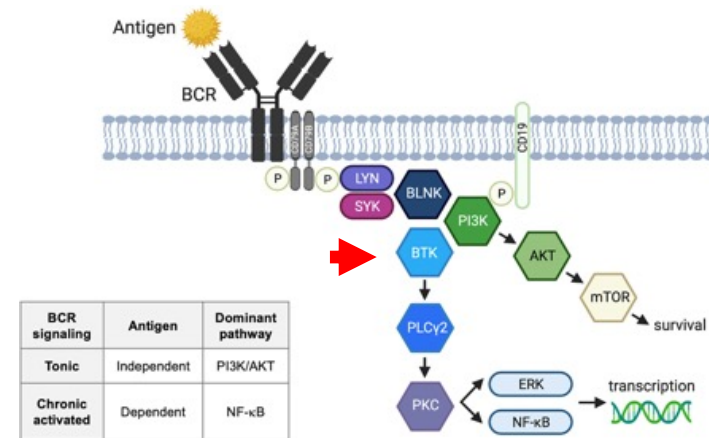


The correct answer is small-bowel infarction secondary to acute superior mesenteric vein thrombosis. For this patient, a long segment of small bowel in the right lower quadrant of the abdomen showed increased wall thickness and decreased enhancement (middle, asterisks). Exploratory laparotomy showed dusky bowel extending from the distal jejunum to the proximal ileum (right). Resection of the infarcted bowel, transvenous thrombolysis and thrombectomy, and a primary anastomosis were performed.

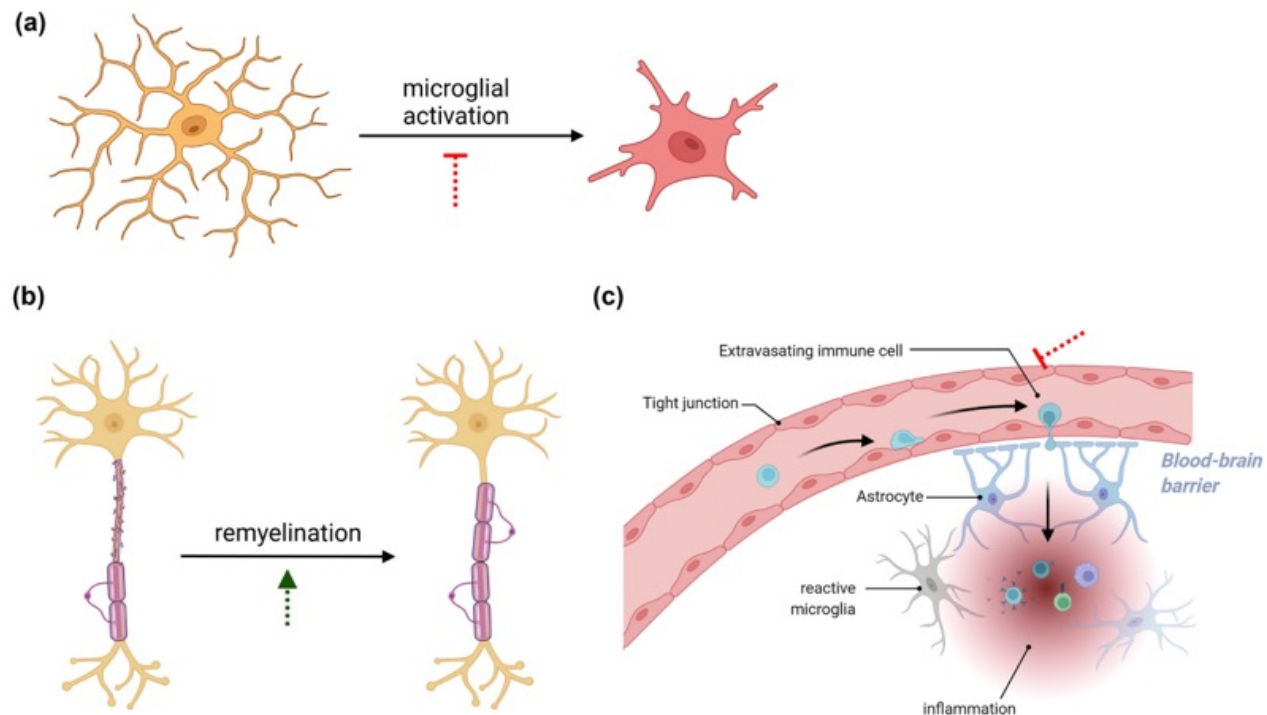
Die **Multiple Sklerose**, kurz MS, ist eine chronische, entzündlich-demyelinisierende Erkrankung des zentralen Nervensystems (ZNS). Das wesentliche Merkmal der MS ist die im Gehirn und im Rückenmark verstreut auftretende Entzündung, die durch den **Angriff körpereigener Abwehrzellen** auf die **Myelinscheiden der Nerven** entsteht. Die dadurch ausgelöste Demyelinisierung bedingt zunächst eine Verlangsamung der Nervenleitgeschwindigkeit, danach einen Untergang der Axone. Anfänglich kommt es häufig noch zu Remyelinisierungen mit gliöser Vernarbung. Die Prädilektionsstellen für das Auftreten solcher Herde sind: Nervus opticus, periventriculäre Hirnsubstanz, Hirnstamm, Kleinhirn, Frontallappen und die Hinterstränge, besonders im Zervikalmark. Der genaue Pathomechanismus der MS ist noch nicht vollständig geklärt. In den Gehirnen erkrankter Versuchstiere ließ sich eine erhöhte Konzentration des Proteins **CD44** nachweisen. Es scheint dafür verantwortlich zu sein, dass die zerstörten Myelinscheiden nicht mehr ersetzt werden. CD44 wird von einer Vielzahl von Zelltypen exprimiert, darunter Immunzellen wie Lymphozyten.



Die Bruton-Tyrosinkinase, kurz BTK, ist eine Tyrosinkinase, die vor allem von B-Zellen exprimiert wird. Die Bruton-Tyrosinkinase spielt eine wichtige Rolle bei der **Reifung der B-Zellen** und bei der **Aktivierung von Mastzellen**. Als Signalmolekül wirkt das Enzym in den intrazellulären Übertragungswegen des B-Zell-Antigenrezeptors (BCR) und des Zytokinrezeptors mit. Die Primärstruktur von BTK besteht aus 658 Aminosäuren. Die Tyrosinkinase enthält eine PH-Domäne am N-Terminus, die Phosphatidylinositol-3,4,5-trisphosphat (PIP3) bindet. Wenn sich PIP3 an die Domäne anlagert, führt das dazu, dass BTK die Phospholipase C phosphoryliert. Diese wiederum hydrolysiert Phosphatidylinositol-4,5-bisphosphat (PIP2) in zwei Second messenger, Inositoltriphosphat (IP3) und Diacylglycerol (DAG). Beide Messenger steuern die Aktivität der B-Zelle im Rahmen der Immunantwort.

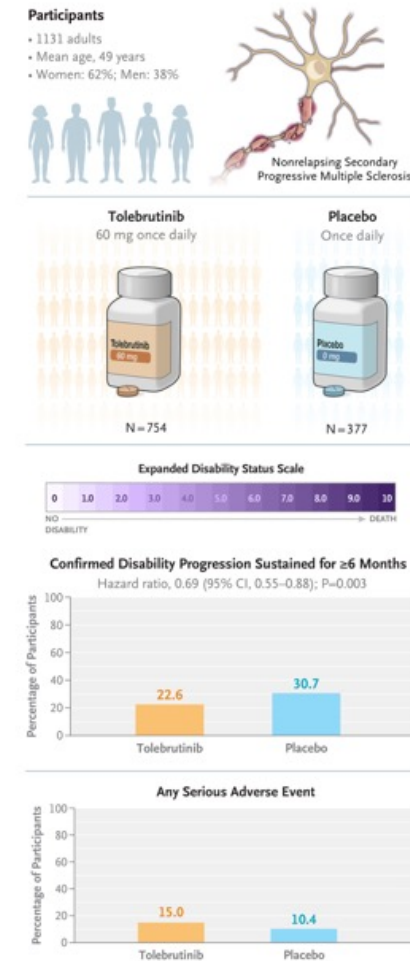


Tolebrutinib ist ein Bruton-Tyrosinkinase (BTK)-Inhibitor, der oral eingenommen wird und zur Behandlung der Multiplen Sklerose (MS) eingesetzt wird, insbesondere bei der nicht-schubförmig progredienten Form. **Es ist ein potenzielles Medikament, das die schwelende Neuroinflammation, eine Ursache für Behinderung bei MS, ansprechen soll.**



Tolebrutinib in Nonrelapsing Secondary Progressive Multiple Sclerosis

Throughout the course of multiple sclerosis, gradually progressive neurologic impairment can occur, which has been called disability accrual. Current disease-modifying therapies for multiple sclerosis have limited effects on disability accrual unrelated to relapses, which is thought to be partially caused by chronic, nonresolving neuroinflammation within the central nervous system. Tolebrutinib is an oral, brain-penetrant Bruton's tyrosine kinase inhibitor that targets myeloid cells (including microglia) and B cells in both the periphery and central nervous system. There are no approved treatments for nonrelapsing secondary progressive multiple sclerosis. In a phase 3, double-blind, placebo-controlled, event-driven trial, we randomly assigned participants with nonrelapsing secondary progressive multiple sclerosis, in a 2:1 ratio, to receive tolebrutinib (60 mg once daily) or matching placebo. The primary end point was confirmed disability progression that was sustained for at least 6 months, assessed in a time-to-event analysis.



Current disease-modifying therapies for multiple sclerosis largely target lymphocyte activity in the periphery to effectively reduce the incidence of focal inflammation in the central nervous system (CNS), which is the pathophysiological basis of lesion formation detected on magnetic resonance imaging (MRI) and acute relapse. Throughout the course of multiple sclerosis, gradually progressive neurologic impairment can occur, which has been called disability accrual. Current disease-modifying therapies have limited effects on disability accrual, especially progression that is independent of relapse activity, which is thought to be caused largely by chronic neuroinflammation within the CNS involving myeloid cells (including macrophages and CNS-resident microglia) and CNS-compartmentalized B cells. Bruton's tyrosine kinase (BTK) is a key signaling element implicated in neuroinflammation that is expressed in microglial cells and CNS-resident and peripheral B lymphocytes and therefore participates in both innate and adaptive immunity. In multiple sclerosis, myeloid cells and B cells interact to drive neuroinflammation and injury, as evidenced by chronic active white-matter lesions in the brain and leptomeningeal tertiary lymphoid structures. Therefore, a BTK inhibitor that targets both myeloid cells and B cells in the periphery and CNS may have a greater effect on CNS neuroinflammation and neurodegeneration than existing therapies.

Participants

Eligible participants were 18 to 60 years of age and had a current diagnosis of secondary progressive multiple sclerosis according to the 2017 revised McDonald criteria, with no superimposed clinical relapses in the 24 months before screening. At screening, the participants were required to have documented evidence of disability progression in the previous 12 months and a score of 3.0 to 6.5 on the Expanded Disability Status Scale (EDSS; scores range from 0 to 10.0, with higher scores indicating greater disability). Before randomization, an adjudication committee evaluated anonymized participant data to endorse the diagnosis of nonrelapsing secondary progressive multiple sclerosis and the presence of disability progression in the previous 12 months.

Trial Design

This phase 3, event-driven, double-blind, randomized, placebo-controlled trial was designed to continue until approximately 288 disability-progression events had occurred across both trial groups.

End Points

The primary end point was confirmed disability progression, defined as an increase from baseline in the EDSS score of 1.0 or more points (if the baseline score was ≤ 5.0) or 0.5 or more points (if the baseline score was > 5.0), that was sustained for at least 6 months.

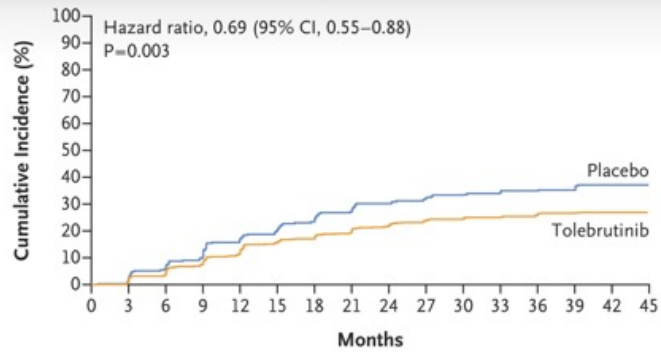
Demographic and Disease Characteristics of the Participants at Baseline (Intention-to-Treat Population).

Characteristic	Tolebrutinib (N=754)	Placebo (N=377)
Age — yr	48.9±8.0	48.9±8.0
Female sex — no. (%)	454 (60.2)	242 (64.2)
Race — no. (%) †		
White	703 (93.2)	348 (92.3)
Black	6 (0.8)	4 (1.1)
Asian	36 (4.8)	19 (5.0)
Other, unknown, or not reported	9 (1.2)	6 (1.6)
EDSS score ‡	5.5±1.0	5.6±0.9
Time since onset of symptoms of relapsing–remitting multiple sclerosis — yr	17.1±8.3	17.6±8.4
Time since diagnosis of secondary progressive multiple sclerosis — yr	7.9±7.3	8.4±7.8
Time since most recent clinical relapse — yr †	7.4±5.3	7.6±5.5
No. of previous disease-modifying therapies received — no. (%)		
0	205 (27.2)	89 (23.6)
1	200 (26.5)	102 (27.1)
≥2	349 (46.3)	186 (49.3)
Previous disease-modifying therapies received — no. (%) ¶		
Interferons †	354 (46.9)	177 (46.9)
Glatiramer acetate	176 (23.3)	99 (26.3)
Fingolimod	113 (15.0)	66 (17.5)
Dimethyl fumarate	93 (12.3)	61 (16.2)
Ocrelizumab	89 (11.8)	48 (12.7)
Teriflunomide	82 (10.9)	49 (13.0)
Natalizumab	72 (9.5)	42 (11.1)
Rituximab	47 (6.2)	23 (6.1)
Other	115 (15.3)	66 (17.5)
≥1 Gadolinium-enhancing lesion on T1-weighted MRI — no./total no. (%)	93/742 (12.5)	49/373 (13.1)
No. of gadolinium-enhancing lesions on T1-weighted MRI ††	0.4±2.0	0.6±3.5
Median volume of lesions on T2-weighted MRI (IQR) — cm ³ ††	15.3 (7.2–25.8)	14.9 (7.6–28.3)

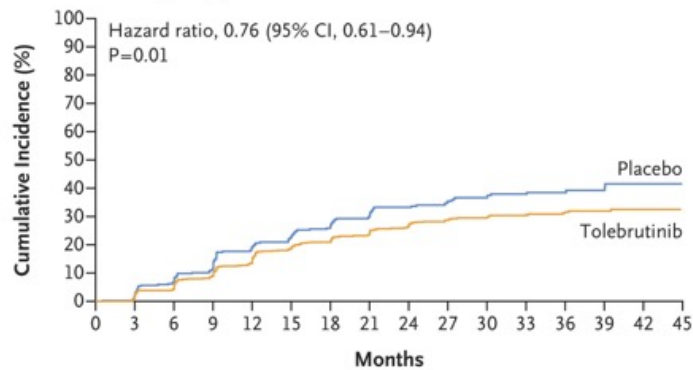
Primary and Secondary End Points (Intention-to-Treat Population).

End Point	Tolebrutinib (N=754)	Placebo (N=377)
Primary end point		
Confirmed disability progression sustained for ≥6 mo †		
No. of events/no. of participants evaluated (%) ‡	171/754 (22.6)	116/377 (30.7)
Kaplan–Meier estimate at 24 mo — % (95% CI)	21.9 (18.8 to 25.1)	30.2 (25.3 to 35.1)
Hazard ratio (95% CI)	0.69 (0.55 to 0.88)	
P value	0.003	
Secondary end points †		
Confirmed disability progression sustained for ≥3 mo †		
No. of events/no. of participants evaluated (%)	208/754 (27.6)	129/377 (34.2)
Kaplan–Meier estimate at 24 mo — % (95% CI)	26.7 (23.5 to 30.2)	33.3 (28.5 to 38.7)
Hazard ratio (95% CI)	0.76 (0.61 to 0.94)	
P value	0.01	
Annualized rate of new or enlarging lesions on T2-weighted MRI		
No. of participants evaluated	719	361
Mean estimate (95% CI)	1.84 (1.44 to 2.34)	2.95 (2.24 to 3.88)
Relative rate (95% CI)	0.62 (0.43 to 0.90)	
P value	0.01	
20% Increase in the score on the nine-hole peg test sustained for ≥3 mo		
No. of events/no. of participants evaluated (%)	143/754 (19.0)	74/377 (19.6)
Kaplan–Meier estimate at 24 mo — % (95% CI)	17.1 (14.5 to 20.2)	16.4 (12.9 to 20.8)
Hazard ratio (95% CI)	0.97 (0.74 to 1.29)	
P value	0.84 ¶	
20% Increase in the score on the timed 25-ft walk sustained for ≥3 mo		
No. of events/no. of participants evaluated (%)	310/754 (41.1)	187/377 (49.6)
Kaplan–Meier estimate at 24 mo — % (95% CI)	36.9 (33.4 to 40.7)	46.9 (41.7 to 52.4)
Hazard ratio (95% CI)	0.77 (0.64 to 0.92)	
Confirmed disability improvement sustained for 6 mo †		
No. of events/no. of participants evaluated (%)	65/754 (8.6)	17/377 (4.5)
Kaplan–Meier estimate at 24 mo — % (95% CI)	8.3 (6.5 to 10.7)	4.3 (2.6 to 7.1)
Hazard ratio (95% CI)	1.88 (1.10 to 3.21)	
Percentage change in brain volume from mo 6 to end-of-trial visit		
No. of participants evaluated	451	223
Least-squares mean change (±SE)	-0.69±0.03	-0.78±0.05
Least-squares mean difference, tolebrutinib vs. placebo (95% CI)	0.08 (-0.03 to 0.20)	

A Confirmed Disability Progression Sustained for ≥ 6 Months



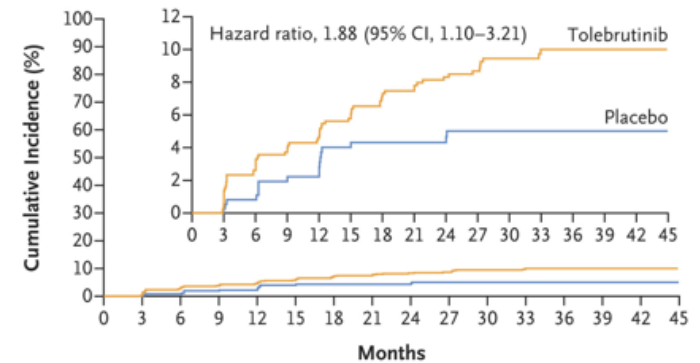
B Confirmed Disability Progression Sustained for ≥ 3 Months

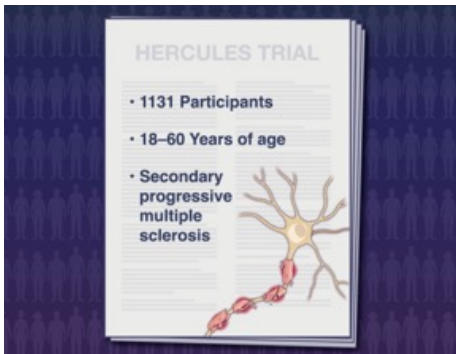
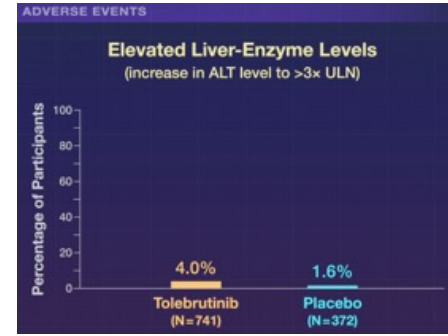
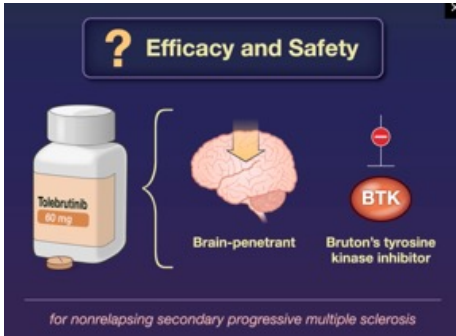
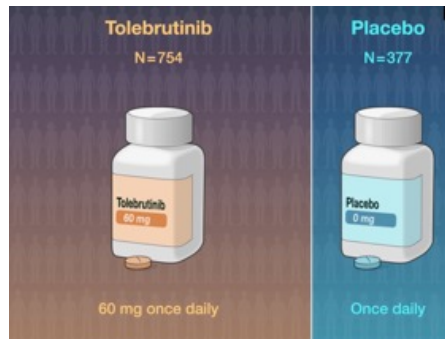


Adverse events

Event	Tolebrutinib (N=752)	Placebo (N=375)
	no./total no. (%)	
Any adverse event	613/752 (81.5)	293/375 (78.1)
Adverse events occurring in $\geq 10\%$ of participants in either group		
Covid-19	192/752 (25.5)	85/375 (22.7)
Urinary tract infection	85/752 (11.3)	49/375 (13.1)
Fall	72/752 (9.6)	41/375 (10.9)
Adverse event leading to discontinuation of tolebrutinib or placebo	29/752 (3.9)	11/375 (2.9)
Any serious adverse event		
Serious infection	39/752 (5.2)	13/375 (3.5)
Death†	2/752 (0.3)	1/375 (0.3)
Increase in ALT level to $>3\times$ ULN		
$>3-5\times$ ULN	15/741 (2.0)	3/372 (0.8)
$>5-10\times$ ULN	8/741 (1.1)	2/372 (0.5)
$>10-20\times$ ULN	3/741 (0.4)	1/372 (0.3)
$>20\times$ ULN	4/741 (0.5)	0
ALT level $>3\times$ ULN and total bilirubin level $>2\times$ ULN‡	3/752 (0.4)	0

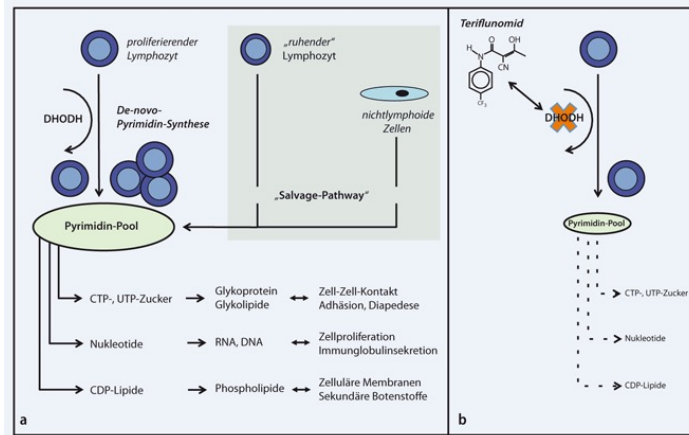
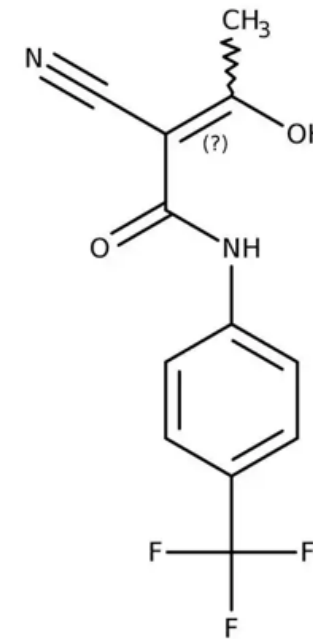
C Confirmed Disability Improvement Sustained for ≥ 6 Months





Teriflunomid ist ein Immunmodulator, der in der Behandlung der schubförmig-remittierenden Multiplen Sklerose (MS) eingesetzt wird. Es hemmt ein Enzym, das für das Wachstum bestimmter Zellen des Immunsystems, insbesondere T- und B-Lymphozyten, wichtig ist, wodurch die Entzündung im Gehirn und Rückenmark reduziert wird.

•**Wirkungsmechanismus:** Teriflunomid wirkt, indem es ein Enzym hemmt, das für die Zellteilung und das Wachstum von T- und B-Lymphozyten, die an der Entzündung bei MS beteiligt sind, notwendig ist.



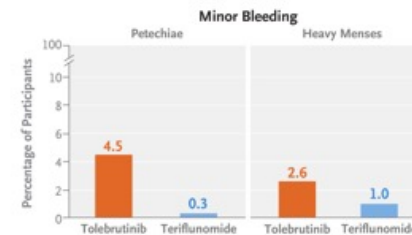
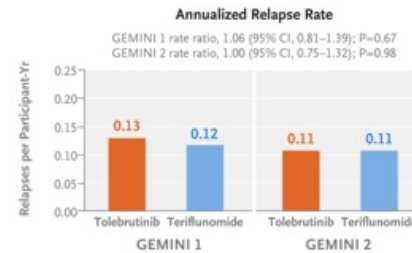
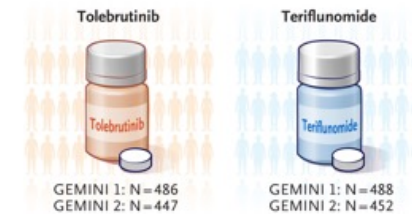
Tolebrutinib versus Teriflunomide in Relapsing Multiple Sclerosis

Tolebrutinib is an oral, brain-penetrant, and bioactive Bruton's tyrosine kinase inhibitor that modulates peripheral inflammation and persistent immune activation within the central nervous system, including disease-associated microglia and B cells. More data are needed on its efficacy and safety in treating relapsing multiple sclerosis. In two phase 3, double-blind, double-dummy, event-driven trials (GEMINI 1 and GEMINI 2), participants with relapsing multiple sclerosis were randomly assigned in a 1:1 ratio to receive tolebrutinib (60 mg once daily) or teriflunomide (14 mg once daily), each with matching placebo. The primary end point was the annualized relapse rate. The key secondary end point was confirmed worsening of disability that was sustained for at least 6 months, which was assessed in a time-to-event analysis that was pooled across trials.

Moreover, specific platelet function tests in blood are described which will help to estimate the probability of bleeding side effects of newly developed BTKi.

Participants

- 1873 adults
- 18 to 55 years of age
- Women: 67%; Men: 33%



Multiple sclerosis is manifested by disseminated focal lesions in the white matter that often precede clinical relapse activity and are accompanied by indolent, insidious, and permanent loss of neurologic function, which is known as disability accrual. The era of disease-modifying therapies that target these features began more than 30 years ago with the approval of interferon beta-1b. Today, more than 20 disease-modifying therapies have been approved largely on the basis of relapse-related outcomes, including clinical relapses and the formation of focal lesions on magnetic resonance imaging (MRI). Anti-CD20 monoclonal antibodies have shown larger effects than most other therapies on focal-lesion formation and relapse activity. However, post hoc analyses of trials on ocrelizumab have shown that although this therapy provided excellent control of focal inflammation, it resulted in limited reduction of disability progression independent of relapse activity. Preventing disability accrual and fostering sustained improvement in neurologic functioning remain unmet clinical needs across all stages of multiple sclerosis.

Participants

Persons were eligible at screening if they were 18 to 55 years of age and had received a diagnosis of relapsing multiple sclerosis according to the 2017 McDonald criteria, had an Expanded Disability Status Scale (EDSS) score of 5.5 or lower (scores range from 0 to 10.0, with higher scores indicating worse disability), and had had at least one relapse within the previous year, at least two relapses within the previous 2 years, or at least one gadolinium-enhancing brain lesion on T1-weighted MRI within the previous year.

Trial Design

The GEMINI 1 and GEMINI 2 trials were double-blind, double-dummy, multicenter, event-driven, active-controlled, randomized trials of similar design that were conducted concurrently. The trials continued until approximately 162 confirmed disability-worsening events lasting at least 6 months occurred in the two treatment groups when the groups were pooled across trials.

End Points

The primary end point for both trials was the annualized relapse rate, which was defined as the number of confirmed (adjudicated) relapses per participant-year according to prespecified criteria.

Demographic and Disease Characteristics of Participants

Characteristic	GEMINI 1		GEMINI 2	
	Tolebrutinib (N=486)	Teriflunomide (N=488)	Tolebrutinib (N=447)	Teriflunomide (N=452)
Age — yr	36.8±9.0	36.6±9.4	36.6±9.3	36.1±9.3
Female sex — no. (%)	334 (68.7)	325 (66.6)	300 (67.1)	293 (64.8)
Race — no. (%)†				
White	395 (81.3)	406 (83.2)	411 (91.9)	417 (92.3)
Black	4 (0.8)	10 (2.0)	7 (1.6)	11 (2.4)
Asian	78 (16.0)	67 (13.7)	23 (5.1)	19 (4.2)
Other, unknown, or not reported	9 (1.9)	5 (1.0)	6 (1.3)	5 (1.1)
Multiple sclerosis subtype — no. (%)				
Relapsing–remitting	480 (98.8)	483 (99.0)	444 (99.3)	450 (99.6)
Secondary progressive	6 (1.2)	5 (1.0)	3 (0.7)	2 (0.4)
Time since diagnosis — yr‡	4.8±6.2	4.6±6.0	3.8±5.4	3.8±5.4
Expanded Disability Status Scale score§	2.4±1.2	2.4±1.2	2.4±1.2	2.3±1.2
Time since most recent relapse — mo¶	6.2±13.5	7.4±17.3	8.5±25.9	7.2±15.5
No. of relapses in the past year	1.2±0.6	1.2±0.6	1.1±0.5	1.2±0.6
Previous disease-modifying therapy — no. (%)**	171 (35.2)	197 (40.4)	146 (32.7)	152 (33.6)
Interferon therapies††	104 (21.4)	100 (20.5)	85 (19.0)	85 (18.8)
Glatiramer acetate	59 (12.1)	61 (12.5)	40 (8.9)	40 (8.8)
Dimethyl fumarate	25 (5.1)	34 (7.0)	21 (4.7)	31 (6.9)
Fingolimod	15 (3.1)	24 (4.9)	15 (3.4)	8 (1.8)
Ocrelizumab	11 (2.3)	10 (2.0)	1 (0.2)	5 (1.1)
Diroximel fumarate	9 (1.9)	15 (3.1)	2 (0.4)	1 (0.2)
Teriflunomide	9 (1.9)	9 (1.8)	7 (1.6)	11 (2.4)
Natalizumab	7 (1.4)	9 (1.8)	5 (1.1)	2 (0.4)
Other	23 (4.7)	22 (4.5)	14 (3.1)	18 (4.0)
≥1 Gadolinium-enhancing lesion on T1-weighted MRI — no./total no. (%)	168/484 (34.7)	186/485 (38.4)	145/447 (32.4)	146/448 (32.6)
No. of gadolinium-enhancing lesions on T1-weighted MRI‡‡	1.3±3.7	1.5±4.2	1.0±2.4	1.0±3.2
Volume of lesion on T2-weighted MRI — cm§§	14.6±13.0	14.0±12.0	11.5±10.6	10.8±9.9

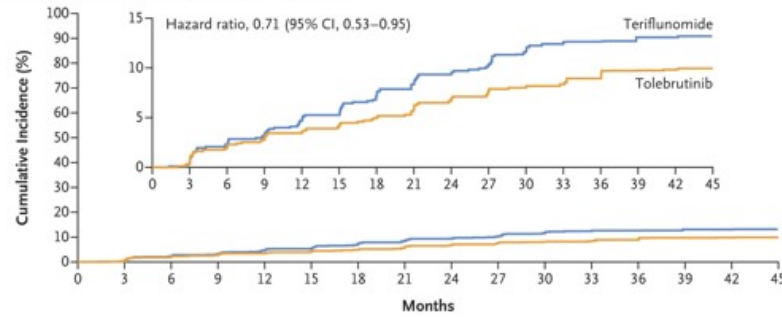
Primary and Secondary End Points in the Intention-to-Treat Population.

End Point	GEMINI 1		GEMINI 2		Pooled Analysis	
	Tolebrutinib (N=486)	Teriflunomide (N=488)	Tolebrutinib (N=447)	Teriflunomide (N=452)	Tolebrutinib (N=933)	Teriflunomide (N=940)
Primary end point						
Adjusted annualized relapse rate (95% CI)	0.13 (0.11 to 0.16)	0.12 (0.10 to 0.15)	0.11 (0.09 to 0.13)	0.11 (0.09 to 0.13)	0.12 (0.11 to 0.14)	0.12 (0.10 to 0.14)
Rate ratio (95% CI)	1.06 (0.81 to 1.39)†		1.00 (0.75 to 1.32)‡		1.03 (0.85 to 1.25)§	
Secondary end points¶						
Confirmed disability worsening for ≥6 mo						
No. of events (%)**					78 (8.3)	106 (11.3)
Kaplan–Meier estimate at 24 mo — % (95% CI)					6.7 (5.2 to 8.5)	9.3 (7.5 to 11.4)
Hazard ratio (95% CI)					0.71 (0.53 to 0.95)	
Confirmed disability worsening for ≥3 mo						
No. of events (%)					109 (11.7)	144 (15.3)
Kaplan–Meier estimate at 24 mo — % (95% CI)					8.8 (7.1 to 10.9)	11.8 (9.8 to 14.1)
Hazard ratio (95% CI)					0.73 (0.57 to 0.94)	
Confirmed disability improvement for ≥6 mo††						
No. of events (%)					118 (12.6)	98 (10.4)
Kaplan–Meier estimate at 24 months — % (95% CI)					11.3 (9.4 to 13.6)	8.8 (7.1 to 10.9)
Hazard ratio (95% CI)					1.22 (0.94 to 1.60)	
Adjusted no. of new gadolinium-enhancing lesions on T1-weighted MRI						
No. of participants with nonmissing data	473	469	436	432		
No. of participants with lesions	218	189	205	151		
Mean estimate (95% CI)	0.53 (0.44 to 0.64)	0.29 (0.22 to 0.37)	0.46 (0.37 to 0.58)	0.22 (0.17 to 0.28)		
Rate ratio (95% CI)	1.86 (1.36 to 2.55)		2.12 (1.50 to 2.99)			
Adjusted no. of new or enlarging lesions on T2-weighted MRI per yr						
No. of participants with nonmissing data	473	474	436	435		
No. of participants with lesions	363	363	331	329		
Mean estimate (95% CI)	5.61 (4.83 to 6.52)	5.18 (4.45 to 6.02)	5.09 (4.34 to 5.98)	4.37 (3.59 to 5.32)		
Rate ratio (95% CI)	1.08 (0.88 to 1.34)		1.17 (0.91 to 1.50)			
Change from baseline to end-of-trial visit in z score for no. of correct substitutions on SDMT						
No. of participants	393	396	366	359		
Least-squares mean	0.364±0.032	0.329±0.032	0.374±0.037	0.428±0.037		
Difference (95% CI)	0.035 (-0.053 to 0.124)		-0.053 (-0.156 to 0.050)			
Change from baseline to end-of-trial visit in CVLT-II total correct standardized score‡‡						
No. of participants	390	391	357	347		
Least-squares mean	17.700±0.724	15.827±0.724	15.819±0.674	16.431±0.683		
Difference (95% CI)	1.873 (-0.135 to 3.880)		-0.612 (-2.493 to 1.269)			
Percentage change in brain volume from 6 mo to end-of-trial visit						
No. of participants	351	346	317	307		
Least-squares mean	-0.69±0.04	-0.88±0.04	-0.70±0.04	-0.74±0.04		
Difference (95% CI)	0.20 (0.09 to 0.30)§§		0.04 (-0.07 to 0.15)¶¶			

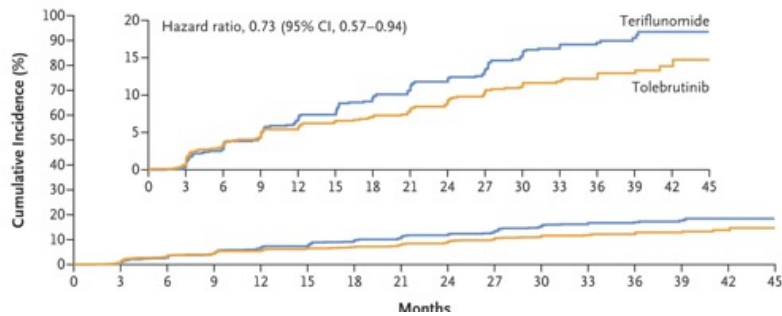
Adverse Events and Elevated ALT Levels in the Safety Population.

Event	Tolebrutinib (N=933)	Teriflunomide (N=939)
Any adverse event — no. (%)	792 (84.9)	810 (86.3)
Adverse events occurring in ≥10% of participants in either treatment group — no. (%)		
Coronavirus disease 2019	225 (24.1)	252 (26.8)
Nasopharyngitis	119 (12.8)	105 (11.2)
Headache	117 (12.5)	98 (10.4)
Alopecia	73 (7.8)	146 (15.5)
Adverse events leading to treatment discontinuation — no. (%)	42 (4.5)	41 (4.4)
Minor bleeding events — no. (%) †		
Heavy menses	24 (2.6)	9 (1.0)
Petechiae	42 (4.5)	3 (0.3)
Any serious adverse event — no. (%)	91 (9.8)	77 (8.2)
Serious infection	23 (2.5)	21 (2.2)
Deaths — no. (%) ‡	1 (0.1)	2 (0.2)
Increase in ALT level to >3× ULN — no./total no. (%)		
>3–5× ULN	20/929 (2.2)	28/926 (3.0)
>5–10× ULN	19/929 (2.0)	21/926 (2.3)
>10–20× ULN	8/929 (0.9)	8/926 (0.9)
>20× ULN	5/929 (0.5)	1/926 (0.1)
Increase in ALT level to >3× ULN and increase in total bilirubin level to >2× ULN — no./total no. (%)	4/929 (0.4)	1/926 (0.1)

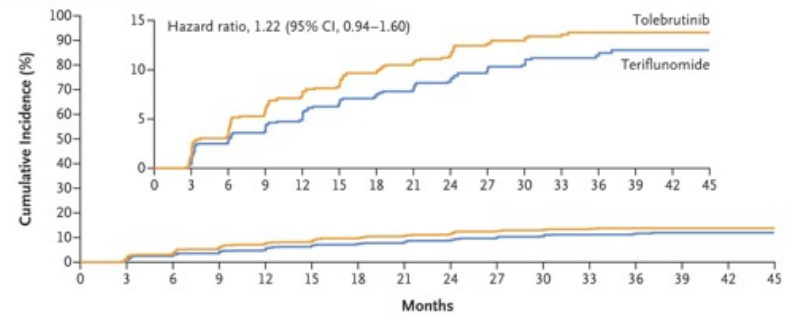
A Confirmed Disability Worsening Sustained for ≥6 Months

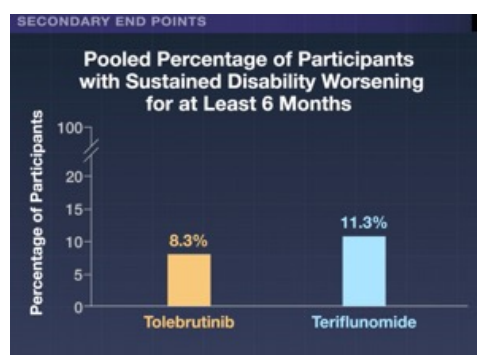
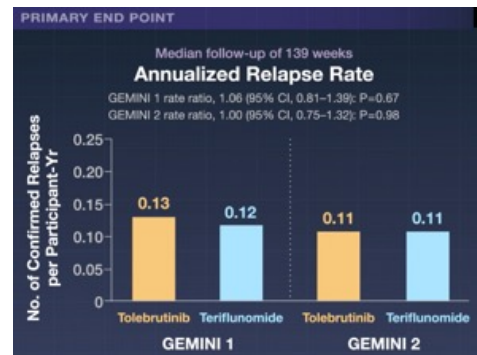
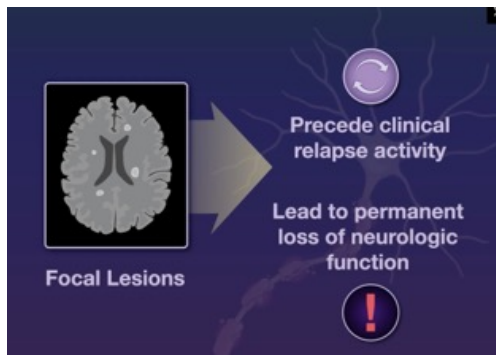
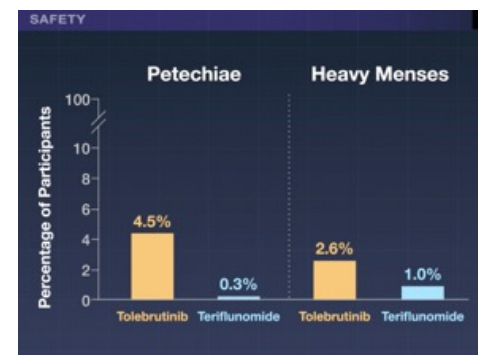
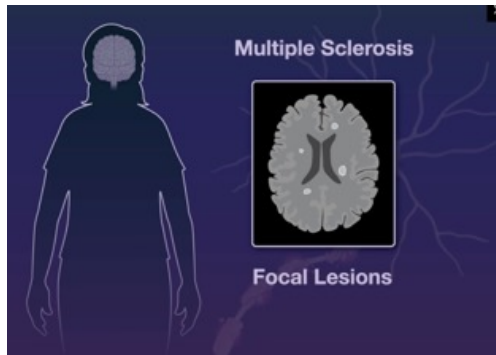


B Confirmed Disability Worsening Sustained for ≥3 Months



C Confirmed Disability Improvement Sustained for ≥6 Months





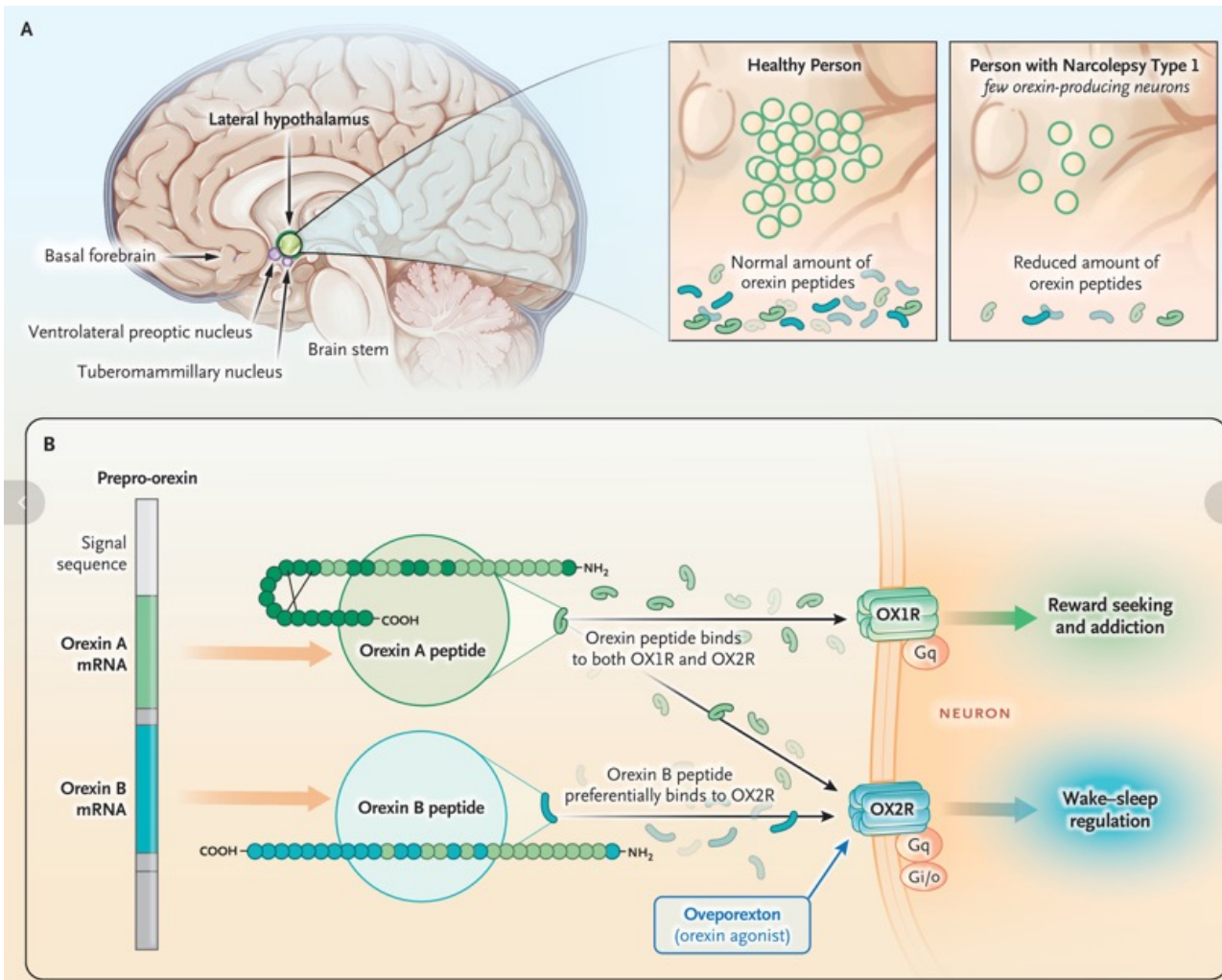
Targeting Orexin Receptors to Treat Narcolepsy

What Is Narcolepsy?

Narcolepsy was first described more than 100 years ago as a disorder that causes a puzzling combination of problems, including excessive daytime sleepiness (hypersomnia), episodes of loss of motor tone associated with emotional responses (cataplexy), and an inability to move (sleep paralysis) or dreamlike states intruding on consciousness at the onset of sleep or waking (hypnagogic or hypnopompic hallucinations). Early pathological studies showed that some patients with narcolepsy who died had damage to the posterior hypothalamus.

What Causes It?

The orexin peptides were discovered independently in 1998 by two groups of investigators. One group identified a messenger RNA (mRNA) that was expressed only in the hypothalamus, which coded for a pair of peptides they named hypocretins. Another group identified two peptides, which they named orexin A and orexin B, that bind two G protein–coupled receptors (see Key Concepts) that they called orexin receptors 1 and 2 (OX1R and OX2R, respectively). Both naming systems are commonly used. The orexin A peptide binds about equally to each receptor, but the orexin B peptide binds preferentially to OX2R. The two receptors are distributed differentially in the brain, with OX2R predominating in many cell groups associated with promoting wakefulness and OX1R in areas associated with addiction and reward-seeking behavior.



Origin and Actions of Orexin Peptides.

Panel A shows the location of the orexin neurons in the lateral hypothalamus, from which they stimulate wake-promoting cell groups (such as the tubero-mammillary nucleus) and inhibit sleep-promoting neurons (such as the ventrolateral preoptic nucleus). The loss of orexin-producing neurons underlies the symptoms of narcolepsy type 1. Panel B shows the location of the orexin A and B sequences in the prepro-orexin messenger RNA (mRNA) and the synthesis of these two peptide neurotransmitters. Orexin B binds to orexin receptor 2 (OX2R), which is important for regulating sleep and wakefulness, whereas orexin A binds to both OX2R and orexin receptor 1 (OX1R), which plays a key role in addiction. Modified from Villano et al.⁵

How Do Orexins Work in the Brain?

The orexin neurons are most active during active wakefulness (e.g., exploring the environment), become less active in quiet wakefulness, and stop firing during sleep. They have widespread projections throughout the brain and spinal cord, including the cerebral cortex and most of the cell groups involved with wake–sleep regulation. Both orexin receptors are excitatory, and orexins activate neurons in the brain stem and basal forebrain that contribute to wakefulness. In the ventrolateral preoptic area, orexin neurons activate GABAergic interneurons, which inhibit the ventrolateral preoptic sleep-promoting cells. Thus, orexin neurons promote wakefulness. Persons or animals with narcolepsy type 1 are excessively sleepy during their normally active periods.

And the Implications for Treating Sleep Disorders?

Although orexins can be administered directly into the CSF in animal models, this approach is not practical in humans, and orexin peptides are too large to cross the blood–brain barrier. Hence, since their discovery, there has been an intensive search for small molecules that interact with the orexin receptors. The orexin antagonists were developed first, and three have been approved by the Food and Drug Administration. As expected, these drugs promote sleep; fortunately, they rarely cause other aspects of narcolepsy (e.g., cataplexy). OX1R antagonists are now being studied for the treatment of addiction.

Oveporexton, an Oral Orexin Receptor 2–Selective Agonist, in Narcolepsy Type 1

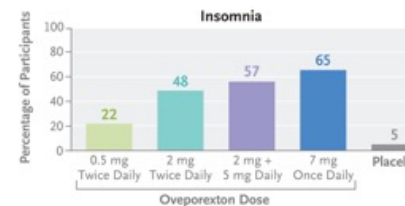
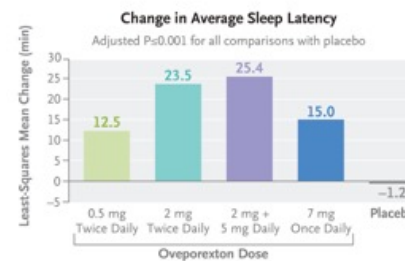
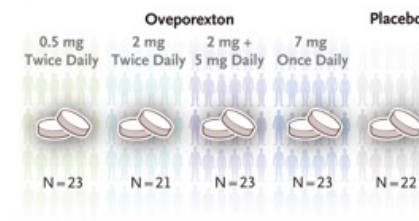
Narcolepsy type 1 is a disorder of hypersomnolence caused by a loss of orexin neurons, which results in low orexin levels in the brain. In this phase 2, randomized, placebo-controlled trial, participants with narcolepsy type 1 received once- or twice-daily oveporexton (TAK-861), an oral orexin receptor 2–selective agonist, or placebo. The primary end point was the mean change from baseline to week 8 in average sleep latency (the time it takes to fall asleep) on the Maintenance of Wakefulness Test (MWT) (range, 0 to 40 minutes; normal, ≥ 20). Secondary end points included the change from baseline to week 8 in the Epworth Sleepiness Scale (ESS) total score (range, 0 to 24; normal, ≤ 10), the weekly cataplexy rate at week 8, and the occurrence of adverse events.

Participants

- 112 adults
- Mean age, 34 years
- Women: 52%; Men: 48%



Loss of hypothalamic orexin-producing neurons



Narcolepsy type 1 is a disorder of hypersomnolence defined by excessive daytime sleepiness, cataplexy, disrupted nighttime sleep, hypnagogic or hypnopompic hallucinations, sleep paralysis, and markedly reduced quality of life. The disorder is characterized by loss of hypothalamic orexin-producing neurons, with low to absent orexin levels in cerebrospinal fluid. Orexins act through two G-protein-coupled receptors, orexin receptor 1 and orexin receptor 2 (OX2R), with overlapping but distinct distributions within the brain. Although both receptors have roles in a range of physiological responses, OX2R has functions in wakefulness, rapid-eye-movement (REM) sleep, and prevention of cataplexy in animal models of narcolepsy. Available treatments do not target pathways underlying the pathophysiological features of narcolepsy type 1 but instead aim to increase daytime wakefulness and reduce cataplexy. Preclinical and clinical evidence with an intravenous OX2R agonist, danavorexton (TAK-925), and an oral OX2R agonist, TAK-994, support the potential for OX2R-selective agonists as treatments for narcolepsy. In participants with narcolepsy type 1, danavorexton promoted wakefulness, and TAK-994 improved measures of wakefulness and cataplexy as compared with placebo over a period of 8 weeks. However, TAK-994 was associated with hepatotoxic effects in three cases (all with a dose of 90 mg or 180 mg twice daily), effects that were thought to be unrelated to OX2R stimulation.

Oveporexton (TAK-861) is a highly selective oral OX2R agonist that crosses the blood-brain barrier and has been shown to improve wakefulness in preclinical models and in sleep-deprived healthy adults. We tested the efficacy and safety of oveporexton for the treatment of narcolepsy type 1 in a phase 2, double-blind, randomized, placebo-controlled trial.

Trial Design

TAK-861-2001 was a phase 2, double-blind, randomized, placebo-controlled trial involving persons with narcolepsy type 1 that was conducted in North America (United States), Europe, Asia (Japan), and Australia.

Participants

The trial included adults 18 to 70 years of age with a diagnosis of narcolepsy type 1 that was made in accordance with the **criteria of the International Classification of Sleep Disorders**, and confirmed by **nocturnal polysomnography and a Multiple Sleep Latency Test** performed within the previous 10 years. Participants also had a baseline Epworth Sleepiness Scale (ESS) total score of more than 12 (range, 0 to 24; normal, ≤ 10), at least four episodes of partial or complete cataplexy per week during screening (2-week average), and either a cerebrospinal fluid orexin-A or hypocretin-1 concentration of less than 110 pg per milliliter (where tested) or a positive test for HLA genotype HLA-DQB1*06:02, to ensure a high likelihood of orexin deficiency in the presence of cataplexy.

End Points

The primary end point was the mean change from baseline to week 8 in average sleep latency on the 40-minute Maintenance of Wakefulness Test (MWT), a measure in minutes of a person's ability to stay awake under soporific conditions. Healthy persons stay awake for 20 minutes or more, as compared with less than 10 minutes for persons with narcolepsy type 1. At baseline, week 4, and week 8, sleep latencies were measured in four MWT sessions at 2, 4, 6, and 8 hours after the 8 a.m. dose (after the 8 a.m. at baseline).

Demographic, Clinical, and Biologic Characteristics

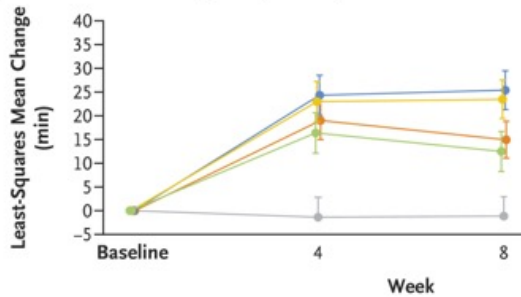
Characteristic	Placebo (N = 22)	Oveporexton, 0.5 mg Twice Daily (N = 23)	Oveporexton, 2 mg Twice Daily (N = 21)	Oveporexton, 2 mg and 5 mg Daily (N = 23)	Oveporexton, 7 mg Once Daily (N = 23)	Total (N = 112)
Age — yr						
Mean	37.5±11.9	32.7±11.1	31.7±11.3	34.7±11.5	33.3±11.9	34.0±11.5
Median (range)	38.0 (19–58)	33.0 (18–59)	32.0 (18–53)	35.0 (18–58)	32.0 (18–57)	34.0 (18–59)
Sex — no. (%)						
Male	8 (36)	12 (52)	12 (57)	9 (39)	13 (57)	54 (48)
Female	14 (64)	11 (48)	9 (43)	14 (61)	10 (43)	58 (52)
Race — no. (%)†						
Asian	1 (5)	2 (9)	0	3 (13)	2 (9)	8 (7)
Black	2 (9)	1 (4)	2 (10)	0	1 (4)	6 (5)
White	19 (86)	19 (83)	19 (90)	19 (83)	20 (87)	96 (86)
Multiple	0	1 (4)	0	1 (4)	0	2 (2)
Average sleep latency on MWT — min‡						
Mean	6.1±8.8	5.6±7.9	3.9±6.0	4.2±3.6	3.6±4.9	4.7±6.5
Median (range)	2.0 (0.5–32.0)	2.3 (0.5–29.0)	1.8 (0.3–26.4)	2.8 (0.1–14.6)	2.5 (0.1–19.6)	2.5 (0.1–32.0)
ESS total score§						
Mean	18.6±2.7	18.3±3.4	19.0±3.1	18.6±3.0	18.0±3.0	18.5±3.0
Median (range)	19.0 (12.0–23.0)	19.0 (11.0–24.0)	19.0 (14.0–24.0)	19.0 (14.0–23.0)	18.0 (12.0–24.0)	19.0 (11.0–24.0)
Weekly cataplexy rate — no. of episodes						
Mean	23.1±25.7	18.6±16.9	21.0±30.0	15.7±13.5	31.1±29.1	21.9±24.0
Median (range)	13.3 (5.0–100.9)	11.0 (2.7–71.0)	11.3 (1.2–130.5)	9.5 (4.0–53.5)	20.0 (7.0–107.5)	12.0 (1.2–130.5)
NSS-CT total score¶						
Mean	32.5±9.3	30.2±9.8	28.8±9.5	28.7±8.3	33.5±6.9	30.7±8.9
Median (range)	30.0 (18–50)	32.0 (14–52)	26.0 (14–53)	27.0 (12–48)	33.0 (22–48)	30.0 (12–53)
Liver-function tests at baseline						
ALT — U/liter	23.6±12.7	19.5±10.0	22.4±12.2	20.0±9.3	21.8±11.5	21.4±11.1
AST — U/liter	21.2±7.4	19.0±6.6	19.9±8.3	19.1±6.9	17.3±4.8	19.3±6.9
Bilirubin — μmol/liter	7.2±7.6	7.3±5.1	8.5±6.9	6.8±4.3	6.1±2.8	7.1±5.4
GGT — U/liter	21.7±17.6	19.1±14.6	19.4±10.1	30.4±33.5	16.9±7.7	21.5±19.4

Efficacy End Points.

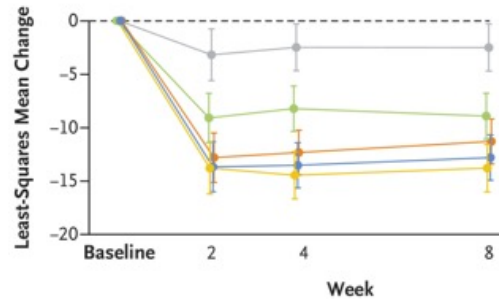
End Point	Placebo (N=22)	Oveporexton, 0.5 mg Twice Daily (N=23)	Oveporexton, 2 mg Twice Daily (N=21)	Oveporexton, 2 mg and 5 mg Daily (N=23)	Oveporexton, 7 mg Once Daily (N=23)
Average sleep latency on MWT†					
No. of participants evaluated	21	19	21	20	23
Mean at wk 8 — min	4.7±8.9	16.5±11.4	27.6±9.5	30.7±9.3	19.5±9.7
Least-squares mean change from baseline to wk 8 (95% CI)	-1.2 (-5.3 to 2.9)	12.5 (8.3 to 16.7)	23.5 (19.5 to 27.6)	25.4 (21.3 to 29.5)	15.0 (11.1 to 18.8)
Least-squares mean difference from placebo (95% CI)	—	13.7 (7.7 to 19.6)	24.7 (18.9 to 30.5)	26.6 (20.8 to 32.4)	16.1 (10.5 to 21.8)
Adjusted P value	—	0.001	<0.001	<0.001	<0.001
Sleep latency of ≥20 min at wk 8 — no./total no. (%)	1/21 (5)	7/19 (37)	17/21 (81)	17/21 (81)	14/23 (61)
ESS total score‡					
No. of participants evaluated	21	21	21	22	23
Mean at wk 8	16.0±5.8	8.9±5.4	4.8±3.0	5.2±4.4	7.0±5.4
Least-squares mean change from baseline to wk 8 (95% CI)	-2.5 (-4.7 to -0.3)	-8.9 (-11.1 to -6.8)	-13.8 (-16.0 to -11.6)	-12.8 (-14.9 to -10.7)	-11.3 (-13.4 to -9.2)
Least-squares mean difference from placebo (95% CI)	—	-6.4 (-9.5 to -3.3)	-11.3 (-14.4 to -8.2)	-10.3 (-13.3 to -7.3)	-8.8 (-11.8 to -5.8)
Adjusted P value	—	0.004	<0.001	<0.001	<0.001
Total score of ≤10 at wk 8 — no. (%)	4 (19)	14 (67)	20 (95)	18 (82)	17 (74)
Weekly cataplexy rate					
No. of participants evaluated	20	21	21	22	23
Mean no. of episodes at wk 8	9.0±9.9	3.3±3.9	3.2±4.3	2.1±3.3	10.1±15.6
Mean change from baseline to wk 8§	-10.3±21.7	-14.5±15.4	-17.9±28.4	-13.9±14.5	-21.0±23.1
Incidence rate (95% CI)¶	8.76 (5.68 to 13.51)	4.24 (2.60 to 6.92)	3.14 (1.65 to 5.98)	2.48 (1.30 to 4.73)	5.89 (3.64 to 9.53)
Incidence rate ratio vs. placebo (95% CI)¶¶	—	0.48 (0.25 to 0.93)	0.36 (0.16 to 0.79)	0.28 (0.13 to 0.60)	0.67 (0.35 to 1.29)
Adjusted P value	—	0.25	0.03	0.003	0.25
VSS-CT total score					
No. of participants evaluated	21	22	21	22	23
Mean at wk 8	26.8±11.0	11.9±6.6	8.8±7.7	8.1±6.0	14.5±10.5
Mean change from baseline to wk 8	-4.9±8.1	-17.6±8.4	-20.0±10.6	-20.7±9.6	-19.0±11.6
Least-squares mean change from baseline to wk 8 (95% CI)	-3.5 (-7.0 to 0.0)	-18.2 (-21.7 to -14.7)	-21.0 (-24.6 to -17.4)	-21.1 (-24.6 to -17.7)	-17.2 (-20.7 to -13.8)
Least-squares mean difference from placebo (95% CI)	—	-14.7 (-19.7 to -9.7)	-17.5 (-22.6 to -12.5)	-17.6 (-22.6 to -12.7)	-13.7 (-18.7 to -8.8)
Total score of 0 to 14: mild disease — no. (%)	2 (10)	18 (82)	18 (86)	20 (91)	15 (65)

● Placebo
 ● Oveporexton, 0.5 mg twice daily
 ● Oveporexton, 2 mg twice daily
 ● Oveporexton, 2 mg and 5 mg daily
 ● Oveporexton, 7 mg once daily

A Change from Baseline in Average Sleep Latency on MWT

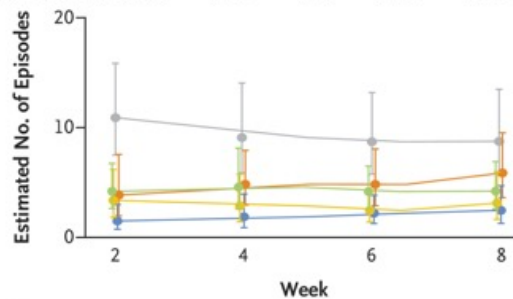


B Change from Baseline in ESS Total Score

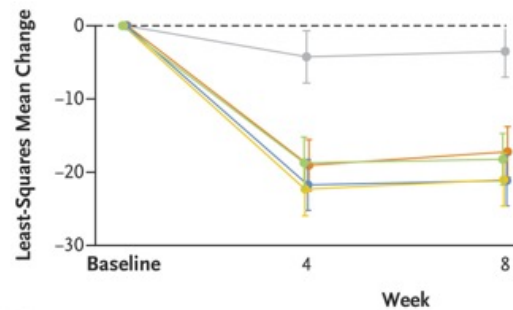


Weekly Cataplexy Rate

	Placebo	Oveporexton			
		0.5 mg twice daily	2 mg twice daily	2 and 5 mg daily	7 mg once daily
Mean Rate at Baseline	23.1	18.6	21.0	15.7	31.1



D Change from Baseline in NSS-CT Total Score

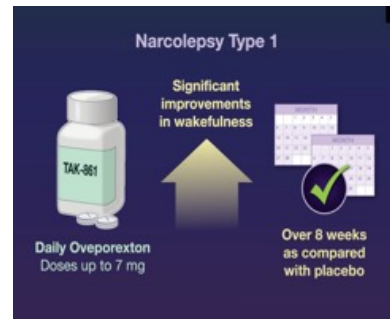
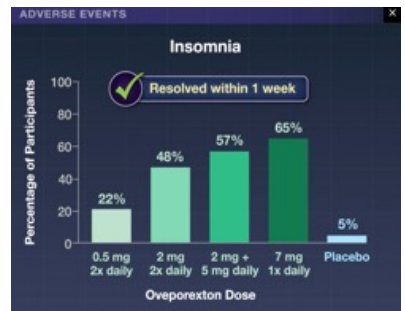
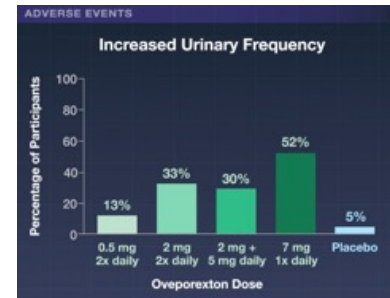
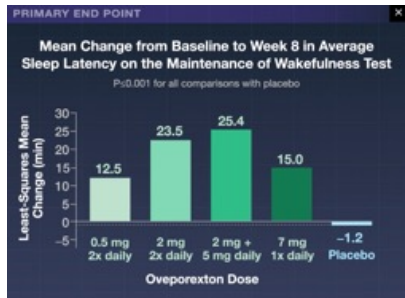
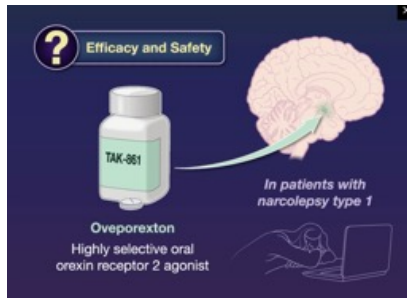
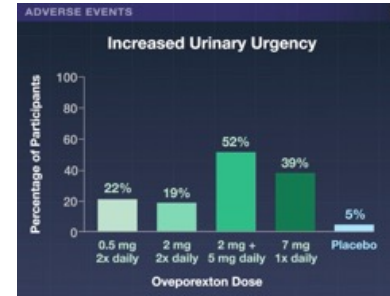
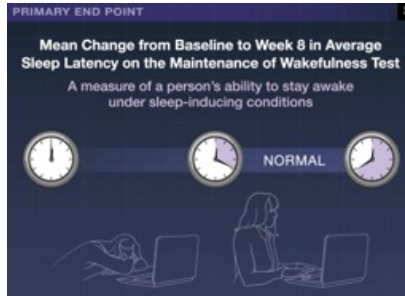
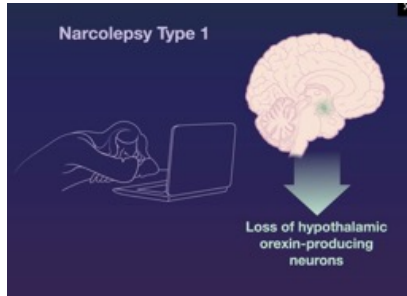


Summary of Efficacy End Points from Baseline to Week 8.

Shown are the change from baseline in average sleep latency on the Maintenance of Wakefulness Test (MWT) (Panel A), the change from baseline in the Epworth Sleepiness Scale (ESS) total score (Panel B), the weekly cataplexy rate (Panel C), and the change from baseline in the Narcolepsy Severity Scale for Clinical Trials (NSS-CT) total score (Panel D). Values on the MWT range from 0 to 40 minutes (normal ability to stay awake, ≥ 20). ESS total scores range from 0 to 24, with higher scores indicating greater daytime sleepiness (normal, ≤ 10). NSS-CT total scores range from 0 to 57, with higher scores indicating greater severity of narcolepsy symptoms. In all groups, doses were administered at 8 a.m. and 11 a.m. each day for 8 weeks (in the once-daily oveporexton group, participants received 7 mg of oveporexton at 8 a.m. and placebo at 11 a.m.). Error bars indicate 95% confidence intervals.

Summary of Safety Evaluations.

Variable	Placebo (N=22)	Oveporexton, 0.5 mg Twice Daily (N=23)	Oveporexton, 2 mg Twice Daily (N=21)	Oveporexton, 2 mg and 5 mg Daily (N=23)	Oveporexton, 7 mg Once Daily (N=23)
Adverse events — no. of participants (%)					
Any	7 (32)	13 (57)	15 (71)	21 (91)	21 (91)
Mild	5 (23)	10 (43)	6 (29)	11 (48)	12 (52)
Moderate	2 (9)	3 (13)	5 (24)	8 (35)	8 (35)
Severe†	0	0	4 (19)	2 (9)	1 (4)
Adverse events related to oveporexton or placebo — no. of participants (%)‡					
Any	3 (14)	12 (52)	14 (67)	20 (87)	20 (87)
Severe‡	0	0	3 (14)	1 (4)	1 (4)
Adverse events resulting in discontinuation from trial — no. of participants (%)					
Any	0	0	0	0	0
Serious adverse events — no. of participants (%)					
Any	0	0	0	1 (4.3)¶	0
Related to oveporexton or placebo‡	0	0	0	0	0
Most frequent adverse events — no. of participants (%)					
Insomnia	1 (5)	5 (22)	10 (48)	13 (57)	15 (65)
Urinary urgency	1 (5)	5 (22)	4 (19)	12 (52)	9 (39)
Urinary frequency	1 (5)	3 (13)	7 (33)	7 (30)	12 (52)
Salivary hypersecretion	1 (5)	2 (9)	2 (10)	6 (26)	2 (9)
Headache	1 (5)	1 (4)	3 (14)	2 (9)	2 (9)
Nasopharyngitis	0	0	2 (10)	2 (9)	2 (9)
Liver-function tests at wk 8					
ALT — U/liter	21.2±14.6	15.3±7.0	20.7±11.8	20.5±10.3	18.7±13.0
AST — U/liter	18.3±4.9	16.8±2.9	19.3±7.1	18.5±5.4	17.0±5.2
Bilirubin — mmol/liter	8.3±7.5	7.9±3.3	8.6±6.0	7.9±3.8	6.3±2.1
GGT — U/liter	20.1±19.6	19.3±19.9	16.7±9.4	28.6±31.7	16.5±8.0



Tenofovirafenamid, kurz TAF, ist ein Medikament zur Behandlung einer Hepatitis-B- oder HIV-Infektion. Es ist ein Prodrug von Tenofovir und gehört zur Gruppe der nukleotidischen Reverse-Transkriptase-Inhibitoren (NtRTI).

Emtricitabin ist ein Arzneimittel, das zur Behandlung von HIV-Infektionen und zur Prävention von HIV-Infektionen eingesetzt wird. Es gehört zur Wirkstoffklasse der nukleosidischen Reverse-Transkriptase-Inhibitoren (NRTI).

Dolutegravir ist ein antiretroviraler Wirkstoff aus der Gruppe der Integrase-Strangtransfer-Inhibitoren (INSTI), der in der HIV-Therapie eingesetzt wird. Er hemmt ein Enzym, das für die Vermehrung des HI-Virus notwendig ist, indem er an das aktive Zentrum der viralen Integrase bindet.

What is the HIV regimen for children?

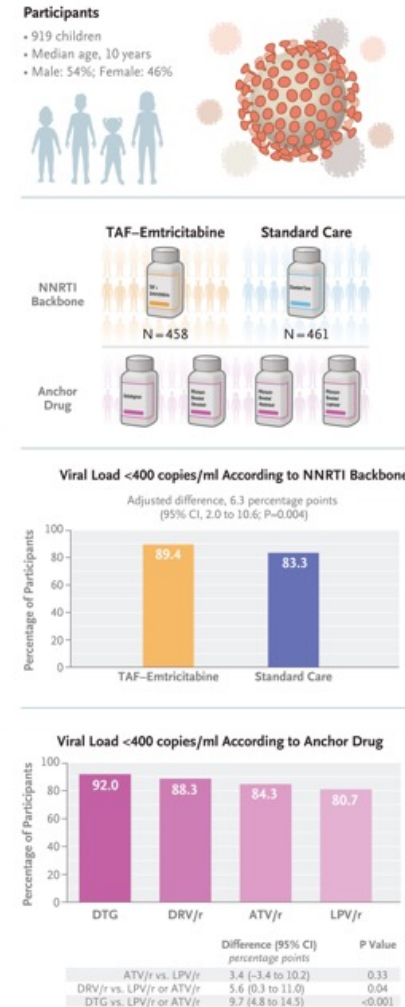
Preferred regimens are as follows: Infants, birth to < 14 days: 2 NRTIs plus nevirapine. Aged ≥ 14 days to < 3 years: 2 NRTIs plus lopinavir/ritonavir. Aged ≥ 2 years to < 3 years: 2 NRTIs plus lopinavir/ritonavir or 2 NRTIs plus raltegravir.

Children with HIV infection face unique challenges due to the severity of the disease and the complexities of managing it in children. Early diagnosis and treatment are crucial for improving outcomes and preventing long-term complications. Approximately 1.4 million children under 15 were living with HIV in 2023, and 120,000 new cases were reported, highlighting the ongoing impact of HIV on children worldwide.



Second-Line Antiretroviral Therapy for Children Living with HIV in Africa

Children living with human immunodeficiency virus (HIV) have limited options for second-line antiretroviral therapy (ART). In this open-label trial with a 2-by-4 factorial design, we randomly assigned children with HIV who had first-line treatment failure to receive **second-line therapy with tenofovir alafenamide fumarate (TAF)–emtricitabine** or **standard care (abacavir or zidovudine, plus lamivudine)** as the backbone and dolutegravir or ritonavir-boosted darunavir, atazanavir, or lopinavir as the anchor drug. The primary outcome was a viral load of less than 400 copies per milliliter at 96 weeks. We hypothesized that TAF–emtricitabine would be noninferior to standard care, that dolutegravir and ritonavir-boosted darunavir would each be superior to ritonavir-boosted lopinavir and atazanavir analyzed in combination, and that ritonavir-boosted atazanavir would be noninferior to ritonavir-boosted lopinavir. Safety was also assessed.



Globally, the number of children living with human immunodeficiency virus (HIV) who are receiving first-line antiretroviral therapy (ART) is increasing. This increase in access to ART, coupled with increased monitoring of HIV viral load, is in turn increasing the number of children in need of second- or subsequent-line ART after virologic failure. Most children with HIV live in Africa, where until recently first-line nonnucleoside reverse-transcriptase inhibitor (NNRTI)-based regimens were widely used. After the failure of first-line NNRTI-based ART, guidelines recommend an anchor drug from a new class (a ritonavir-boosted protease inhibitor or integrase inhibitor), plus a backbone of two nucleoside (or nucleotide) reverse-transcriptase inhibitors (NRTIs). Maximizing effectiveness and acceptability to patients while minimizing side effects is particularly important for children in need of lifelong ART. Which backbone and anchor drugs are safest and most effective for pediatric second-line ART remains unclear.

Participants

Participants were children with HIV who were 3 to 15 years of age, weighed at least 14 kg, were receiving first-line NNRTI-based ART, had treatment failure according to World Health Organization (WHO) criteria (a confirmed viral load of >1000 copies per milliliter after receiving counseling about adherence to the treatment regimen, or immunologic or clinical criteria for failure), and had a viral load above 400 copies per milliliter at the screening visit. Postmenarchal girls were required to have a pregnancy test with negative results.

Randomization and Procedures

Participants were randomly assigned to receive one of two backbone drug combinations — TAF-emtricitabine or standard care (abacavir-lamivudine or zidovudine-lamivudine, whichever was not used in first-line ART) — and were simultaneously randomly assigned to receive one of four anchor drugs (dolutegravir, ritonavir-boosted darunavir, ritonavir-boosted atazanavir, or ritonavir-boosted lopinavir).

Outcomes

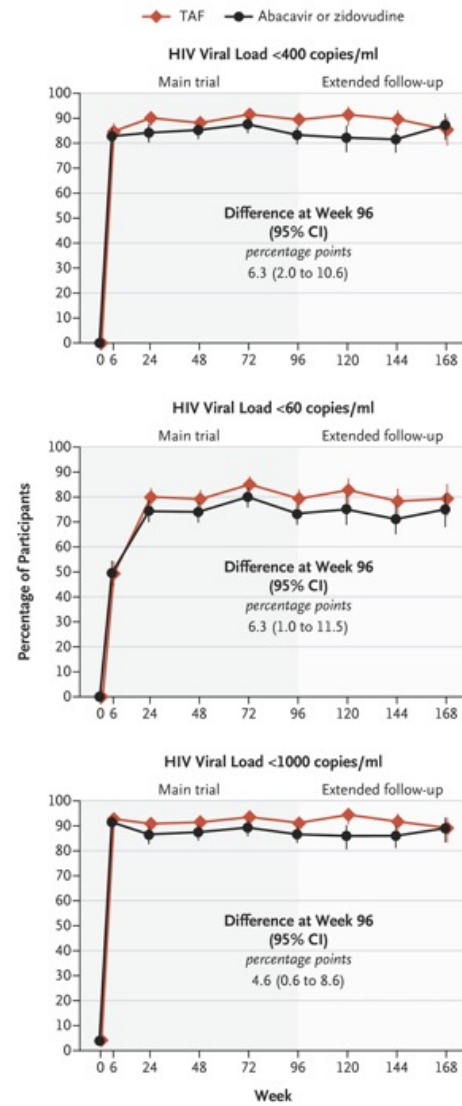
The primary outcome was a viral load of less than 400 copies per milliliter at 96 weeks; death before week 96 was considered to be treatment failure.

Grade 3 and 4 Adverse Events

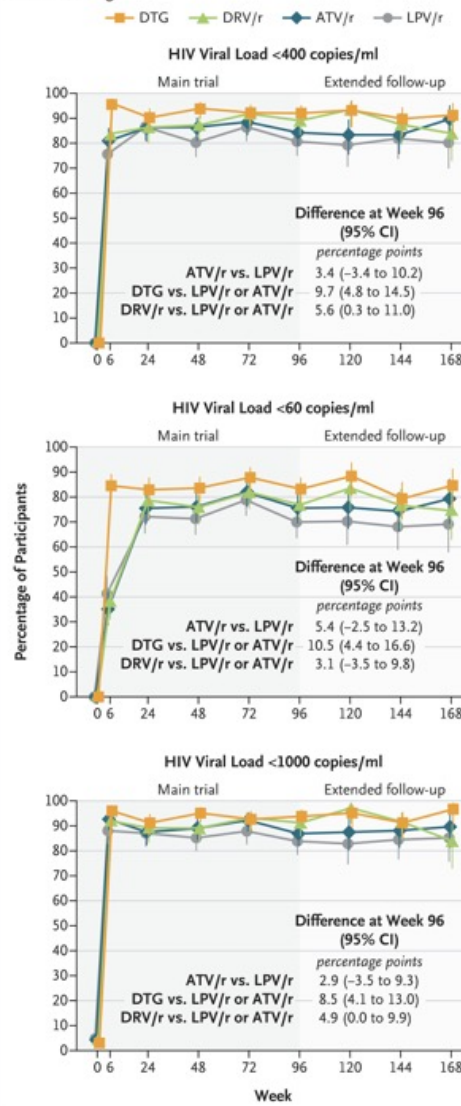
Characteristic	NRTI Backbone Randomization		Anchor Drug Randomization				All (N=919)
	Standard Care (N=461)	TAF (N=458)	Ritonavir-Boosted Lopinavir (N=227)	Ritonavir-Boosted Atazanavir (N=231)	Ritonavir-Boosted Darunavir (N=232)	Dolutegravir (N=229)	
Male sex — no. (%)	256 (55.5)	241 (52.6)	120 (52.9)	129 (55.8)	121 (52.2)	127 (55.5)	497 (54.1)
Age							
Median (IQR) — yr	10 (7–13)	10 (8–13)	10 (7–12)	10 (8–13)	10 (8–12)	11 (8–13)	10 (8–13)
Distribution — no. (%)							
3–4 yr	21 (4.6)	18 (3.9)	12 (5.3)	14 (6.1)	7 (3.0)	6 (2.6)	39 (4.2)
5–9 yr	178 (38.6)	180 (39.3)	95 (41.9)	83 (35.9)	96 (41.4)	84 (36.7)	358 (39.0)
10–15 yr	262 (56.8)	260 (56.8)	120 (52.9)	134 (58.0)	129 (55.6)	139 (60.7)	522 (56.8)
WHO clinical stage — no. (%)†							
1	244 (52.9)	239 (52.2)	114 (50.2)	121 (52.4)	130 (56.0)	118 (51.5)	483 (52.6)
2	140 (30.4)	154 (33.6)	79 (34.8)	74 (32.0)	65 (28.0)	76 (33.2)	294 (32.0)
3	63 (13.7)	50 (10.9)	30 (13.2)	29 (12.6)	27 (11.6)	27 (11.8)	113 (12.3)
4	14 (3.0)	15 (3.3)	4 (1.8)	7 (3.0)	10 (4.3)	8 (3.5)	29 (3.2)
Median CD4 cell count (IQR) — cells/mm ³ ‡	667 (405 to 963)	673 (434 to 982)	692 (432 to 1035)	685 (446 to 943)	685 (416 to 1000)	625 (349 to 891)	669 (413 to 971)
Median CD4 cell percentage (IQR)§	27.5 (19.0 to 35.4)	28.3 (20.3 to 37.0)	28.7 (19.2 to 36.0)	28.0 (20.5 to 35.2)	28.0 (19.4 to 37.1)	27.0 (18.0 to 36.0)	28.0 (19.2 to 36.0)
Median viral load (IQR) — copies/ml	17,909 (5,117 to 58,359)	17,265 (5,764 to 50,655)	16,885 (6,333 to 59,994)	16,784 (5,070 to 56,600)	16,875 (6,673 to 49,668)	15,409 (4,992 to 57,076)	17,573 (5,549 to 55,700)
Median weight (IQR) — kg	26.1 (20.2 to 33.5)	25.8 (21.0 to 32.8)	25.1 (20.0 to 33.4)	25.2 (20.3 to 32.1)	26.0 (21.0 to 32.3)	27.0 (21.3 to 34.0)	25.9 (20.5 to 33.1)
Median weight-for-age z score (IQR)¶	-1.6 (-2.4 to -0.9)	-1.6 (-2.4 to -0.9)	-1.5 (-2.3 to -0.8)	-1.6 (-2.5 to -0.9)	-1.7 (-2.4 to -0.9)	-1.6 (-2.5 to -0.9)	-1.6 (-2.4 to -0.9)
Median height (IQR) — cm	130.9 (118.0 to 142.5)	130.1 (120.7 to 141.6)	130.0 (118.2 to 142.0)	129.5 (119.0 to 140.8)	131.6 (118.7 to 142.3)	133.0 (120.6 to 143.5)	130.5 (119.4 to 142.0)
Median height-for-age z score (IQR)¶	-1.5 (-2.3 to -0.9)	-1.6 (-2.4 to -0.8)	-1.5 (-2.3 to -0.6)	-1.7 (-2.4 to -1.0)	-1.6 (-2.3 to -0.8)	-1.5 (-2.5 to -0.9)	-1.6 (-2.3 to -0.8)
Median BMI (IQR)‡	15.4 (14.4 to 16.5)	15.5 (14.3 to 16.8)	15.5 (14.4 to 16.8)	15.5 (14.3 to 16.7)	15.4 (14.1 to 16.5)	15.5 (14.5 to 16.8)	15.5 (14.3 to 16.7)
Median BMI-for-age z score (IQR)¶	-1.0 (-1.6 to -0.4)	-0.9 (-1.8 to -0.3)	-0.8 (-1.6 to -0.3)	-1.0 (-1.8 to -0.3)	-1.0 (-1.7 to -0.5)	-1.0 (-1.7 to -0.3)	-1.0 (-1.7 to -0.4)
Median duration of first-line ART (IQR) — yr	5.6 (3.2 to 7.8)	5.5 (3.3 to 7.7)	5.2 (3.2 to 7.5)	5.4 (3.0 to 7.6)	6.0 (3.3 to 7.8)	5.7 (3.5 to 8.1)	5.6 (3.3 to 7.8)
First-line NRTI — no. (%)							
Abacavir	244 (52.9)	246 (53.7)	121 (53.3)	124 (53.7)	123 (53.0)	122 (53.3)	490 (53.3)
Zidovudine	217 (47.1)	212 (46.3)	106 (46.7)	107 (46.3)	109 (47.0)	107 (46.7)	429 (46.7)
First-line NNRTI — no. (%)							
Efavirenz	247 (53.6)	267 (58.3)	131 (57.7)	128 (55.4)	124 (53.4)	131 (57.2)	514 (55.9)
Nevirapine	214 (46.4)	191 (41.7)	96 (42.3)	103 (44.6)	108 (46.6)	98 (42.8)	405 (44.1)
Assigned NRTI backbone therapy — no. (%)							
Standard care	461 (100)	0	115 (50.7)	115 (49.8)	114 (49.1)	117 (51.1)	461 (50.2)
TAF	0	458 (100)	112 (49.3)	116 (50.2)	118 (50.9)	112 (48.9)	458 (49.8)
Assigned anchor drug — no. (%)							
Ritonavir-boosted lopinavir	115 (24.9)	112 (24.5)	227 (100)	0	0	0	227 (24.7)
Ritonavir-boosted atazanavir	115 (24.9)	116 (25.3)	0	231 (100)	0	0	231 (25.1)
Ritonavir-boosted darunavir	114 (24.7)	118 (25.8)	0	0	232 (100)	0	232 (25.2)
Dolutegravir	117 (25.4)	112 (24.5)	0	0	0	229 (100)	229 (24.9)

Grade 3 or 4 adverse events	NRTI Backbone Randomization		Anchor Drug Randomization				All (N=919)
	Standard Care (N=461)	TAF (N=458)	Ritonavir-Boosted Lopinavir (N=227)	Ritonavir-Boosted Atazanavir (N=231)	Ritonavir-Boosted Darunavir (N=232)	Dolutegravir (N=229)	
Any grade 3 or 4 adverse event							
No. of participants (%)	64 (13.9)	63 (13.8)	26 (11.5)	69 (29.9)	20 (8.6)	12 (5.2)	127 (13.8)
No. of events	93	83	36	92	28	20	176
Elevated bilirubin							
No. of participants (%)	25 (5.4)	34 (7.4)	1 (0.4)	57 (24.7)	1 (0.4)	0	59 (6.4)
No. of events	32	36	1	66	1	0	68
Serious adverse events							
Any serious adverse event							
No. of participants (%)	14 (3.0)	15 (3.3)	10 (4.4)	5 (2.2)	8 (3.4)	6 (2.6)	29 (3.2)
No. of events	14	17	10	6	9	6	31
Death†							
No. of participants (%)	0	1 (0.2)	0	0	0	1 (0.4)	1 (0.1)
No. of events	0	1	0	0	0	1	1
Any life-threatening event							
No. of participants (%)	1 (0.2)	1 (0.2)	1 (0.4)	1 (0.4)	0	0	2 (0.2)
No. of events	1	2	1	2	0	0	3
Any event leading to or prolonging hospitalization							
No. of participants (%)	13 (2.8)	14 (3.1)	9 (4.0)	5 (2.2)	8 (3.4)	5 (2.2)	27 (2.9)
No. of events	13	16	9	6	9	5	29
Any important medical condition emerging during the trial‡							
No. of participants (%)	1 (0.2)	1 (0.2)	2 (0.9)	0	0	0	2 (0.2)
No. of events	1	1	2	0	0	0	2
Events leading to ART modification							
Any event leading to ART modification							
No. of participants (%)	13 (2.8)	11 (2.4)	7 (3.1)	5 (2.2)	5 (2.2)	7 (3.1)	24 (2.6)
No. of events	22	19	11	11	9	10	41
Psychiatric disorder							
No. of participants (%)	0	1 (0.2)	0	0	0	1 (0.4)	1 (0.1)
No. of events	0	1	0	0	0	1	1
Acute hepatitis							
No. of participants (%)	1 (0.2)	0	1 (0.4)	0	0	0	1 (0.1)
No. of events	1	0	1	0	0	0	1
Hypersensitivity reaction							
No. of participants (%)	2 (0.4)	0	2 (0.9)	0	0	0	2 (0.2)
No. of events	4	0	4	0	0	0	4
Tuberculosis							
No. of participants (%)	9 (2.0)	9 (2.0)	4 (1.8)	5 (2.2)	4 (1.7)	5 (2.2)	18 (2.0)
No. of events	16	17	6	11	8	8	33
Pregnancy							
No. of participants (%)	0	1 (0.2)	0	0	0	1 (0.4)	1 (0.1)
No. of events	0	1	0	0	0	1	1
Anemia							
No. of participants (%)	1 (0.2)	0	0	0	1 (0.4)	0	1 (0.1)
No. of events	1	0	0	0	1	0	1

A Backbone



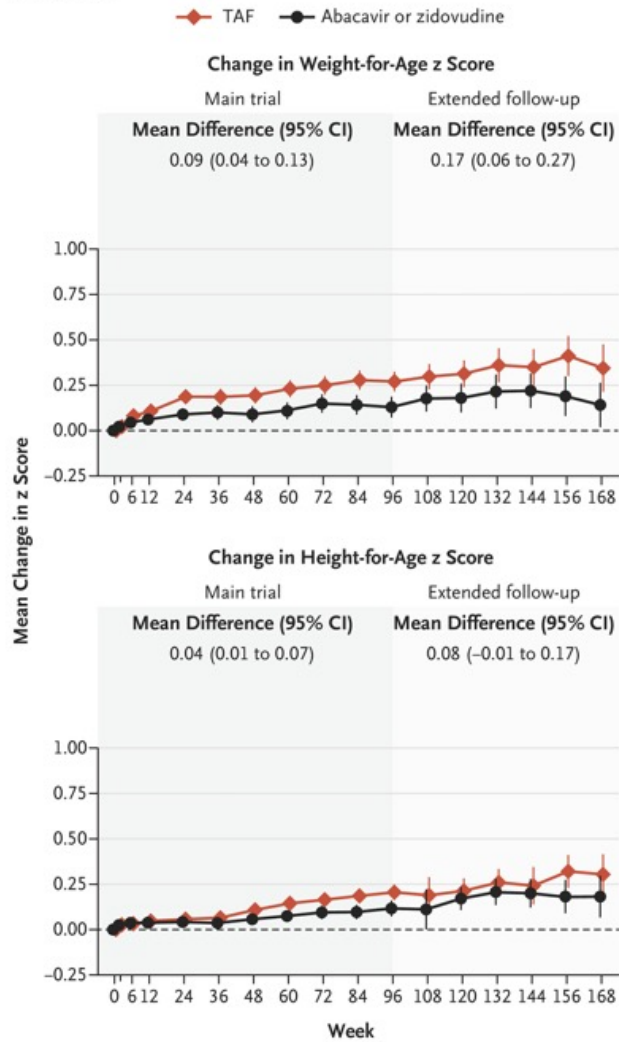
B Anchor Drug



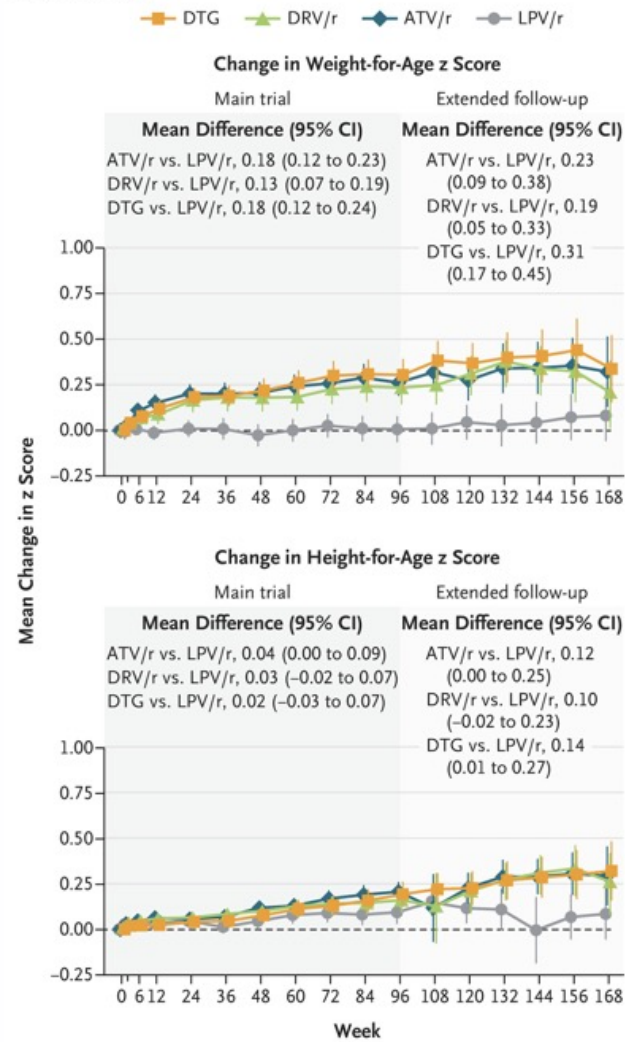
HIV Viral Load According to Assigned Treatment.

Shown are percentages of participants with a human immunodeficiency virus (HIV) viral load of less than 400 copies per milliliter, less than 60 copies per milliliter, and less than 1000 copies per milliliter over time during the main trial and during the extended follow-up period according to the assigned backbone (Panel A) or anchor drug (Panel B).

A Backbone

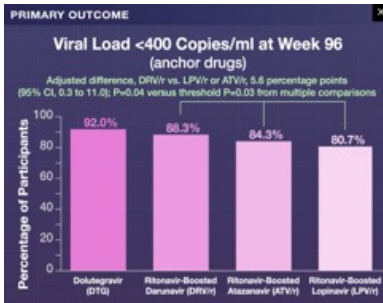
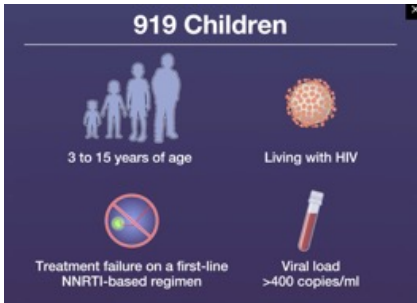
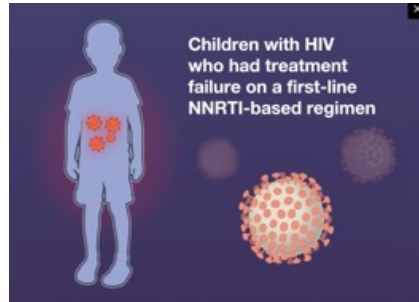
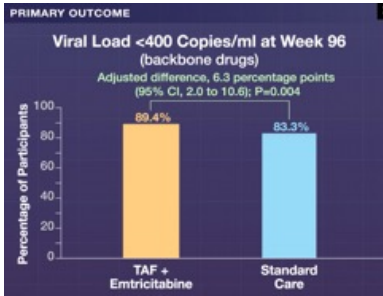
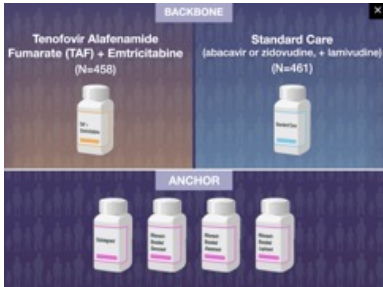
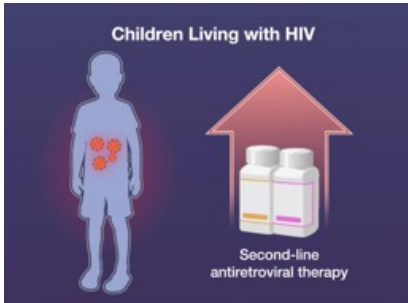


B Anchor Drug

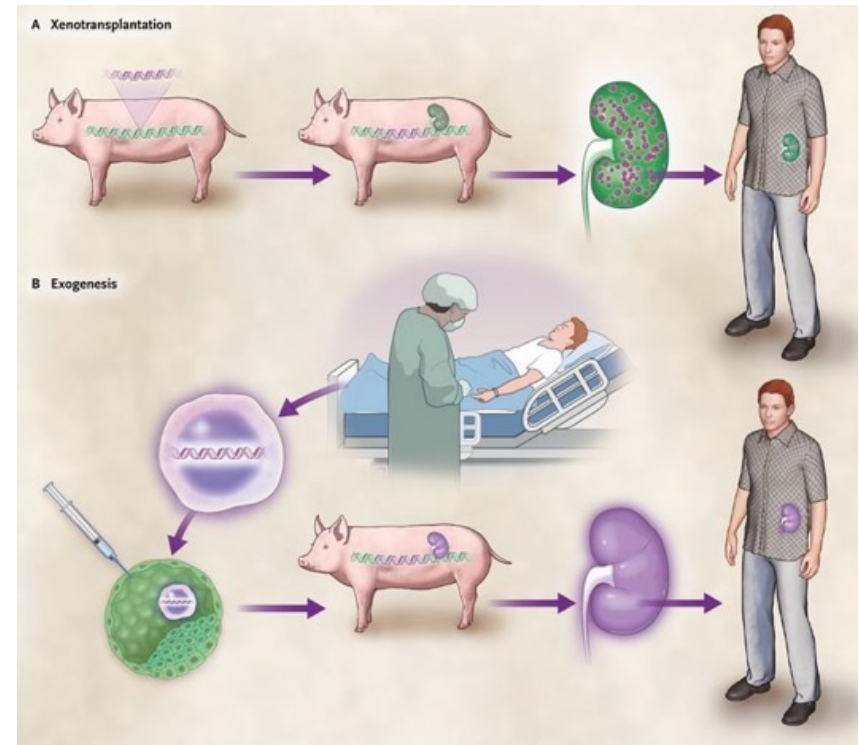
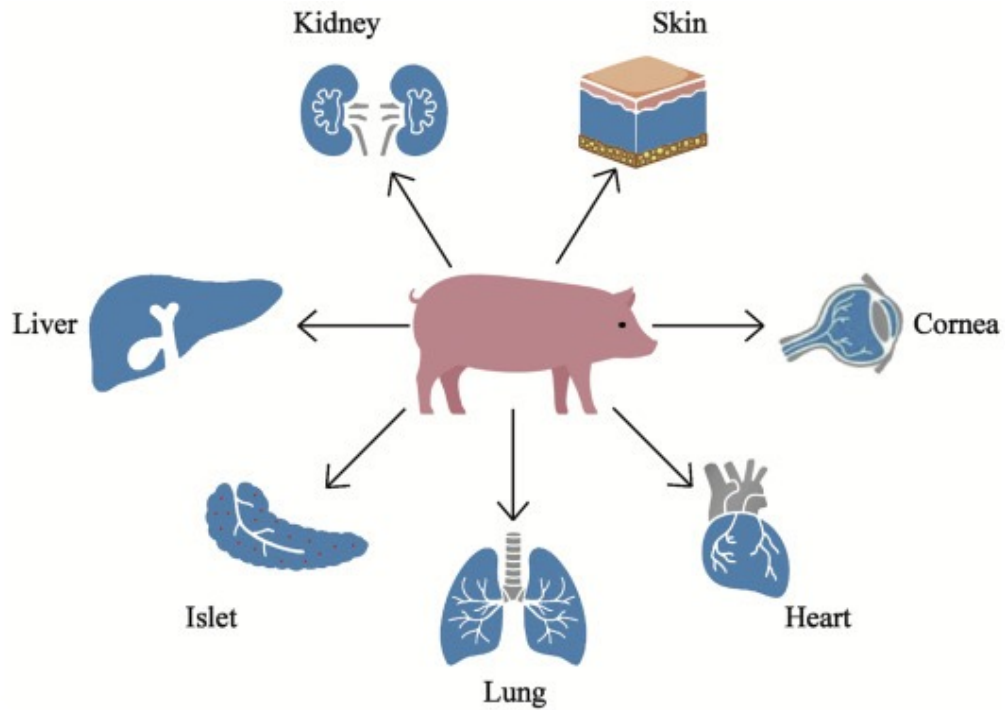


Changes in Weight-for-Age and Height-for-Age z Scores.

Changes are shown according to the assigned backbone (Panel A) or anchor drug (Panel B).



Kein Schwein ruft mich an!



Xenotransplantation of a Porcine Kidney for End-Stage Kidney Disease

Summary

Xenotransplantation offers a potential solution to the organ shortage crisis. A 62-year-old hemodialysis-dependent man with long-standing diabetes, advanced vasculopathy, and marked dialysis-access challenges received a gene-edited porcine kidney with 69 genomic edits, including deletion of three glycan antigens, inactivation of porcine endogenous retroviruses, and insertion of seven human transgenes. The xenograft functioned immediately. The patient's creatinine levels decreased promptly and progressively, and dialysis was no longer needed. After a T-cell-mediated rejection episode on day 8, intensified immunosuppression reversed rejection. Despite sustained kidney function, the patient died from unexpected, sudden cardiac causes on day 52; autopsy revealed severe coronary artery disease and ventricular scarring without evident xenograft rejection. (Funded by Massachusetts General Hospital and eGenesis.)

Methods

Pig Kidney Xenograft

A Yucatan miniature pig was engineered to carry 69 genomic edits, eliminating three major glycan antigens, overexpressing seven human transgenes (*TNFAIP3*, *HMOX1*, *CD47*, *CD46*, *CD55*, *THBD*, and *EPCR*), and inactivating porcine endogenous retroviruses.

Recipient Evaluation

The patient was a 62-year-old man with end-stage kidney disease caused by type 2 diabetes mellitus who had exhausted nearly all viable vascular access for dialysis. His history included myocardial infarction, severe vasculopathy, heart failure, total parathyroidectomy, and receipt of a deceased-donor kidney in 2018. After having graft failure in May 2023 associated with BK virus infection and recurrent diabetic nephropathy, he returned to receiving hemodialysis.

Table S2. Infectious disease surveillance post-transplantation.

Organisms	Assay	Time points			
PCMV	NAT	Weekly for 8 weeks	Monthly through Month 6	Months 9, 12, 15, 18, 24	
PLHV 1-3	NAT	Weekly for 4 weeks	Monthly through Month 6	Months 9, 12, 15, 18, 24	
PCV	NAT	Weekly for 4 weeks	Monthly through Month 6	Months 9, 12, 15, 18, 24	
PERV (A,B,C,AC)	NAT	Weekly for 4 weeks	Monthly through Month 6	Months 9, 12, 15, 18, 24	
Karius metagenomics	Nondirected DNA amplification	Weekly for 4 weeks	Monthly through Month 6	Months 9, 12, 15, 18, 24	
Cytomegalovirus (CMV)	PCR	Weekly for 8 weeks	Monthly through Month 6	Months 9, 12, 15, 18, 24	
Epstein-Barr virus (EBV)	PCR	Weekly for 8 weeks	Monthly through Month 6	Months 9, 12, 15, 18, 24	
BK polyomavirus	PCR	Weekly for 8 weeks	Monthly through Month 6	Months 9, 12, 15, 18, 24	

pCMV:porcine cytomegalovirus, PLHV: porcine lymphotropic virus, PCV: porcine circovirus, PERV: porcine endogenous retrovirus, NAT: nuclear acid test, PCR: polymerase chain reaction

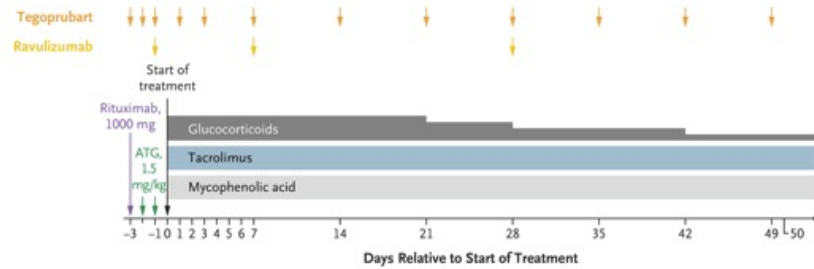
Xenograft Rejection Episode

On day 8, the patient's plasma creatinine level increased from 2.2 (day 7) to 2.9 mg per deciliter, accompanied by fever, allograft tenderness, and decreased urine output. An infectious disease workup was negative. Empirical therapy with glucocorticoid pulse (500 mg of methylprednisolone) and monoclonal antibody against interleukin-6 receptor (tocilizumab at a dose of 8 mg per kilogram of body weight) was initiated for suspected antibody-mediated rejection.

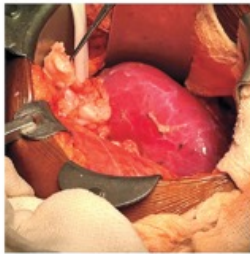
Table S3. Nanostring gene set of B-HOT panel and homology to pig's genes.

Gene	Note*	% Pig Homology	Gene	Note*	% Pig Homology	Gene	Note*	% Pig Homology	Gene	Note*	% Pig Homology	Gene	Note*	% Pig Homology	Gene	Note*	% Pig Homology			
ABCA1	95		CD47			EB3	87		IGHM			LAMP1			PNOC	93		ST8IA4	92	
ABCF1	90		CD7	87		EBV LMP2			IGKC			LAP3	87		POLR2A	HK	91	STAT3	94	
ABCF1	90		CD7A			EB1	96		IGLC1			LOC	93		POU2AF1			STAT4	95	
ABCF1	HK	93	CD7B			EBF14	92		KZP1			LCF2	92		PR3	HK	93	STAT5A	91	
ACTA2	92		CD38			EGPR	96		KZP2			LCR	96		PPP3CA	97		STAT6	92	
ACVR1	94		CD3E			EGP1	91		IL10	88		LEP1	96		PRDM1	93		STAT6	95	
ADAM4	89		CD3D			END3	93		IL10RA	92		LGAL3	90		PRP1	94		STAT6	95	
ADORA2A	89		CD3E			EMP3	92		IL10RB			LHX9	96		PROX1	91		TANK	90	
ADGR	92		CD3D	88		EMRE5	89		IL12A	87		LEBR1	91		PSEN1	95		TAP1	89	
ADG2	91		CD4			ERG	98		IL12B			LRB2	92		PSMB9	88		TAP2	86	
ADG3	89		CD48	88		ERKFF1	88		IL12RB1	80		LRBM	94		PSMB9	91		TAPBP	94	
ALAD1	91		CD48L2			EVH2	91		IL12RB2	88		LOC	89		PSMB9	89		TAP1	89	
ALG3	93		CD44	90		ED2	89		IL13	95		LAP2	91		P18E2	91		TBP	HK	94
ANKRD1	94		CD48RB			FASLG	88		IL17RA	90		L78	89		P27NP1	91		TE21	90	
ANKK1	88		CD48A			FCAR	93		IL17RB	83		L78R	90		PTGDR4	89		TCF7	95	
ADAM	86		CD48RB			FCER14			IL18RAP	90		LY96	91		PTGDR3	88		TCL1A	90	
ADP2	94		CD46	N Tg		FCER1G	96		IL18	84		MAP3K1	91		PTF2L	86		TEK	91	
AR20	96		CD47	N Tg		FCGR1A	90		IL1R1	85		MAPK11	90		PTF2L2	91		TFP3	86	
AR31	90		CD48			FCGR2A			IL1R2			MAPK12	91		PTF2L	96		TFRC	90	
AR32	94		CD5	90		FCGR2B			IL1RAP	88		MAPK13	93		PTF2L	91		TFPI1	91	
ATM	93		CD58			FCGR2BB			IL1	83		MAPK14	87		PTF2L	85		TFPI2	93	
AXL	91		CD58			FCRL3			IL21	85		MAPK3	90		PTF2L	92		TFPI3	88	
B2M	N Tg		CD59			FGD2	90		IL21R			MAPK8	94		PTX3	90		TFPI4	96	
B3GAT1	94		CD6			FOXP2			IL22	88		MAP3	89		RAF1	88		TFPI5	92	
BATF	87		CD68	82		FXY1	87		IL23A	91		MBP	88		RAO2	90		TFPI1	91	
BATF3	95		CD69			FKBP14	89		IL23R			MC9N	96		RARGP9	88		THSD7	N Tg	81
BAX	93		CD7			FLT3	89		IL27	89		MEF2C	94.1		RAD51	95		THSD1	92	
BCL2	100		CD79			PN1	87		IL27RA			MEK7C	92		REL	93		THSD2	93	
BCL2L1	92		CD72	84		FOXP1	91		IL2RA			MEK7	90		RELA	93		THSD3	85	
BCL3	85		CD74	86		FOXP3	96		IL2RB	85		MEP	95		RELB	90		THSD4	94	
BCL6	95		CD79A			FTK	88		IL2RG	85		MEK	92		ROX	89		TLR2	96	
BDNF	93		CD80			GAPD	HK	94	IL4			WMP12			RGS5	92		TLR4	90	
BK large T Ag			CD81			GAPDH	91		IL4R	83		WMP14	96		RNF149	91		TLR7		
BK VP1			CD82			GATA3			IL5			WMP9			ROSA	96		TM4SF1		
BLK	89		CD83			GMP2			IL6	88		MRG1	89		ROCC	95		TM4SF18	88	
BLANK	90		CD84			GMP4			IL6R	82		MS4A1	83		RPL19	91		TMEM77A	93	
BMP2	86.8		CD86			GMP6	92		IL6ST	89		MS4A2			RPS9	98		TNP		
BMP4	91		CD8A			GMS17			IL7	97		MS4A4	97		RPS48B1	98		TNFAIP3	N Tg	92
BMPER	95		CD8B			GMLY			IL7R			MS4A4	83		RTN4	95		TNFAIP6	91	
BMPR1A	90		CD96	81		G2MA			IL20A	93		MS4A7	83		RUNX1	94		TNFRSF14		
BMPR1B	90		CDKX1A	91		G2MB			IL20R2	88		MTOR	89		RORA	94		TNFRSF17	84	
BRWD1	99		CEACAM3			G2MH	82		IL20R3	92		MYB	98		SI10A12			TNFRSF18		
BT22	86		CMCHD19	94		G2MK			IL20R3	91		MYBL1	93		SI10A8			TNFRSF19		
BTX	97		CMUK	91		KAVCR2			IL21	92		MYC	89		SI10A9	83		TNFRSF24	85	
BTLA	CTED4					H2AC3	96		IL21R	92		MYDM	92		SI10F1	92		TNFRSF29	83	
C10A	94		GLEIC			H2AC9	92		IL22	97		MYL9	92		SI10H1	88		TNFRSF30	81	
C1QB	91		CMKL1	94		HDC	92		IL23	92		NCAB1	88		SELE	83		TNFRSF34	84	
C13orf1	92		GMV L1E3			HPE			ITGAA	80		NCR1	83		SELL	94		TNFRSF38		
C3	96		COL13A1	93		HLA-C			ITGAB	91		NPATC1	85		SEMA7A	93		TNFRSF4		
C3AR1	91		COL3A1	92		HLA-DRA	89		ITGAX	83		NPATC2	83		SERPINC5	95		TNFRSF6		
C9	86		COL4A1	92		HLA-DQB2	86		ITGB2	83		NPFB1	87		SERPINA3			TNFRSF9		
CASP2	86		COL4A3	92		HLA-E			JAK1	91		NPXB2	89		SERTAD1			TOX2	90	
CAV1	90		COL4A4	96		HLA-G			JAK2	91		NKX2	91		SFTR2			TFPI1	91	
CCL19			COL4A5	93		HMSBT	97		JAK3	92		NO22	90		SFTR8			TFPI2	90	
CCL21	87		CRI1			INP1A	94		JAK3	91		NO23	96		SFTR9			TFPI3	95	
CCL27	86		CSHBP	90		INP1T1	96		KDR	89		NO2YH1	87		SH2D4	85		TRAF1		
CCL4	87		CRP2	92		INS1B1	95		KIR_Activating_Subgroup_1			NO2YH2	91		SH2D6	90		TRDC		
CCR1	95		CSF1	93		NSP9AA1	90		KIR_Activating_Subgroup_2			NOX4	96		SHROOM3	88		TROV	81	
CCR2			CSF2RB			NSP412B	90		KIR_Inhibiting_Subgroup_1			NPDC1	87		SIORR			TROV2		
CCR3			CSF3R	84		JCOS			KIR_Inhibiting_Subgroup_2			NPFS1	89		SIOLCS3			TRIM1		
CCR4	87		CTLA4			JCOSL2	84		KIR3DL1			NPFS2	87		SIRPB			UMOD	88	
CCR5			CTNNA1	96		IF30	82		KIR3DL2			NRDE2	HK	90	SKI	90		VEGFA	88	
CCR6			CTSW	81		IFM6			KIT	91		NRX1	HK	93	SLA	96		VEGFB	91	
CD27	96		CD25R1	97		IFB			KITL	87		OSIP			SLAMF6			V5R	83	
CD44	83		CD44L1	90		IFNG			KLF2	91		P2RX4	87		SLAMF9			WNT3A	94	
CD160	83		CD44L2	88		IFNGR1			KLF4	91.2		PAD4	90		SLC11A1	90		XAF1	88	
CD183	90		CD483			IFNGR2			KLHL13	93		PAAR	82		SMAD2	92		XBP1	90	
CD19			CD484			JG1	94		KLRB1			POD1			SMAD4	96		XCL12	84	
CD19			CD485	84		JG1R			KLRG1			POD1L2			SMAD5	94		ZAP70	88	
CD2			CD486			JG1L1			KLRD1			POGFA			SOC3	91		ZEB1	88	
CD397	88		CD487	92		JG1H1			KLRP1	84		PP4			SOX7	90				
CD399			CD488	87		JG1H2			KLRP2			PKKX	88		SPH4	87				
CD32			CD487A	96		JG1H3	90		KLRK1	88		PKX3D	91		SPB					
CD24	92		CD487B	93		JG1H1	87		KRT19			PKX3D	92		SRC	93				
CD244			CD487C	92		JG1H4			LAG3	84		PLAT	89		ST3	87				

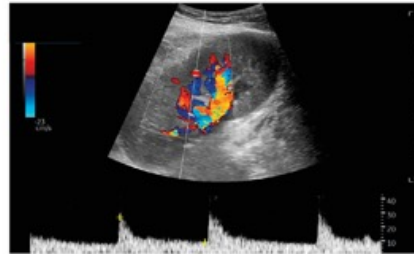
A Planned Immunosuppressive Regimen



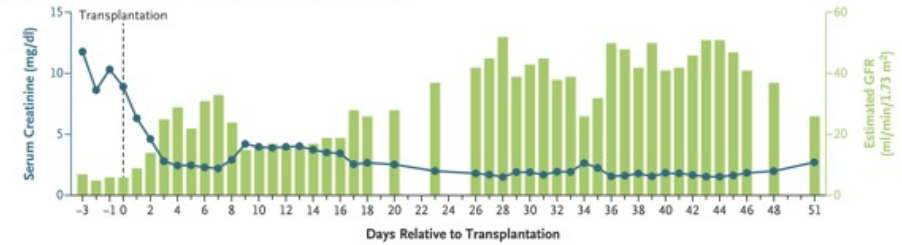
B Intraoperative View of Xenograft Immediately after Reperfusion



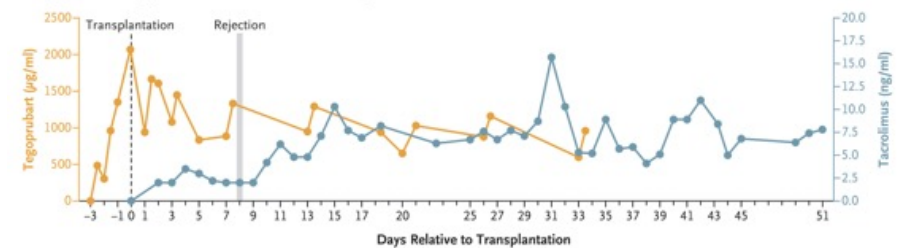
C Renal Ultrasound after Transplantation



D Plasma Creatinine and Estimated GFR Following Transplantation



E Drug Levels of Tegoprubart and Tacrolimus after Transplantation

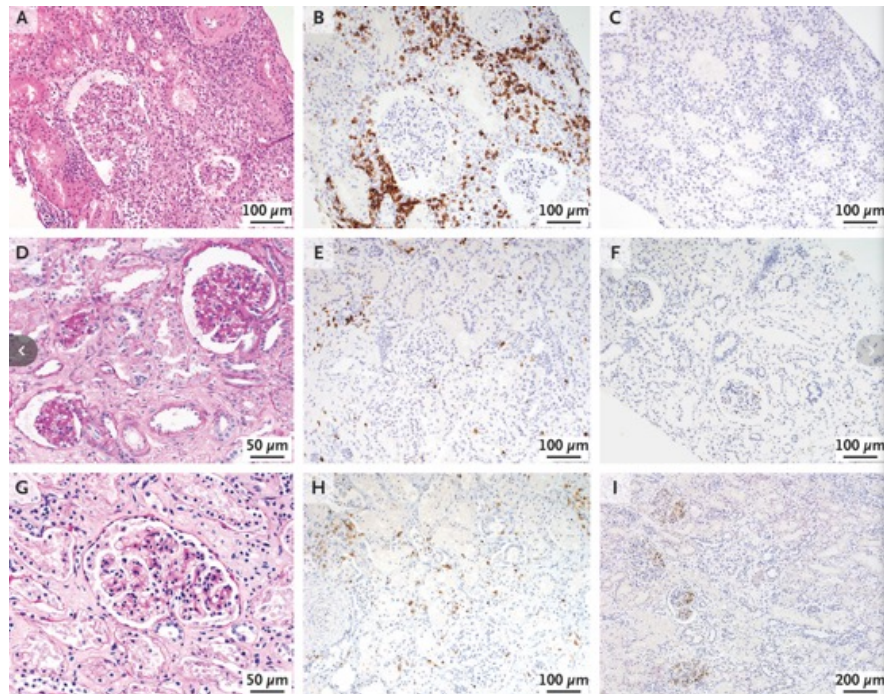


Immunosuppressive Regimen and Post-Transplantation Clinical Course.

Panel A shows the planned immunosuppressive regimen including antithymocyte globulin (ATG) (1.5 mg per kilogram of body weight on days -2 and -1), rituximab (anti-CD20 antibody) (1000 mg on day -3), Fc-modified anti-CD154 monoclonal antibody (**tegoprubart at a dose of 20 mg per kilogram** on days -3, -2, -1, 1, 3, 7, and then weekly), and anti-C5 antibody (ravulizumab at a dose of 3330 mg on days -1, 7, and 28) combined with a conventional immunosuppressive regimen of tacrolimus, mycophenolic acid (540 mg twice a day), and glucocorticoids (starting on day 0). As T cells were completely depleted from the circulation after the first dose and the patient had a severe reaction, the second dose of ATG was not administered. Panel B shows an intraoperative view of the xenograft immediately after reperfusion. Panel C shows a renal ultrasound performed after transplantation indicating excellent blood flow within the kidney xenograft with normal resistive index of 0.67. Panel D shows the plasma creatinine and estimated glomerular filtration rate (GFR) after transplantation.

Xenograft Rejection Episode

On day 8, the patient's plasma creatinine level increased from 2.2 (day 7) to 2.9 mg per deciliter, accompanied by fever, allograft tenderness, and decreased urine output. An infectious disease workup was negative. Empirical therapy with glucocorticoid pulse (500 mg of methylprednisolone) and monoclonal antibody against interleukin-6 receptor (tocilizumab at a dose of 8 mg per kilogram of body weight) was initiated for suspected antibody-mediated rejection. A pretreatment, same-day biopsy confirmed acute T-cell-mediated rejection, Banff grade 2A, without evidence of thrombotic microangiopathy or antibody-mediated rejection.



Pathological Analyses of Biopsy Samples Obtained from the Kidney Xenograft.

A biopsy sample obtained 8 days after transplantation shows a prominent, extensive mononuclear infiltrate in the cortex that was associated with tubulitis and focal endarteritis, which is typical of T-cell-mediated rejection (Panel A). Abundant CD3+ cells are seen in the interstitium and focally in an artery (Panel B), and staining for C4d is negative (Panel C). At 34 days, the sample shows normal arteries and glomeruli with mild interstitial fibrosis (Panel D). The CD3+ infiltrate is sparse and substantially reduced from the 8-day biopsy (Panel E), and the C4d stain is negative (Panel F). At 52 days after transplantation in a sample obtained on autopsy, the glomeruli are normal except for minimal glomerulitis (Panel G); sparse CD3+ cells are seen (Panel H), similar to the biopsy sample at 34 days. The C4d stain is segmentally present in glomerular capillaries and not detected in peritubular capillaries (Panel I). Analyses include hematoxylin and eosin staining (Panels A, D, and G) and immunohistochemical analyses of CD3 (Panels B, E, and H) and C4d (Panels C, F, and I).

Banff Scores on Xenograft Biopsy Samples.

Variable	Interstitial Inflammation	Tubulitis	Endarteritis	Glomerulitis	Peritubular Capillaritis	C4d Deposition in Peritubular Capillaries	Thrombotic Microangiopathy
Contralateral donor kidney not transplanted	0	0	0	0	0	0	None
Timing after transplantation							
5 minutes after reperfusion	0	0	0	0	0	0	None
Day 8	3	1	1	1	2	0	None
Day 34	0	1	0	0	0	0	None
Day 52 on autopsy	0	0	0	1	0	0	None

Cardiac Complication

The patient was also evaluated in the outpatient clinic on day 51 after transplantation. He reported low fluid intake, and the plasma creatinine level of 2.7 mg per deciliter was relatively elevated, despite tacrolimus trough levels within target range. He had no symptoms of congestive heart failure or worrisome findings on physical examination, and kidney ultrasonography showed no abnormalities. The overall presentation was similar to a previous episode of an elevated creatinine level on day 34, which had resolved with hydration. Intravenous magnesium (2 g) and a 500-ml bolus of normal saline were administered over a 30-minute period to address hypomagnesemia and presumed volume depletion. The patient's blood pressure, heart rate, and respiratory rate were all normal.

Later that evening, the patient had respiratory distress and rapidly became unresponsive. Despite resuscitative efforts, he died.

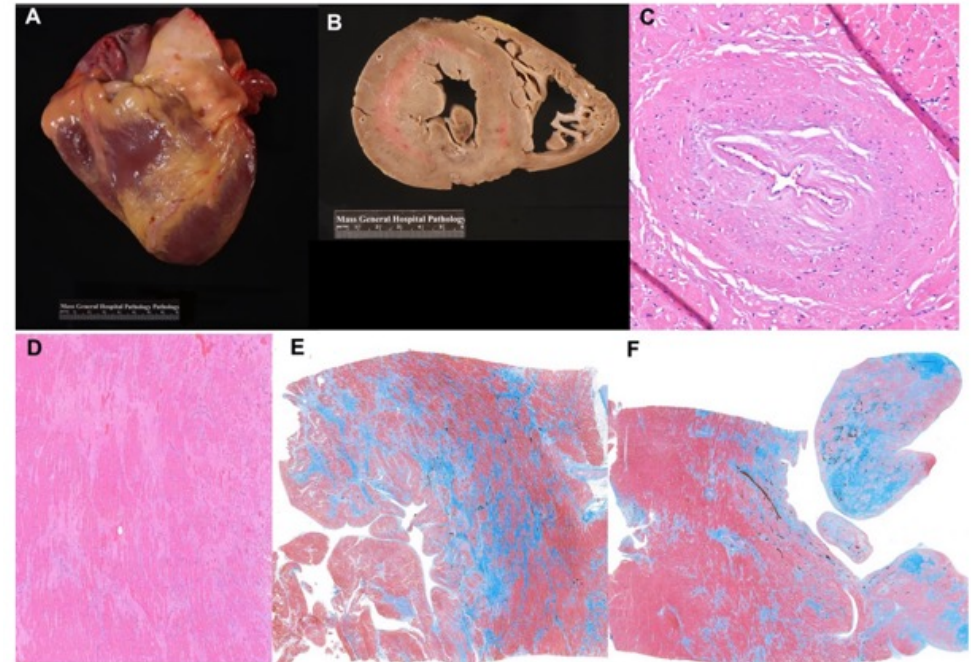
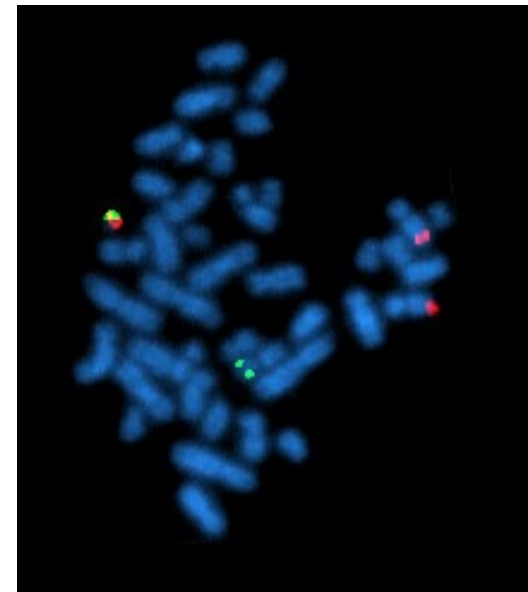
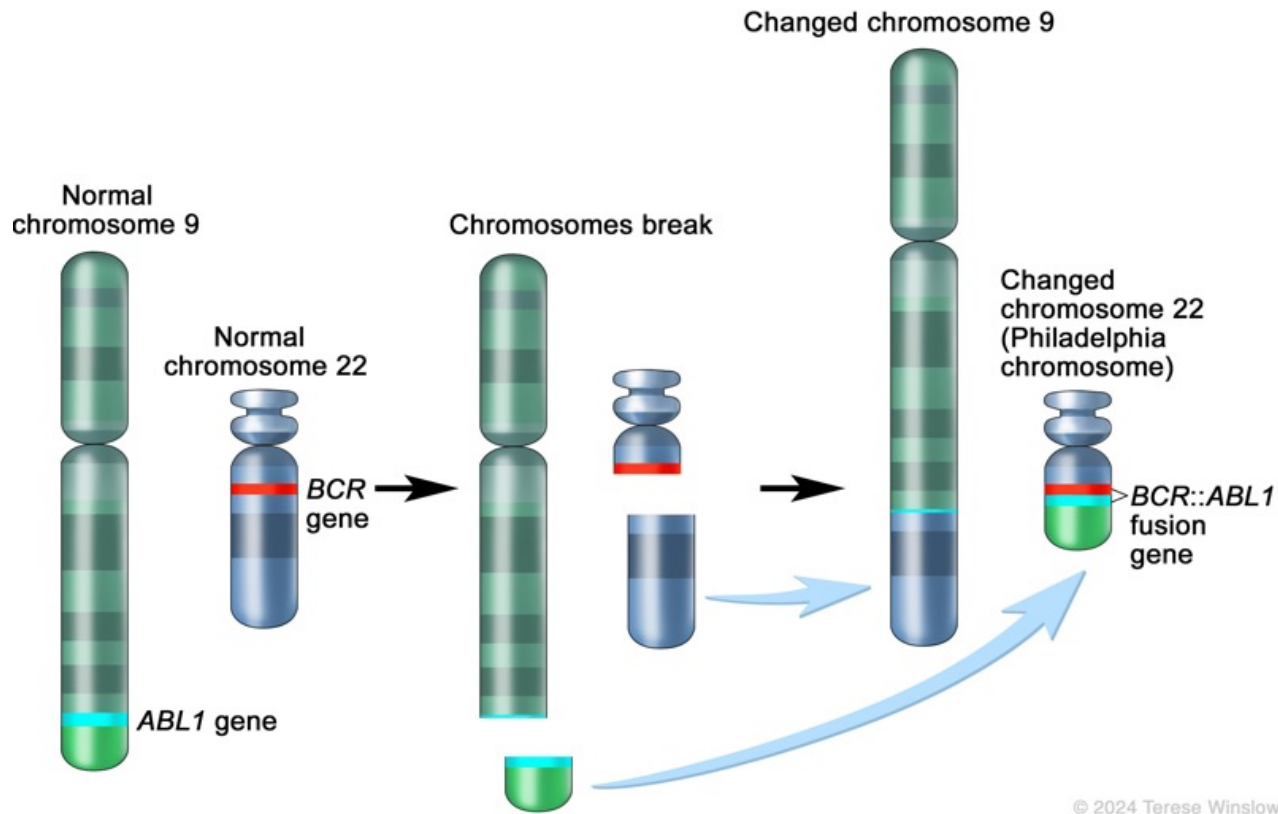


Figure S12. Heart autopsy findings. A, Anterior view of the heart weighing 725 grams, with the upper limit of normal for height being 536 grams. B, Mid-cross section of the heart. The left ventricle and septum exhibit uniform thickness of two inches, exceeding the upper normal limit of 1.5 inches. A pale, remote infarct is visible in the posterior septum, along with an infarct in the posterior papillary muscle. C, H&E staining of a hypertrophied intramyocardial artery. D, H&E staining of the septum is showing pale pink, and diffuse fibrosis. E, Trichrome staining of the lateral left ventricle showing diffuse fibrosis (blue). F, Trichrome staining of the posterior left ventricle showing diffuse fibrosis (blue) and old infarcted posterior papillary muscle (upper right, blue).

Discussion

This report documents the transplantation of a 3KO kidney xenograft with seven human transgenes into a patient with end-stage kidney disease, which built on our preclinical studies. Tegoprubart, an Fc-modified anti-CD154 monoclonal antibody in phase 2 trials for kidney allotransplantation, was part of the immunosuppressive regimen. This agent has shown potent inhibition of antibody production, as well as suppression of innate immune responses by blocking CD11b, another receptor of CD154. The pattern and timing of rejection in this patient suggested that early subtherapeutic levels of tacrolimus and mycophenolic acid may have contributed to the development of T-cell-mediated rejection, which was successfully treated with standard antirejection therapy. On biopsy, there was no evidence of antibody-mediated rejection, a common complication observed in the preclinical and decedent models of kidney xenotransplantation.

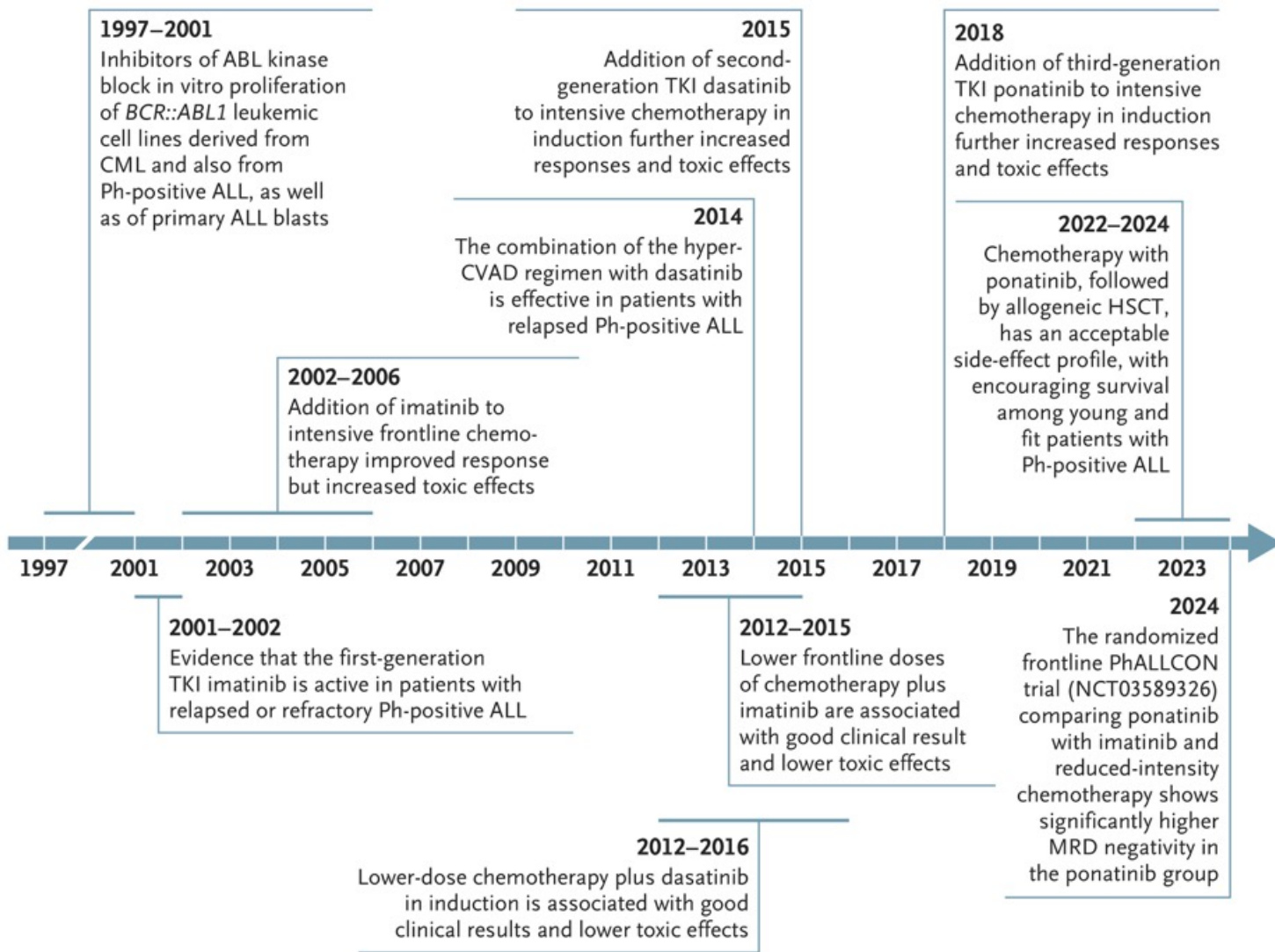
Despite the short observation period, this case demonstrated that a genetically modified kidney xenograft with human transgenes provided life-supporting kidney function in a living human patient. This outcome supports the feasibility of using genetically modified pig kidney xenografts to expand transplant access for patients with end-stage kidney disease. Although the identification of suitable candidates for kidney xenotransplantation is complex and debated, a small, pilot clinical trial for well-informed dialysis patients who face a high risk of dying while awaiting a human transplant may be a logical next step. Despite stable kidney function, our study patient who had undergone kidney xenotransplantation died from apparent sudden cardiac causes on day 52. The autopsy revealed severe coronary artery disease and ventricular scarring but no evidence of xenograft rejection.



Ph-Positive Acute Lymphoblastic Leukemia — 25 Years of Progress

Ph-Positive Acute Lymphoblastic Leukemia

- Philadelphia chromosome–positive acute lymphoblastic leukemia (Ph-positive ALL) is the most common genetic ALL subgroup in adulthood, with a prevalence that increases with age. In patients over the age of 50 years, Ph-positive disease accounts for about 50% of cases of B-lineage ALL.
- Before the advent of tyrosine kinase inhibitors (TKIs), Ph-positive ALL was the hematologic cancer with the worst outcome. Only the few patients who could undergo allogeneic stem-cell transplantation had a chance of long-term survival.
- Initially, TKIs were added to conventional intensive chemotherapy. Since this approach had notable toxic effects, reduced-intensity chemotherapy programs, plus TKIs, were used, an approach resulting in improved responses and outcomes, with fewer toxic effects.
- In the year 2000, the GIMEMA cooperative study group started using a TKI plus glucocorticoids for induction without systemic chemotherapy. First-, second-, and third-generation TKIs have been used over the years. These studies have shown the feasibility of this approach, with hematologic complete responses in 94 to 100% of adults, irrespective of age, and with limited toxic effects.
- The addition of the bispecific monoclonal antibody blinatumomab (an anti-CD19 and anti-CD3 antibody) in consolidation therapy has further improved molecular response and survival.
- As for all forms of ALL, a sustained molecular MRD negativity in the bone marrow should be the primary goal of frontline treatment.
- The combination of TKI (targeted treatment) and blinatumomab (immunotherapy) is associated with long-term survival of 75 to 80%, with many patients never receiving systemic chemotherapy or undergoing transplantation.

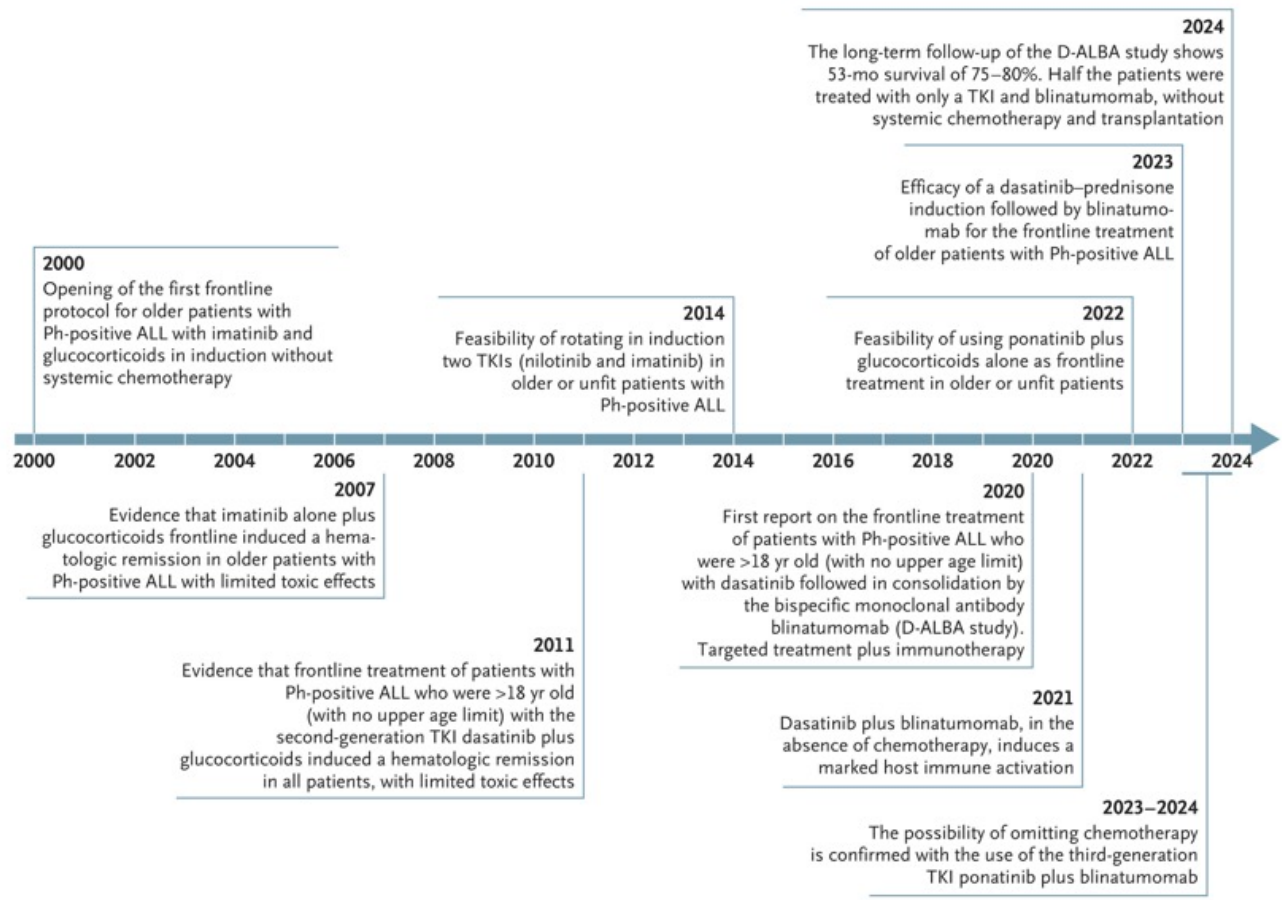


Timeline for Studies of Frontline TKIs plus Intensive or Lower-Dose Chemotherapy in Adults with Ph-Positive ALL, 1997–2024.^{10–12,15–29}

ALL denotes acute lymphoblastic leukemia; CML chronic myeloid leukemia; CVAD cyclophosphamide, vincristine sulfate, doxorubicin, dexamethasone, methotrexate, and cytarabine; HSCT hematopoietic stem-cell transplantation; TKI tyrosine kinase inhibitor; MRD minimal or measurable residual disease; and Ph Philadelphia chromosome.

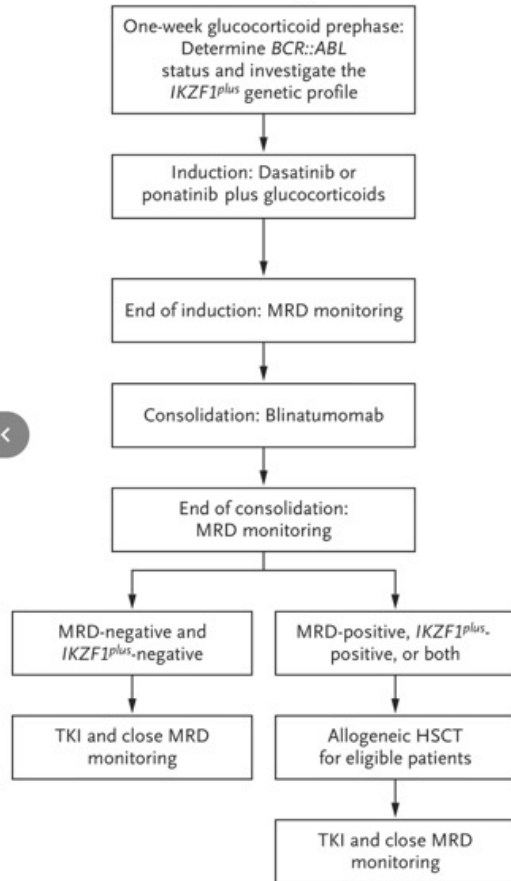
The GIMEMA Frontline Strategy without Chemotherapy from 2000 to 2025 in Patients with Ph-Positive ALL.

Study Protocol	Age <i>yr</i>	Induction Therapy	Complete Remission <i>% of patients</i>
LAL0201-B ³⁰	>60	Imatinib	100
LAL1205 ³¹	>18	Dasatinib	100
LAL0904, 3rd amendment ²⁰	16–60	Imatinib followed by chemotherapy (with or without HSCT)	96
LAL1408 ³²	>60 or unfit	Nilotinib and imatinib	94
LAL1509 ³³	18–60	Dasatinib and total therapy†	97
LAL1811 ³⁴	>60 or unfit	Ponatinib	95
LAL2116 ^{35,36}	>18	Dasatinib plus blinatumomab	98
ALL2820 ^{37,38}	>18	Ponatinib plus blinatumomab	95

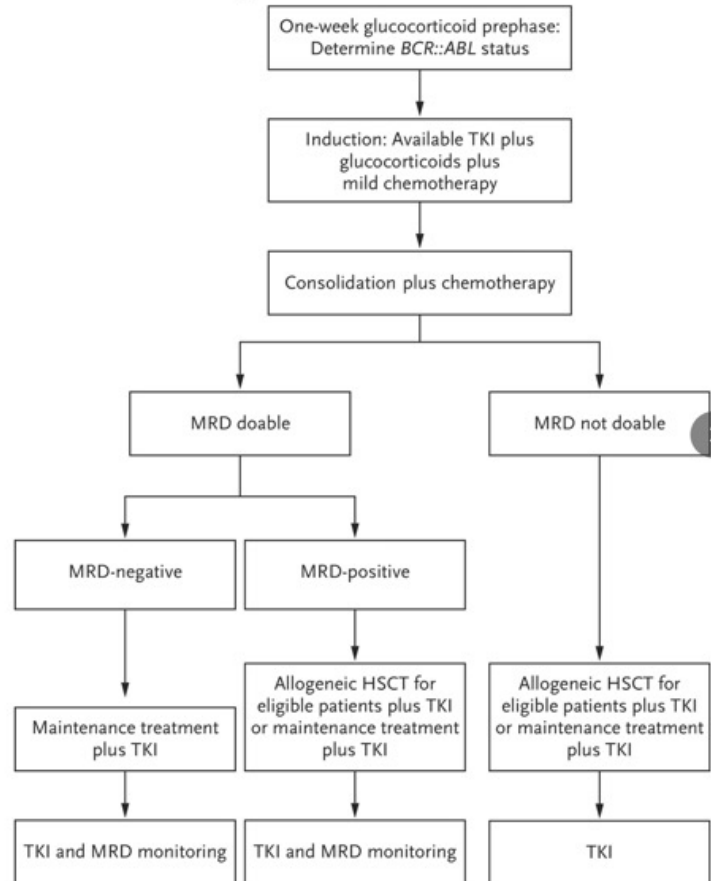


Timeline for Studies of Induction and Consolidation Treatment without Systemic Chemotherapy in Adults with Ph-Positive ALL, 2000–2024. [30–38,60,62,63](#)

A Recommended Frontline Strategy



B Real-Life Frontline Strategy



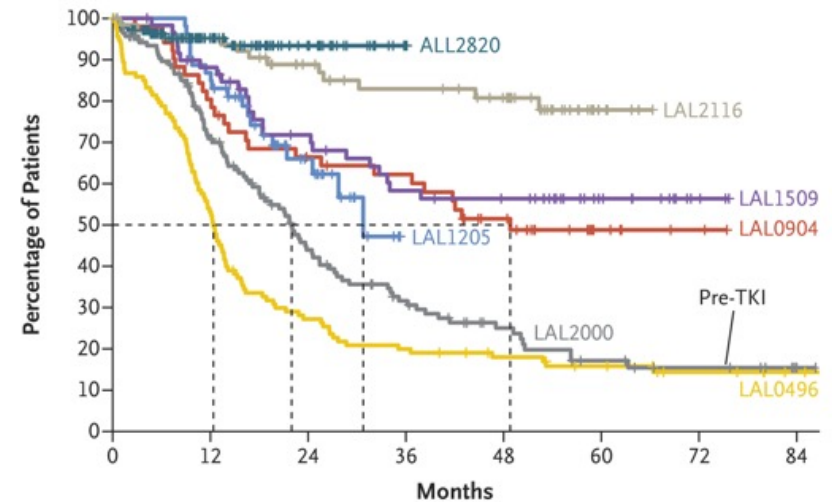
Recommended and Real-Life Strategies for Frontline Treatment in Adults of All Ages with Ph-Positive ALL.

Panel A shows the frontline strategy that is recommended when all the required components of frontline treatment are available. Panel B shows the strategy in real-life scenarios when one or more of the components of the recommended strategy are not available.

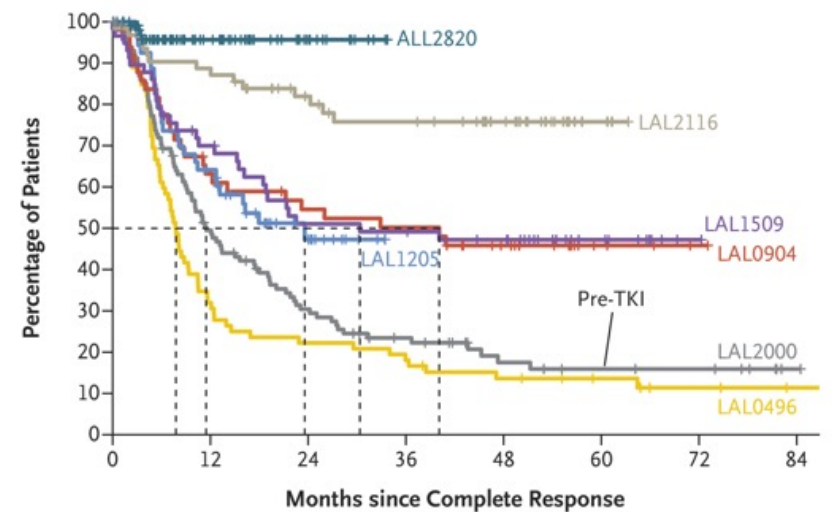
Conclusions

In the year 2000, a TKI without chemotherapy was introduced for the frontline treatment of older adults with Ph-positive ALL, which gave rise to a new era in the management of this disease. If every piece of the puzzle is in place — early diagnosis, TKI and blinatumomab availability, and MRD monitoring — today, 25 years later, we can expect to cure most adults with Ph-positive ALL, irrespective of age. Efforts to do so should ensure that all these components are widely available, including availability in middle- and low-income countries. A subcutaneous formulation of blinatumomab is under active investigation, with very encouraging early results. We can thus expect that soon most patients with Ph-positive ALL will be treated with an oral TKI plus subcutaneous blinatumomab. These past 25 years have witnessed a true revolution in the management and outcome of what used to be the most lethal hematologic cancer, as illustrated by the increases in overall and disease-free survival shown.

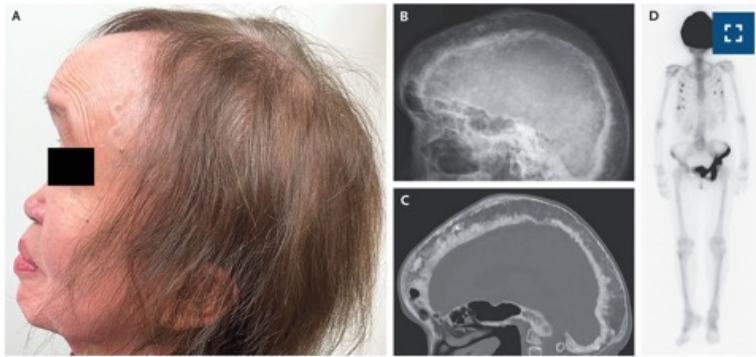
A Overall Survival



B Disease-free Survival

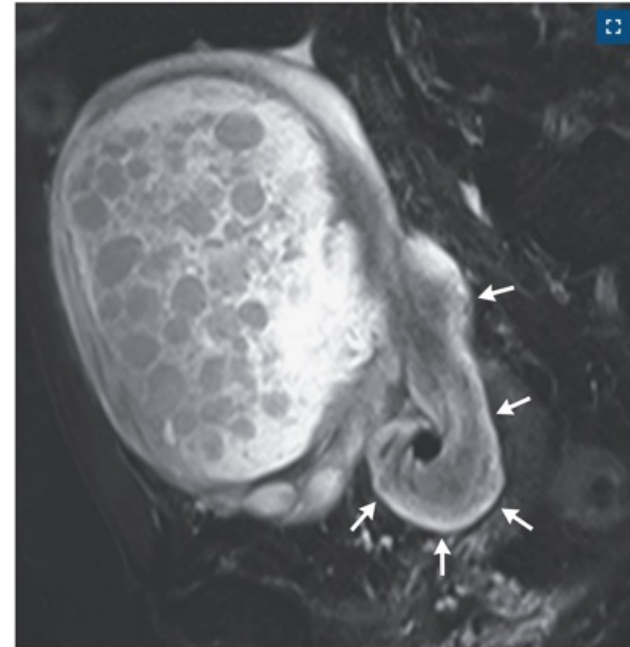


Paget's Disease of Bone



An 80-year-old woman presented to the endocrinology clinic with a several-year history of gradual forehead enlargement and progressive hearing loss. She reported no headache or bone pain. Sixteen years earlier, mild thickening of the skull had been noted on imaging studies that had been conducted to evaluate early-stage breast cancer, which was successfully treated. However, the patient had not followed up on the incidental radiographic finding as recommended. At the current presentation, physical examination was notable for frontal bossing (Panel A). The alkaline phosphatase level was 592 IU per liter (reference range, 38 to 113). A radiograph of the skull showed marked thickening of the calvarium with irregular patches of sclerosis and lucency, resulting in a cotton-wool appearance (Panel B). Whole-body computed tomography showed no evidence of cancer but did reveal severe cortical thickening, sclerosis, and focal osteolysis of the skull (Panel C). Audiometry confirmed sensorineural hearing loss. A radionuclide bone scan revealed increased uptake in the skull and the left side of the pelvis (Panel D). A diagnosis of Paget's disease of bone was made. Treatment with a bisphosphonate was initiated. At a 3-month follow-up visit, the alkaline phosphatase level had decreased, but the hearing loss and frontal bossing remained unchanged.

Torsion of a Mature Cystic Ovarian Teratoma



A 59-year-old woman presented with a 1-day history of sudden-onset, sharp pain in her left lower abdomen. Physical examination was notable for tenderness to palpation and a firm, nonmobile mass in the left lower quadrant. On pelvic examination, there was cervical motion tenderness. Although ultrasonography is the ideal imaging method for assessment of adnexal masses, magnetic resonance imaging of the abdomen and pelvis was performed in this case. A cystic mass measuring 11.9 cm by 9.0 cm by 12.5 cm was seen in the left adnexa (T2-weighted, fat-saturated sequence; sagittal view). Multiple free-floating, hypointenuating nodules were seen within the mass. This finding — known as the sack-of-marbles sign — represents globules of sebum or fat within a cystic lesion. There was also twisting of the ovarian pedicle — a finding known as the whirlpool sign — indicating ovarian torsion (arrows). A diagnosis of torsion of a mature cystic ovarian teratoma was confirmed during a laparotomy in which the cyst, left ovary, and left fallopian tube were removed. Sebaceous material, fat, and hair were found when the resected cyst was incised. Histopathological findings were consistent with a mature cystic teratoma with extensive hemorrhagic necrosis. The patient recovered well and had no recurrence over 10 years of follow-up.

Case 14-2025: A 29-Year-Old Woman with Peritonsillar Swelling and Bleeding

A 29-year-old woman was admitted to this hospital because of sore throat and peritonsillar swelling and bleeding. The patient had been well until 7 weeks before the current admission, when sore throat developed. When the soreness did not abate after 1 week, she sought evaluation at a primary care clinic of another hospital. Screening tests of a nasopharyngeal swab for severe acute respiratory syndrome coronavirus 2 RNA and streptococcal antigen were negative. The patient was instructed to rest and drink fluids.

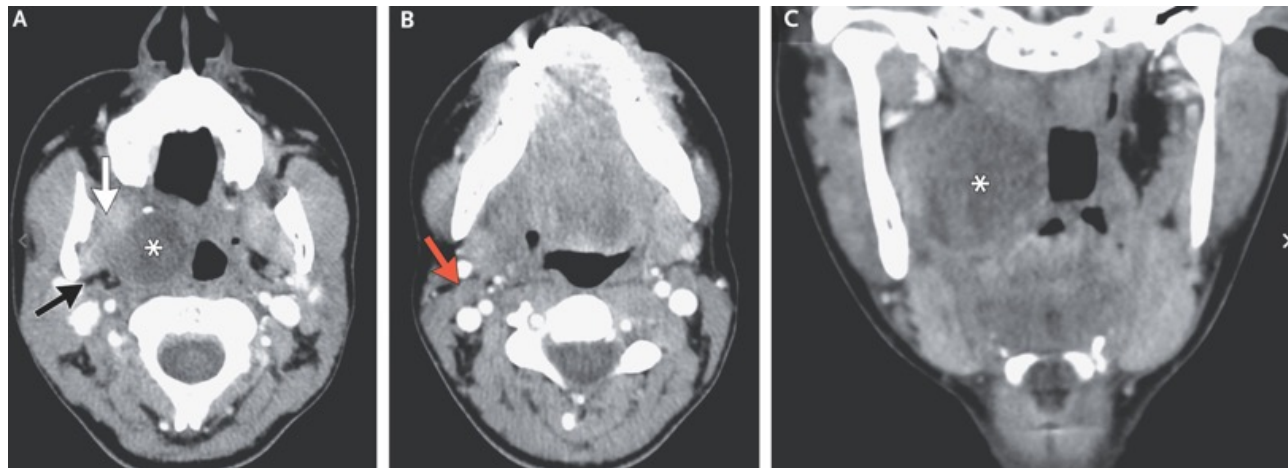
During the next 4 days, the throat soreness increased in severity to the point that the patient was unable to sleep through the night. She returned to the primary care clinic, and azithromycin was prescribed. During the subsequent 5 days, she took the prescribed antibiotic, but the throat soreness did not abate. She called the primary care clinic and was instructed to go to the emergency department of the other hospital.

On evaluation in the emergency department, 31 days before the current admission, the patient described pain and swelling on the right side of the throat and noted that when she swallowed food, it felt as though the food became “stuck.” She reported fatigue but no fever, headache, shortness of breath, cough, nausea, vomiting, abdominal pain, diarrhea, or rash.

On examination, the temporal temperature was 36.9°C, the blood pressure 105/77 mm Hg, the heart rate 74 beats per minute, and the oxygen saturation 99% while the patient was breathing ambient air. She appeared well and had a normal voice without hoarseness or stridor. The mucous membranes were moist. Edema and fluctuance were seen in the right peritonsillar area of the soft palate. The right tonsil had no erythema, swelling, or exudate. The uvula deviated to the left. No trismus was noted. The lungs were clear on auscultation. There was no palpable lymphadenopathy and no rash. The white-cell count was 6700 per microliter (reference range, 4000 to 11,000). Other laboratory test results are shown.

Variable	Reference Range, Other Hospital	On Initial Presentation, Other Hospital	Reference Range, Adults, This Hospital*	On Admission, This Hospital
White-cell count (per μl)	4000–11,000	6700	4500–11,000	13,470
Differential count (per μl)				
Neutrophils	1600–8300	4400	1800–7700	8970
Lymphocytes	600–5900	1800	1000–4800	2750
Monocytes	200–1400	500	200–1200	1420
Eosinophils	0–800	0	0–900	200
Basophils	0–100	0	0–300	70
Hemoglobin (g/dl)	11.2–15.7	13.9	12.0–16.0	15.1
Hematocrit (%)	34.1–44.9	41.5	36.0–46.0	44.9
Platelet count (per μl)	150,000–400,000	261,000	150,000–400,000	339,000
Prothrombin time (sec)	—	—	11.5–14.5	12.5
Prothrombin-time international normalized ratio	—	—	0.9–1.1	0.9
Activated partial-thromboplastin time (sec)	—	—	22.0–36.0	28.5

Computed tomography (CT) of the neck, performed after the intravenous administration of contrast material, revealed a hypodense lesion in the right peritonsillar region of the oropharynx that measured 2.6 cm by 2.1 cm by 3.8 cm. There was minimal peripheral enhancement. The presence of the lesion resulted in mild effacement of the oropharynx. Minimal fat stranding was present in the right parapharyngeal fat. No edema was noted in the right medial pterygoid muscle. A right jugulodigastric lymph node had a normal appearance. The patient was discharged home with a prescription for amoxicillin–clavulanate and was advised to schedule a follow-up visit at the otolaryngology clinic of the other hospital. Twenty-six days before the current admission, the patient was evaluated at the otolaryngology clinic of the other hospital. The right peritonsillar lesion was incised, and 3 ml of sanguineous fluid was drained. The next day, the patient returned to the otolaryngology clinic because of increased pain and swelling on the right side of the throat and bleeding from the incision site.



Initial CT Scans of the Neck.

Contrast-enhanced CT of the neck was performed on initial presentation to the other hospital. Axial (Panels A and B) and coronal (Panel C) images at the level of the oropharynx show a hypodense lesion (Panels A and C, asterisks) with no substantial rim enhancement centered in the right peritonsillar region of the oropharynx. The presence of the mass has resulted in mild effacement of the oropharynx. There is minimal, if any, fat stranding in the right parapharyngeal fat (Panel A, black arrow). The right medial pterygoid muscle (Panel A, white arrow) and right jugulodigastric lymph node (Panel B, red arrow) have a normal appearance.

On examination, the right peritonsillar area was more edematous than it had been the previous day, and ecchymosis, friable mucosa, and some necrotic granulation tissue were noted. The incision site was partially open with oozing of bloody fluid. A repeat drainage of fluid at this site was attempted, and a hematoma was evacuated with suction. Bleeding was treated with silver nitrate and oxidized regenerated cellulose; however, oozing at the site continued. The patient was taken to the operating room urgently.

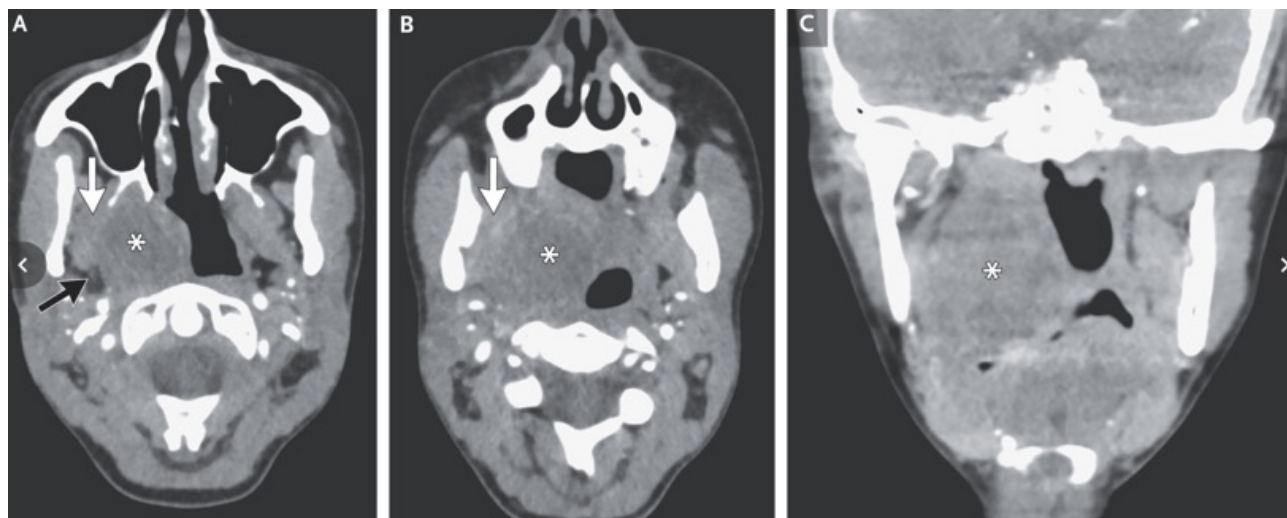
On examination while the patient was under anesthesia, there was oozing of bloody fluid from multiple sites in the right peritonsillar area. Oxymetazoline-soaked gauze and a human gelatin–thrombin matrix sealant were used to achieve hemostasis. The patient was admitted to the other hospital. Dexamethasone and ampicillin–sulbactam were administered, and an infusion of lactated Ringer’s solution was initiated. On the second hospital day, after confirmation that bleeding had stopped, she was discharged home with instructions to resume treatment with amoxicillin–clavulanate and to take acetaminophen and oxycodone as needed for pain.

During the next 2 weeks, the pain and swelling on the right side of the throat decreased. However, 8 days before the current admission, the patient noticed that her voice sounded “froggy.” She returned to the otolaryngology clinic of the other hospital, and treatment with clindamycin and methylprednisolone was started. During the subsequent 4 days, the patient noticed intermittent bleeding on the right side of the throat. She was referred to the otolaryngology clinic of a second hospital. Four days before the current admission, aspiration of the swollen area of the right peritonsillar region reportedly yielded dark blood.

On the morning of the current admission, the patient awoke with increased pain and swelling on the right side of the throat. Several hours later, she felt a “pop” and noticed bleeding on the right side of the throat. She presented to the otolaryngology clinic of the second hospital, where she received oral vitamin K and aminocaproic acid. She was advised to seek evaluation in the emergency department of this hospital.

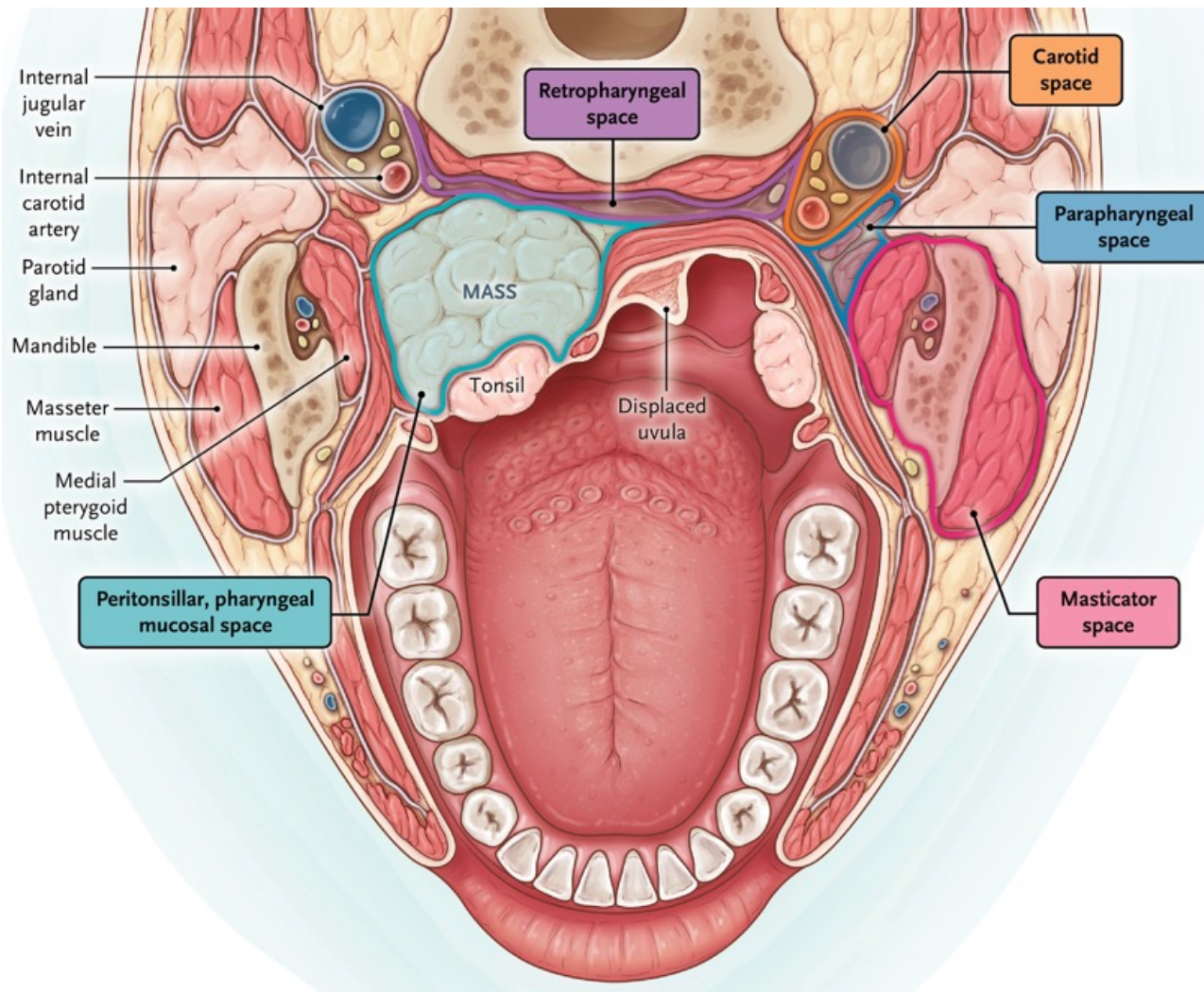
CT angiography of the neck, performed after the intravenous administration of contrast material, revealed that the size of the hypodense right peritonsillar lesion had increased to 3.4 cm by 3.6 cm by 4.6 cm, with mildly complex attenuation. The lesion involved the soft palate and extended into the submucosal nasopharynx. Minimal rim enhancement and mild fat stranding in the right parapharyngeal fat were unchanged from the previous imaging study. The lesion was inseparable from the right medial pterygoid muscle, which was not enlarged or edematous. No extravasation of contrast material was seen.

Treatment with ampicillin–sulbactam was started. Vitamin K and aminocaproic acid therapy were stopped. Intravenous hydromorphone, acetaminophen, and ondansetron were administered. The patient was admitted to the surgical intensive care unit.



CT Angiogram of the Neck Obtained 1 Month after Initial Presentation.

Contrast-enhanced CT angiography of the neck was performed 1 month after the patient's initial presentation to the first hospital. Axial (Panels A and B) and coronal (Panel C) images show enlargement of the right peritonsillar lesion (asterisks), which now extends above the soft palate and into the submucosal nasopharynx. Although the lesion is inseparable from the right medial pterygoid muscle, no enlargement or edema is present within the muscle (Panels A and B, white arrows). Minimal fat stranding is seen in the right parapharyngeal fat (Panel A, black arrow).



Deep Neck Spaces and Their Associated Tissues.

Shown is the location of the patient's mass (approximately 4 cm in diameter) in the right peritonsillar, pharyngeal mucosal space with medial displacement of the palatine tonsil. The mass does not invade the pterygoid muscles in the masticator space. The parapharyngeal fat is displaced posterolaterally, without fat stranding that would have suggested inflammation. The neurovascular structures within the carotid space are intact and displaced posteriorly. There is no extension into the retropharyngeal space.

Peritonsillar Abscess

This patient initially presented for a consultation with an otolaryngologist after a 3-week history of pain on the right side of the throat, dysphagia, peritonsillar edema, and identification of a 3.8-cm hypodense lesion within the peritonsillar space on CT.

Benign Neoplasm

At this point, a neoplastic process rises to the top of the differential diagnosis. A number of benign neoplasms (papillomas, fibromas, muscle and connective-tissue tumors, vascular tumors, and salivary-gland tumors) are related to the tissue types located in the peritonsillar and pharyngeal mucosal spaces of the oropharynx.

Malignant Neoplasm

Malignant neoplasms that warrant consideration in this patient are squamous-cell carcinoma, lymphoma, salivary-gland cancer, and sarcoma.

Squamous-Cell Carcinoma

Squamous-cell carcinoma is the most common cancer that involves the tonsils. Although squamous-cell carcinoma of the tonsils has historically been caused primarily by tobacco-related and alcohol-related carcinogenesis, it is now more commonly associated with human papillomavirus types 16 and 18.

Lymphoma

When a rapidly growing tonsillar mass is encountered in a young patient, it is important to consider lymphoma. Extranodal non-Hodgkin's lymphoma of the head and neck region usually develops within the lymphoid tissues of Waldeyer's ring; the palatine tonsils are the most common site of involvement.

Salivary-Gland Cancer

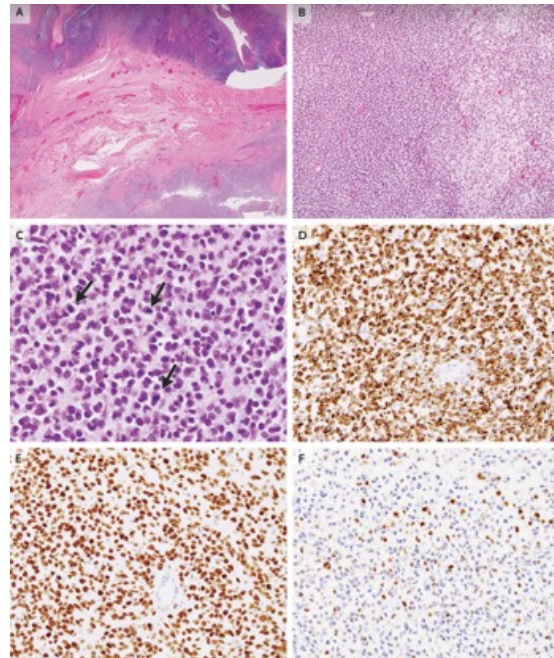
Minor salivary-gland cancers, which account for less than 3% of head and neck cancers, may develop within the soft tissues surrounding the tonsils and inside the soft palate.³ Low-grade tumors may lack the clinical and radiographic evidence of local invasion and lymphadenopathy, as in this patient, but would also have a slow rate of growth

Sarcoma

Sarcomas are rare tumors that may arise from the musculoskeletal and connective tissues of the neck. Nearly 200 different subtypes have been reported in adults. These tumors may appear as a painless mass without lymph-node involvement. When I evaluated this patient, I thought that the most likely diagnosis was a malignant neoplasm — possibly minor salivary-gland cancer, lymphoma, or sarcoma — but it is not possible to distinguish among these cancers without first obtaining tissue for pathological evaluation. Given this patient's presentation involving bleeding from a large oropharyngeal mass and concerns about airway complications, examination and biopsy while the patient was under anesthesia was recommended.

Diagnosis

Malignant neoplasm consistent with minor salivary-gland cancer, lymphoma, or sarcoma.



Biopsy Specimen of the Oropharyngeal Mass.

Hematoxylin and eosin staining of the oropharyngeal tissue specimen (Panel A) shows an infiltrative round-cell neoplasm deep in the tonsil tissue. At higher magnification, an alternating hypocellular and hypercellular pattern of growth is seen in a myxoid background (Panel B), and round-to-oval cells with a high nuclear-to-cytoplasmic ratio, scant amphophilic cytoplasm, and numerous mitoses are noted (Panel C, arrows). Immunohistochemical staining shows that the tumor cells are diffusely positive for desmin (Panel D) and myoD1 (Panel E) and multifocally positive for myogenin (Panel F).

A representative formalin-fixed, paraffin-embedded tissue specimen containing tumor cells was sent for molecular testing. Fluorescence in situ hybridization, performed with break-apart probes to the *FOXO1* locus, did not detect the presence of *FOXO1* rearrangements, which effectively ruled out a diagnosis of alveolar rhabdomyosarcoma. Next-generation sequencing revealed variants in the RAS pathway, including single-nucleotide variants in *HRAS* and *GNAS* and copy-number variants in *HRAS*. Somatic driver mutations involving the RAS pathway have been identified in genomic studies of embryonal rhabdomyosarcoma. Cytogenetic analysis of fresh tumor tissue obtained from this patient revealed a complex karyotype, including trisomy 8. Although not specific, trisomy 8 is a recurrent aberration observed in patients with rhabdomyosarcoma.

Management

Diagnostic tonsillectomy, chemotherapy, and radiotherapy.

Pathological Diagnosis

Embryonal rhabdomyosarcoma.

Patient Perspective

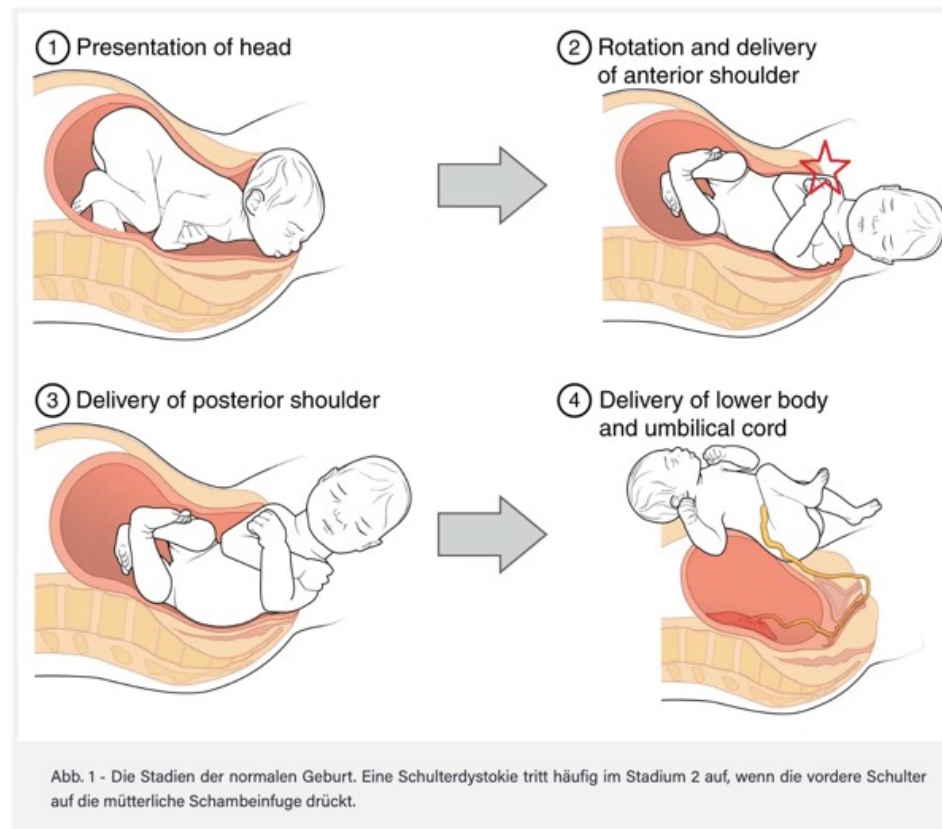
The Patient: My first symptom was a sore throat that never went away. As the swelling and list of unusual symptoms grew, my confidence that it was nothing shrank. It was confusing and exhausting.

Self-advocacy is often imagined as tenacity, but it was just how I was channeling my frustration. Frustration at my body for being so mysterious and stumping a competent medical community. Frustration at not having answers. Looking for a diagnosis felt like being underwater and seeing the reflection of the sun, trying to swim to the surface but realizing you're too far below and running out of air. I firmly believe that if patients speak up in these moments and physicians use stories like mine to inform how they approach the unusual, maybe one fewer person will experience what I did.

Final Diagnosis

Embryonal rhabdomyosarcoma of the pharynx.

Schulterdystokie, auch "Schulterblock" genannt, ist eine Situation, in der die vordere Schulter des Kindes auf der mütterlichen Schambeinfuge oder die hintere Schulter auf dem Kreuzbein des Beckenbodens festhängt. Nach der Geburt des Kopfes kann der Rest des Körpers nicht vollständig entbunden werden, da die Schultern durch den Geburtskanal passen müssen, ein Prozess, der dann durch die Schulterblockade verhindert wird.



Induction of labour versus standard care to prevent shoulder dystocia in fetuses suspected to be large for gestational age in the UK (the Big Baby trial): a multicentre, open-label, randomised controlled trial

Summary

Background The benefits and harms of early induction of labour to reduce shoulder dystocia in fetuses suspected to be large for gestational age (LGA) are uncertain. We aimed to investigate whether early induction of labour is associated with a reduced risk of shoulder dystocia compared with standard care.

Methods In this open-label, randomised controlled phase 3 trial, women aged ≥ 18 years with a suspected LGA fetus (estimated fetal weight >90 th customised percentile) as identified by ultrasound scan between 35 weeks and 0 days (35^{+0} weeks) of gestation and 38^{+0} weeks' gestation, recruited from 106 hospitals across England, Scotland, and Wales in the UK, were randomly assigned (1:1) by web app to standard care or induction of labour between 38^{+0} weeks' gestation and 38^{+4} weeks' gestation using minimisation, balancing site, estimated fetal weight percentile (≤ 95 th EFW percentile or >95 th EFW percentile), and maternal age (≤ 35 years or >35 years). Key exclusion criteria included drug-treated diabetes, gestational diabetes, and elective caesarean section or induction already planned or indicated for any reason. Our primary outcome was incidence of shoulder dystocia, assessed by a masked independent expert adjudication panel who reviewed participants' delivery notes. Induction of labour was anticipated to result in birth 10.5 days earlier with a 300 g lower birthweight on average than standard care. We did an intention-to-treat (ITT) analysis in all participants for whom we had primary outcome data, and a per-protocol analysis in participants in the induction group who went into labour or were induced at 38^{+0} to 38^{+4} weeks' gestation versus participants in the standard care group who had not started labour, been induced, or had an elective caesarean section before 38^{+4} weeks' gestation. This study was registered with ISRCTN (18229892) and is no longer recruiting.

Findings Between June 8, 2018, and Oct 25, 2022, 2893 women were randomly assigned to induction of labour (n=1447) or standard care (n=1446); the trial was terminated before the target of 4000 participants was reached on advice of the data monitoring committee following the lower-than-expected incidence of shoulder dystocia in the standard care group. Two participants in the induction group and seven in the standard care group had missing data for the primary outcome and were excluded from the ITT analysis. In the ITT analysis, 33 (2.3%) of 1445 babies in the induction group versus 44 (3.1%) of 1439 in the standard care group had shoulder dystocia (risk ratio [RR] 0.75 [95% CI 0.51–1.09]; p=0.14) with a mean difference of –6.0 days' (95% CI –6.3 to –5.6) gestation and –163.6 g (–190.0 to –137.1) birthweight between trial groups. 355 (24.6%) of 1446 mothers in the standard care group were induced, delivered, or went into labour at or before 38⁺⁴ weeks' gestation. In the per-protocol analysis, 27 (2.3%) of 1180 babies in the induction group versus 40 (3.7%) of 1074 in the standard care group had shoulder dystocia (RR 0.62 [0.41–0.92]; p=0.019), and there was a mean difference of –8.1 days' (–8.4 to –7.9) gestation and –213.3 g (–242.0 to –184.6) birthweight between trial groups. One neonatal death occurred from perinatal asphyxia after shoulder dystocia in the standard care group, and one neonatal death occurred following sepsis and congenital pneumonia in the induction group. 88 (6.1%) of 1447 mothers in the induction group had an adverse event versus 108 (7.5%) of 1446 in the standard care group (RR 0.81 [0.62 to 1.06]; p=0.13). Similar numbers of serious adverse events were reported in both groups.

Interpretation No significant difference in incidence of shoulder dystocia was found between trial groups in the ITT analysis, probably due to the high proportion of earlier-than-expected deliveries in the standard care group reducing the intended between-group differences in gestational age and birthweight. However, in the per-protocol analysis, compared with all deliveries after 38⁺⁴ weeks' gestation, induction of labour between 38⁺⁰ weeks' gestation and 38⁺⁴ weeks' gestation did show a significant reduction in shoulder dystocia. This study provides pregnant women with suspected LGA fetuses and their clinicians important information about choices and decision making for timing and mode of birth.

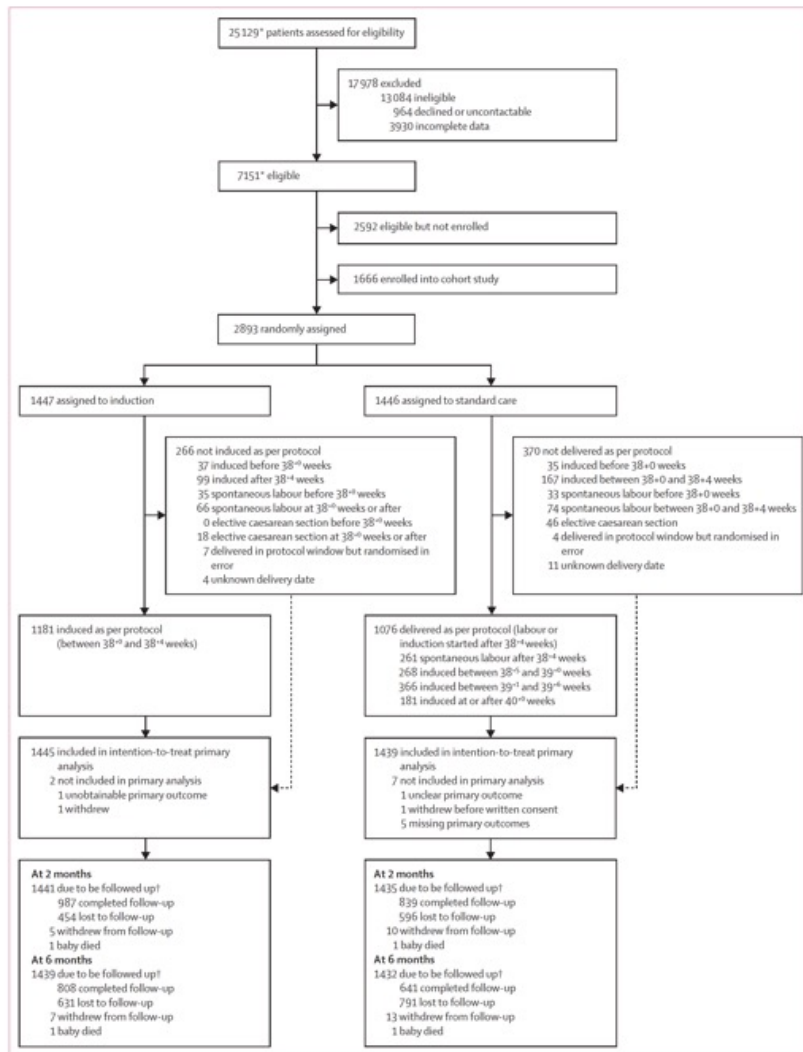


Figure: CONSORT diagram
Weeks refers to weeks of gestation. *Including three not included in screening logs. †Including 8-week follow-up period after due date, after which participant was considered lost to follow-up if no response had been received.

	Induction (n=1447)	Standard care (n=1446)
Age at recruitment, years*		
Mean (SD)	28.8 (5.3)	28.8 (5.4)
≤35 years	1286 (88.9%)	1286 (88.9%)
>35 years	161 (11.1%)	160 (11.1%)
Previous pregnancies of ≥24 weeks' gestation†		
0	808 (55.8%)	831 (57.5%)
1	386 (26.7%)	344 (23.8%)
2	149 (10.3%)	177 (12.2%)
3+	104 (7.2%)	92 (6.4%)
Missing	0 (0.0%)	2 (0.1%)
Ethnicity‡		
British European	1228 (84.9%)	1191 (82.4%)
East European	32 (2.2%)	46 (3.2%)
West African	19 (1.3%)	16 (1.1%)
Indian	39 (2.7%)	30 (2.1%)
Pakistani	30 (2.1%)	51 (3.5%)
Declined	2 (0.1%)	2 (0.1%)
Other	97 (6.7%)	108 (7.5%)
Missing	0	2 (0.1%)
BMI at early pregnancy visit, kg/m²		
Underweight (<18.5)	32 (2.2%)	40 (2.8%)
Healthy (≥18.5 to <25)	518 (35.8%)	510 (35.3%)
Overweight (≥25 to <30)	404 (27.9%)	398 (27.5%)
Obese (≥30)	493 (34.1%)	496 (34.3%)
Missing	0	2 (0.1%)
Diet-controlled gestational diabetes§		
Yes	60 (4.1%)	72 (5.0%)
No	1387 (95.9%)	1372 (94.9%)
Missing	0	2 (0.1%)
Smoker at early pregnancy visit§		
Yes	134 (9.3%)	154 (10.7%)
No	1313 (90.7%)	1290 (89.2%)
Missing	0	2 (0.1%)
Received corticosteroid for fetal lung maturation during pregnancy§		
Yes	45 (3.1%)	25 (1.7%)
No	1401 (96.8%)	1413 (97.7%)
Missing	1 (0.1%)	8 (0.6%)

Data are n (%) or mean (SD). Age, ethnicity, and BMI data were collected at recruitment. Gestational diabetes, smoking status, and corticosteroid use data were collected at baseline visit. †Stratification variable. ‡For information on previous pregnancies see appendix (p 9). §Ethnicity categories containing <1% of participants were grouped together in the Other category; for full details see appendix pp 10-12. §Collected at baseline visit.

	Induction	Standard care	Mean difference (95% CI) or adjusted analysis*
Intention-to-treat analysis			
n	1447	1446	--
Gestation at delivery, days	270 (3.0; n=1446)	276 (5.6; n=1446)	-6.0 (-6.3 to -5.6)
Birthweight, g	3893 (349.8; n=1446)	3857 (375.2; n=1446)	-163.6 (-190.0 to -137.1)
Birthweight >90th percentile	610 (42.2%)	576 (39.8%)	--
Birthweight >4000 g	260 (18.0%)	469 (32.4%)	--
Shoulder dystocia†	33/1445 (2.3%)	44/1439 (3.1%)	0.75 (0.51 to 1.09); p=0.14*
Per-protocol analysis			
n	1180	1074	--
Gestation at delivery, days	270 (2.0)	278 (4.1)	-8.1 (-8.4 to -7.9)
Birthweight, g	3686 (337.0)	3899 (357.5)	-213.1 (-242.0 to -184.6)
Birthweight >90th percentile	487 (41.3%)	402 (37.4%)	--
Birthweight >4000 g	195 (16.5%)	384 (35.8%)	--
Shoulder dystocia	27 (2.3%)	40 (3.7%)	0.62 (0.41 to 0.92); p=0.033*

Data are n (%) or mean (SD). Statistical analysis based on complete data. All caesarean sections were counted as no shoulder dystocia. *Relative risk (95% CI) and p value from generalised linear model, with family binomial and link log, adjusted by site, estimated fetal weight percentile (<10th or >90th) and maternal age (≤35 years or >35 years), with clustering adjustments for site. †Primary analysis.

Table 2: Gestational age, birthweight, and incidence of shoulder dystocia by study group, according to intention-to-treat and per-protocol analyses

2/3 >27 BMI to obese

Table 1: Demographic and baseline characteristics

	Induction (n=1447)	Standard care (n=1446)	Adjusted estimate (95% CI)	p value*
Delivery timings				
Time between delivery of head and delivery of body, min†				
Mean (SD)	1.09 (0.94; n=996)	1.21 (1.02; n=923)	-0.13 (-0.21 to -0.04)	0.0047
Missing	40/1036 (3.9%)	46/969 (4.7%)	--	--
Time from commencement of active second stage of labour until fetal expulsion, min†				
Mean (SD)	46.2 (49.1; n=939)	50.9 (51.2; n=859)	-4.81 (-9.43 to -0.20)	0.041
Missing	2/1036 (0.2%)	6/969 (0.6%)	--	--
NA or unknown due to timing of arrival at hospital	95/1036 (9.2%)	104/969 (10.7%)	--	--
Time in labour ward, h				
Mean (SD)	21.2 (17.2; n=1407)	19.0 (16.6; n=1419)	2.19 (0.94 to 3.43)	0.0006
Missing	40 (3%)	27 (2%)	--	--
Duration of hospital stay before delivery, days‡				
Mean (SD)	1.97 (1.45; n=1444)	1.46 (1.41; n=1436)	0.50 (0.40 to 0.60)	<0.0001
Missing	2 (0.1%)	7 (0.5%)	--	--
NA (not born in hospital)	1 (0.1%)	3 (0.2%)	--	--
Duration of hospital stay after delivery, days‡				
Mean (SD)	1.46 (1.46; n=1446)	1.56 (1.47; n=1440)	-0.11 (-0.21 to 0.001)	0.052
Missing	1 (0.1%)	6 (0.4%)	--	--
Total duration in hospital from admission to discharge, days				
Mean (SD)	3.42 (2.13; n=1445)	3.02 (2.14; n=1436)	0.40 (0.24 to 0.55)	<0.0001
NA (not born in hospital)	1 (0.1%)	3 (0.2%)	--	--
Missing	1 (0.1%)	7 (0.5%)	--	--
Delivery characteristics				
Labour type onset				
Spontaneous	89 (6.2%)	358 (24.8%)	RRR 0.19 (0.15 to 0.24)	<0.0001§
Induced	1327 (91.7%)	1021 (70.6%)	1 (ref)	--
No labour (caesarean section)	30 (2.1%)	61 (4.2%)	RRR 0.38 (0.24 to 0.59)	<0.0001§
Missing	1 (0.1%)	6 (0.4%)	--	--
Mode of delivery				
Spontaneous vaginal delivery	799 (55.2%)	704 (48.7%)	1 (ref)	--
Vaginal delivery, ventouse	57 (3.9%)	61 (4.2%)	RRR 0.82 (0.57 to 1.20)	0.315
Vaginal delivery, forceps	157 (10.9%)	177 (12.2%)	RRR 0.78 (0.62 to 0.99)	0.042§
Vaginal delivery, rotational forceps	22 (1.5%)	21 (1.5%)	RRR 0.92 (0.50 to 1.69)	0.79§
Elective caesarean section	39 (2.7%)	61 (4.2%)	RRR 0.56 (0.37 to 0.85)	0.0064§
Emergency caesarean section	372 (25.7%)	416 (28.8%)	RRR 0.79 (0.66 to 0.94)	0.0066§
Missing	1 (0.1%)	6 (0.4%)	--	--
Presentation at birth				
Cephalic	1439 (99.5%)	1428 (98.8%)	1 (ref)	--
Breech	3 (0.2%)	5 (0.4%)	RRR 0.60 (0.14 to 2.48)	0.48§
Transverse lie	3 (0.2%)	7 (0.5%)	RRR 0.43 (0.11 to 1.69)	0.23§
Missing	2 (0.1%)	6 (0.4%)	--	--
Maternal outcomes				
Primary postpartum haemorrhage (≥500 mL blood loss)				
Yes	648 (44.8%)	709 (49.0%)	RR 0.91 (0.84 to 0.98)	0.016
Missing	1 (0.1%)	6 (0.4%)	--	--
Major primary postpartum haemorrhage (≥1000 mL blood loss)				
Yes	203 (14.0%)	220 (15.2%)	RR 0.91 (0.77 to 1.09)	0.32
Missing	1 (0.1%)	6 (0.4%)	--	--
Episiotomy				
Yes	286 (19.8%)	327 (22.6%)	RR 0.87 (0.76 to 1.00)	0.054
Missing	1 (0.1%)	6 (0.4%)	--	--

(Table 3 continues on next page)

	Induction (n=1447)	Standard care (n=1446)	Adjusted estimate (95% CI)	p value*
(Continued from previous page)				
Perineal injury degree¶				
First	161 (11.1%)	148 (10.2%)	RR 1.08 (0.88 to 1.34)	0.47
Second	405 (28.0%)	354 (24.5%)	RR 1.14 (1.01 to 1.29)	0.037
Third	33 (2.3%)	32 (2.2%)	RR 1.03 (0.64 to 1.66)	0.91
Fourth	4 (0.3%)	5 (0.4%)	RR 0.79 (0.21 to 2.94)	0.73
Unknown	2 (0.4%)	3 (0.6%)	--	--
Cervical laceration				
Yes	13 (0.9%)	13 (0.9%)	RR 0.99 (0.46 to 2.14)	0.99
Missing	1 (0.1%)	6 (0.4%)	--	--
Retained placenta requiring manual removal				
Yes	39 (2.7%)	37 (2.6%)	RR 1.05 (0.67 to 1.64)	0.83
Missing	1 (0.1%)	6 (0.4%)	--	--
Maternal death				
Yes	0	0	NA	NA
Missing	1 (0.1%)	6 (0.4%)	--	--
Sepsis in labour or within 24 h postpartum				
Yes	84 (5.8%)	95 (6.6%)	RR 0.88 (0.66 to 1.17)	0.38
Missing	1 (0.1%)	7 (0.5%)	--	--
Fever >38°C in labour or within 24 h postpartum				
Yes	93 (6.4%)	106 (7.3%)	RR 0.87 (0.67 to 1.14)	0.31
Missing	1 (0.1%)	7 (0.5%)	--	--
Maternal readmissions				
Hospital readmission within 30 days of discharge				
Yes	80 (5.5%)	100 (6.9%)	RR 0.80 (0.60 to 1.06)	0.12
Missing	1 (0.1%)	8 (0.6%)	--	--
Composite outcome				
Third-degree or fourth-degree perineal tear, cervical laceration or tear, primary postpartum haemorrhage, or a combination of these complications				
Yes	663 (45.8%)	727 (50.3%)	RR 0.91 (0.84 to 0.98)	0.013
Missing	3 (0.2%)	6 (0.4%)	--	--
Adverse events				
Any maternal adverse events up to the point of discharge from hospital following delivery				
Yes	88 (6.1%)	108 (7.5%)	RR 0.81 (0.62 to 1.06)	0.13
Missing	1 (0.1%)	8 (0.6%)	--	--
Data are n (%) unless otherwise stated. RR=risk ratio. RRR=relative risk ratio. NA=not applicable. *Unless otherwise stated, for continuous outcomes: linear regression adjusted for site, estimated fetal weight percentile (≤95th or >95th), and maternal age (≤35 years or >35 years), with standard care as the reference group. For categorical outcomes: generalised linear model, with family binomial and link log adjusted for site, estimated fetal weight percentile (≤95th or >95th), and maternal age (≤35 years or >35 years), with standard care as the reference group. Statistical analysis based on complete data. †Vaginal deliveries only. ‡The end of the third stage of labour was used as the delivery timepoint. §Multinomial logistic regression, adjusted for site, maternal age, and estimated fetal weight percentile. ¶Some participants reported multiple degrees of tears.				
Table 3: Hospital stay, mode of delivery, and maternal outcomes				

	Induction (n=1447)	Standard care (n=1446)	Adjusted estimate (95% CI)	p value*
Neonatal outcomes				
Stillbirth				
Yes	0	0	NA	NA
Missing	1 (0.1%)	6 (0.4%)	–	–
Neonatal death				
Yes	1 (0.1%)	1 (0.1%)	OR 1.00 (0.10 to 9.59)	>0.99†
Missing	1 (0.1%)	6 (0.4%)	–	–
Apgar score at 5 min				
Score 7–10 (good)	1417 (97.9%)	1421 (98.3%)	RR 1.62 (0.87 to 3.01)	0.13
Score 0–6 (poor)	26 (1.8%)	16 (1.1%)	–	–
Missing	4 (0.3%)	9 (0.6%)	–	–
Humeral fracture				
Yes	0	0	NA	NA
Missing	1 (0.1%)	6 (0.4%)	–	–
Clavicular fracture				
Yes	0	0	NA	NA
Missing	1 (0.1%)	6 (0.4%)	–	–
Brachial plexus palsy				
Yes‡	4 (0.3%)	2 (0.1%)	RR 1.95 (0.36 to 10.65)	0.44
Missing	1 (0.1%)	6 (0.4%)	–	–
Admission to neonatal unit or additional care received§				
Yes	155 (10.7%)	139 (9.6%)	RR 1.11 (0.90 to 1.38)	0.34
Missing	1 (0.1%)	6 (0.4%)	–	–
Duration of stay at neonatal unit, days¶				
Mean (SD)	3.2 (4.0; n=155)	2.9 (2.3; n=139)	0.37 (–0.39 to 1.12)	0.34
Missing	0/155	0/139	–	–
Hypoxic ischaemic encephalopathy				
Yes	2 (0.1%)	0	OR 4.96 (0.24 to 103.17)	0.30†
Missing	1 (0.1%)	7 (0.5%)	–	–
Use of phototherapy				
Yes	44 (3.0%)	28 (1.9%)	RR 1.57 (0.98 to 2.50)	0.061
Missing	1 (0.1%)	7 (0.5%)	–	–
Supplemental oxygen				
Yes	46 (3.2%)	51 (3.5%)	RR 0.90 (0.61 to 1.33)	0.60
Missing	1 (0.1%)	6 (0.4%)	–	–
Mechanical ventilation				
Yes	8 (0.6%)	3 (0.2%)	RR 2.65 (0.70 to 10.05)	0.15
Missing	1 (0.1%)	6 (0.4%)	–	–
Non-invasive respiratory support				
Yes	30 (2.1%)	30 (2.1%)	RR 1.00 (0.60 to 1.64)	0.99
Missing	1 (0.1%)	6 (0.4%)	–	–
Extracorporeal membrane oxygenation				
Yes	0	0	NA	NA
Missing	1 (0.1%)	6 (0.4%)	–	–
Nitric oxide therapy				
Yes	2 (0.1%)	0	OR 4.95 (0.24 to 103.07)	0.30†
Missing	1 (0.1%)	6 (0.4%)	–	–
Hypoglycaemia				
Yes	50 (3.5%)	43 (3.0%)	RR 1.16 (0.77 to 1.73)	0.48
Missing	1 (0.1%)	8 (0.6%)	–	–

(Table 4 continues on next page)

	Induction (n=1447)	Standard care (n=1446)	Adjusted estimate (95% CI)	p value*
(Continued from previous page)				
Neonatal readmissions				
Hospital readmission within 30 days of postnatal inpatient discharge				
Yes	190 (13.1%)	160 (11.1%)	RR 1.18 (0.97 to 1.44)	0.092
Unknown	24 (1.7%)	20 (1.4%)	–	–
Missing	3 (0.2%)	9 (0.6%)	–	–
Composite outcomes				
Intrapartum birth injury—fractures, brachial plexus injury, or both injuries				
Yes	4 (0.3%)	2 (0.1%)	RR 1.95 (0.36 to 10.65)	0.44
Missing	1 (0.1%)	6 (0.4%)	–	–
Prematurity associated problems—use of phototherapy, respiratory support, or both				
Yes	90 (6.2%)	77 (5.3%)	RR 1.16 (0.87 to 1.56)	0.32
Missing	1 (0.1%)	7 (0.5%)	–	–

Data are n (%) unless otherwise stated. OR=odds ratio. RR=risk ratio. NA=not applicable. *Unless otherwise stated, for continuous outcomes: linear regression adjusted for site, estimated fetal weight percentile (<95th or >95th), and maternal age (<35 years or >35 years), with standard care as reference group. For categorical outcomes: generalised linear model, with family binomial and link log adjusted for site, estimated fetal weight percentile (<95th or >95th), and maternal age (<35 years or >35 years), with standard care as reference group. Statistical analysis based on complete data. †Penalised logistic regression (Firth algorithm) used due to small frequencies. ‡Of these infants, three in the induction group and one in the standard care group had transient brachial plexus palsy, and one in the induction group and one in the standard care group required treatment for more than 8 weeks, neither of which were associated with shoulder dystocia. §Counted if admitted to intensive care, high-dependency care, special care, or transitional care. ¶Only calculated if they received additional care. Both same and different hospital transfers were included. If babies were admitted into multiple hospitals, the durations of both stays have been combined for the admissions that were either intensive care, high-dependency care, special care, or transitional care. ||Sites specifically returned forms saying unknown, whereas missing refers to cases where no information was given.

Table 4: Neonatal outcomes

Research in context

Evidence before this study

Fetuses that are large for gestational age (LGA) have an increased risk of perinatal complications, and earlier delivery by induction of labour might reduce this risk. We searched MEDLINE for systematic reviews from Jan 1, 2000 to May 31, 2017 with the search terms “induction of labour”, “macrosomia”, “large for gestational age”, and “shoulder dystocia”. Our search identified two systematic reviews (2016 and 2017) of four trials with a total of 1190 participants. These reviews found a reduced risk of shoulder dystocia, fracture, and brachial plexus injury following early induction of labour compared with expectant care; however, only one review concluded that these differences were statistically significant. The conclusions of both reviews were largely driven by the results of a single trial, which had a protocol of induction of labour starting from 37 weeks’ gestation.

Added value of this study

To our knowledge, this is the largest randomised controlled trial of induction of labour to prevent shoulder dystocia, and included more than twice as many pregnancies as the combined total of all trials included in the two selected systematic reviews. The study assessed a protocol of induction from 38 weeks’ gestation compared with delivery after 39 weeks’ gestation and found that early delivery of a baby suspected to

be LGA can reduce the risk of shoulder dystocia and can have no effect on secondary neonatal outcomes. Contrary to previous evidence, induction was found to decrease the need for caesarean sections and did not increase third-degree and fourth-degree perineal tears. The study provides important information for clinical management options, and empowers pregnant women to choose the time and mode of delivery of their suspected LGA baby.

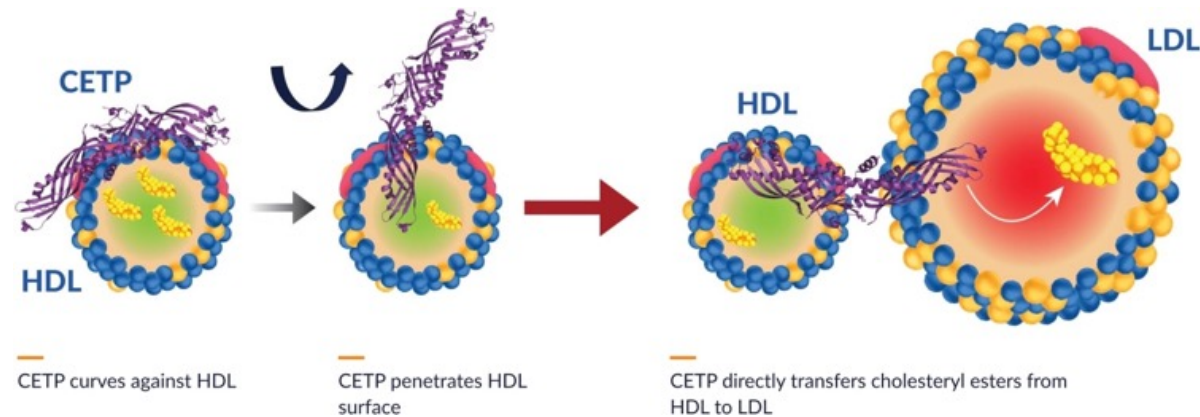
Implications of all the available evidence

On the basis of our per-protocol analysis, we found that induction of labour in pregnancies with LGA fetuses can reduce shoulder dystocia at 38 weeks’ gestation as well as from the previously reported 37 weeks’ gestation. Contrary to previous studies, our large trial found that induction of labour did not increase maternal trauma in terms of third-degree and fourth-degree tears, and reduced postpartum haemorrhage and emergency caesarean sections. We also found no change in adverse neonatal outcomes with induction of labour. Therefore, the timing and mode of delivery in LGA pregnancies can account for maternal choice and include planned caesarean section to eliminate the risk of shoulder dystocia, or induction of labour to reduce risk of shoulder dystocia, without increasing the risk of adverse maternal outcomes.

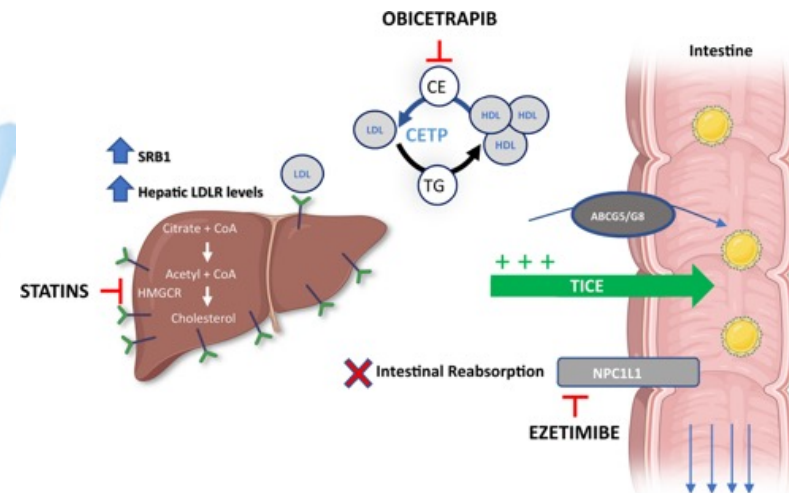
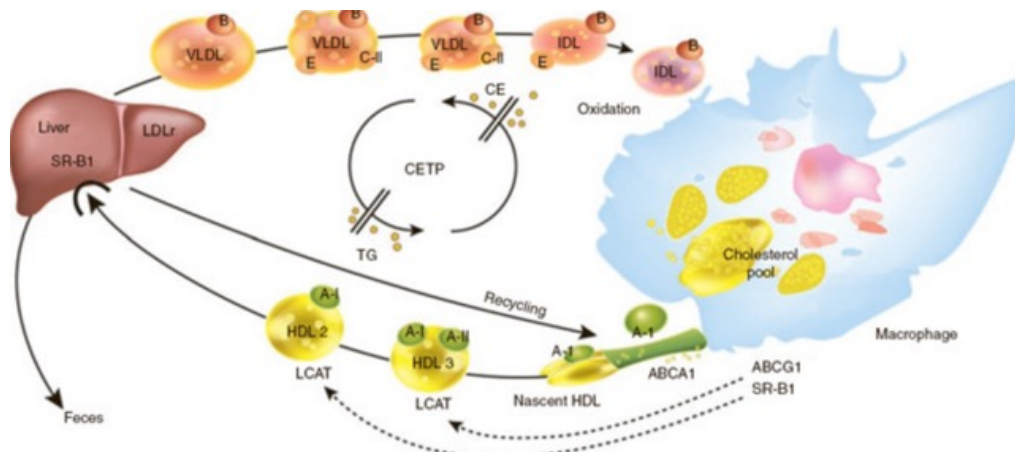
Das **Cholesterinester-Transferprotein, kurz CETP**, ist ein Glykoprotein, das am Lipidstoffwechsel beteiligt ist und dem Austausch von Lipiden zwischen Apolipoproteinen dient.

CETP vermittelt einen Austausch von Lipiden zwischen den proteinreichen HDL und den lipidreichen VLDL. Dabei werden Triglyceride von VLDL auf HDL transferiert, während HDL Cholesterinester an VLDL abgibt. Mutationen des CETP-Gens sind mit Hyperalphalipoproteinämie 1 und Fettstoffwechselstörungen assoziiert. Darüber hinaus wird vermutet, dass CETP eine Rolle bei der Atherogenese spielt.

CETP-Inhibitoren, die den HDL-C-Spiegel erhöhen sollen (z.B. Ancetrapib, Dalcetrapib, Evacetrapib, Torcetrapib), haben in großen Studien zur kardiovaskulären Prävention weitgehend enttäuscht. Präventiv scheint die Hemmung der CETP-Aktivität nur zu wirken, wenn sie mit einem Abfall der ApoB- und LDL-C-Spiegel einhergeht. Obicetrapib, ein Inhibitor, der ein solches Wirkprofil aufweist, befindet sich als Monotherapie und zusätzlich zu einer hochdosierten Statintherapie gegenwärtig (2024) in klinischer Testung.



Obicetrapib ist ein experimenteller CETP-Inhibitor, der in klinischen Studien untersucht wird, um die Lipidsenkerwirkung von Statinen zu verbessern und das Risiko kardiovaskulärer Erkrankungen zu reduzieren. Es senkt LDL-Cholesterin und erhöht HDL-Cholesterin.



Fixed-dose combination of obicetrapib and ezetimibe for LDL cholesterol reduction (TANDEM): a phase 3, randomised, double-blind, placebo-controlled trial

Summary

Background Reducing LDL cholesterol prevents atherosclerotic cardiovascular disease (ASCVD) events. The aim of this study was to evaluate the LDL cholesterol-lowering efficacy of a fixed-dose combination (FDC) of obicetrapib, a CETP inhibitor, and ezetimibe.

Methods This randomised, double-blind trial across 48 US sites including hospitals, private and group practices, and independent research centres included participants at least 18 years old with pre-existing or high risk for ASCVD or heterozygous familial hypercholesterolaemia with LDL cholesterol concentrations of 1.8 mmol/L (70 mg/dL) or greater despite maximally tolerated lipid-lowering therapy excluding ezetimibe, or having statin intolerance. Participants were randomly assigned (1:1:1:1) to obicetrapib 10 mg plus ezetimibe 10 mg FDC, obicetrapib 10 mg monotherapy, ezetimibe 10 mg monotherapy, or placebo administered daily for 84 days. The co-primary endpoints in the intention-to-treat population were the percent LDL cholesterol changes in the FDC group compared with placebo, ezetimibe monotherapy, and obicetrapib monotherapy, and the placebo-adjusted change in the obicetrapib monotherapy group. The trial was prospectively registered (NCT06005597) and is completed.

FDC = Fixed-dose combination

Findings Between March 4 and July 3, 2024, 407 participants were randomly assigned. The median age was 68.0 years (IQR 62.0–73.0) and 177 (43%) were female. Mean baseline LDL cholesterol was 2.4 mmol/L, 2.5 mmol/L, 2.6 mmol/L, and 2.5 mmol/L in the placebo (n=102), ezetimibe monotherapy (n=101), obicetrapib monotherapy (n=102), and FDC groups (n=102), respectively. At day 84, percent differences in LDL cholesterol reduction with the FDC were -48.6% (95% CI -58.3 to -38.9) versus placebo, -27.9% (-37.5 to -18.4) versus ezetimibe, and -16.8% (-26.4 to -7.1) versus obicetrapib. Obicetrapib monotherapy decreased LDL cholesterol by 31.9% (22.1 to 41.6) versus placebo. Adverse event rates were similar in the FDC (52 [51%] of 102), obicetrapib (55 [54%] of 102), and ezetimibe (54 [53%] of 101) groups and lowest with placebo (38 [37%] of 102). Serious adverse event rates were generally similar across FDC (three [3%] of 102), obicetrapib (six [6%] of 102), ezetimibe (seven [7%] of 101), and placebo (four [4%] of 102) groups. Deaths occurred in one [1%] of 102 participants with FDC, one [1%] of 102 with obicetrapib, one [1%] of 101 with ezetimibe, and none with placebo.

Interpretation Combination therapy of obicetrapib and ezetimibe significantly reduced LDL cholesterol. This oral, single-pill therapy could improve LDL cholesterol management in patients with pre-existing or high risk for ASCVD.

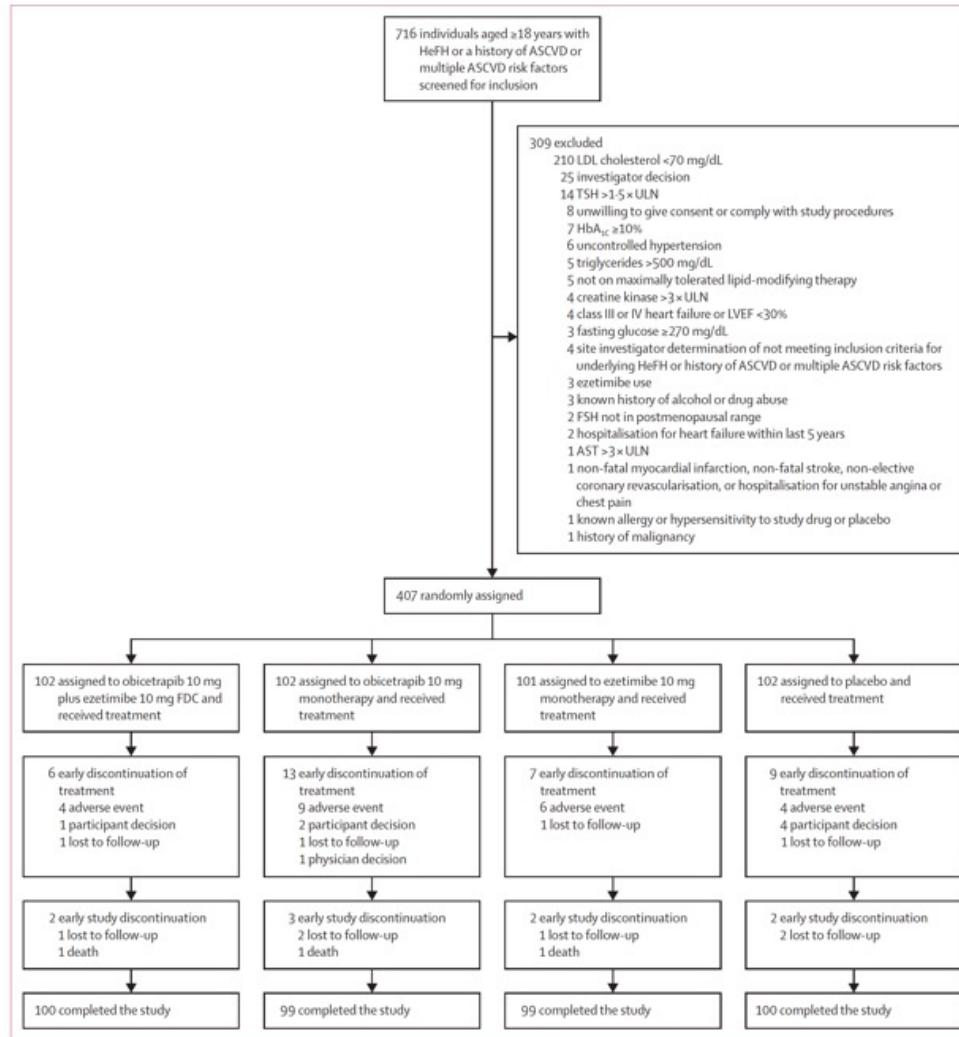


Figure 1: Trial profile

ASCVD=atherosclerotic cardiovascular disease, AST=aspartate aminotransferase, FDC=fixed-dose combination, FSH=follicle-stimulating hormone, HbA_{1c}=glycated haemoglobin, HeFH=heterozygous familial hypercholesterolaemia, LVEF=left ventricular ejection fraction, TSH=thyroid-stimulating hormone, ULN=upper limit of normal.

	Obicetrapib plus ezetimibe FDC (n=102)	Obicetrapib monotherapy (n=102)	Ezetimibe monotherapy (n=101)	Placebo (n=102)
Median age (IQR), years	68.0 (63.0-72.0)	67.0 (61.0-74.0)	68.0 (64.0-73.0)	67.5 (62.0-72.0)
Sex				
Female	48 (47%)	33 (32%)	45 (45%)	51 (50%)
Male	54 (53%)	69 (68%)	56 (55%)	51 (50%)
Race				
White	86 (84%)	85 (83%)	82 (81%)	84 (82%)
Black or African American	14 (14%)	15 (15%)	13 (13%)	17 (17%)
Asian	1 (1%)	0	3 (3%)	1 (1%)
Unspecified or other	1 (1%)	0	2 (2%)	0
Ethnicity				
Hispanic or Latino	4 (4%)	2 (2%)	1 (1%)	2 (2%)
Not Hispanic or Latino	98 (96%)	100 (98%)	100 (99%)	100 (98%)
Mean LDL cholesterol (SD), mmol/L	2.5 (0.7)	2.6 (0.9)	2.5 (0.8)	2.4 (0.7)
Mean non-HDL cholesterol (SD), mmol/L	3.2 (1.0)	3.3 (1.1)	3.2 (1.1)	3.0 (0.7)
Mean HDL cholesterol (SD), mmol/L	1.2 (0.3)	1.2 (0.4)	1.3 (0.4)	1.3 (0.4)
Mean apolipoprotein B (SD), mg/dL	88.9 (23.0)	90.6 (25.6)	89.2 (24.9)	85.3 (18.4)
Median triglycerides (IQR), mmol/L	1.6 (1.1-1.9)	1.4 (1.0-2.0)	1.3 (0.9-1.9)	1.3 (1.0-1.9)
Median lipoprotein (a) (IQR), mmol/L	50.9 (13.8-199.8)	33.7 (14.5-175.7)	32.8 (8.1-154.8)	48.3 (7.7-196.4)
Median hsCRP (IQR), mg/L	2.3 (0.9-4.5)	1.9 (1.1-3.2)	1.3 (0.7-3.7)	1.7 (0.8-4.6)
Lipid-lowering therapies				
Statin	91 (89%)	87 (85%)	93 (92%)	93 (91%)
High-intensity statin	75 (74%)	66 (65%)	71 (70%)	75 (74%)
PCSK9 inhibitor	6 (6%)	1 (1%)	3 (3%)	6 (6%)
Bempedoic acid	0	2 (2%)	2 (2%)	2 (2%)
No statin therapy due to intolerance	11 (11%)	16 (16%)	7 (7%)	9 (9%)
History of ASCVD				
Coronary artery disease	72 (71%)	76 (75%)	67 (66%)	65 (64%)
Peripheral arterial disease	4 (4%)	7 (7%)	7 (7%)	4 (4%)
Cerebrovascular disease	22 (22%)	20 (20%)	15 (15%)	19 (19%)
HeFH	7 (7%)	5 (5%)	6 (6%)	12 (12%)
Diabetes	49 (48%)	52 (51%)	49 (49%)	49 (48%)
Hypertension	84 (82%)	82 (80%)	86 (85%)	85 (83%)
Current cigarette smoking	15 (15%)	13 (13%)	12 (12%)	16 (16%)
Family history of coronary heart disease*	26 (25%)	32 (31%)	37 (37%)	28 (27%)

Data are n (%) unless otherwise indicated. The conversion factors between conventional units and SI units for LDL, HDL, and total cholesterol are 38.67 mg/dL = 1 mmol/L, and for triglycerides, 88.57 mg/dL = 1 mmol/L. ASCVD=atherosclerotic cardiovascular disease, FDC=fixed-dose combination, HeFH=heterozygous familial hypercholesterolaemia, hsCRP=high-sensitivity C-reactive protein. *Family history of coronary heart disease was defined as a first-degree relative with clinical coronary heart disease (males <55 years or females <65 years of age).

Table 1: Baseline characteristics

Fixed combination

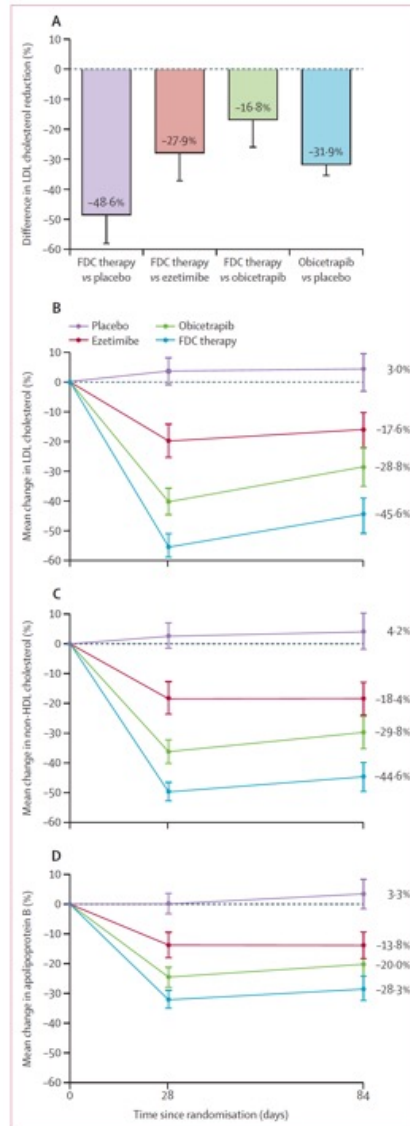
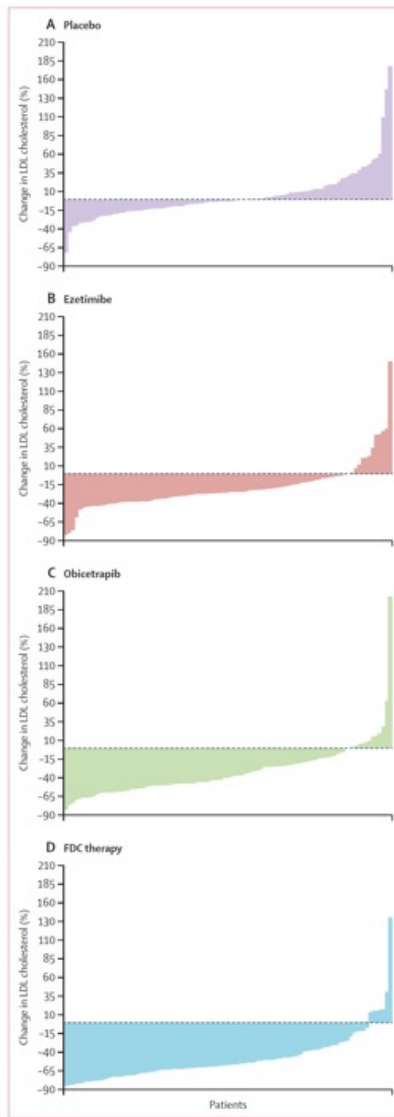


Figure 2: Co-primary and secondary endpoints

(A) Co-primary endpoints—percent difference in LDL cholesterol reduction at day 84. Least-squares mean percent differences in the reduction of LDL cholesterol concentrations measured by preparative ultracentrifugation at day 84 following randomisation in the intention-to-treat population. An ANCOVA model with a fixed effect for the treatment group and a covariate of baseline LDL cholesterol was used to assess the primary efficacy parameter to obtain the values for the difference in least-squares mean percent change. The number of missing observations at day 84 were as follows: 3 in the FDC group, 5 in the obicetrapib monotherapy group, 5 in the ezetimibe monotherapy group, and 4 in the placebo group. (B) Change in LDL cholesterol over time. Mean percent change in LDL cholesterol concentrations from baseline during the 84 days following randomisation in the intention-to-treat population. The markers at day 28 represent the mean percent change as measured by the Martin–Hopkins estimation method. The markers at day 84 represent the least-squares mean percent change measured using beta quantification. An ANCOVA model with a fixed effect for the treatment group and a covariate of baseline LDL cholesterol was used to assess the primary efficacy parameter to obtain the values for the least-squares mean percent changes at day 84. The number of missing observations at day 84 were as follows: 3 in the FDC group, 5 in the obicetrapib monotherapy group, 5 in the ezetimibe monotherapy group, and 4 in the placebo group. (C) Change in non-HDL cholesterol over time. Mean percent change in non-HDL cholesterol concentrations from baseline during the 84 days following randomisation in the intention-to-treat population. The markers at day 28 and day 84 represent the mean percent change at each timepoint. The number of missing observations at day 84 were as follows: 3 in the FDC group, 5 in the obicetrapib monotherapy group, 5 in the ezetimibe monotherapy group, and 4 in the placebo group. (D) Change in apolipoprotein B over time. Mean percent change in apolipoprotein B concentrations from baseline during the 84 days following randomisation in the intention-to-treat population. The markers at day 28 and day 84 represent the mean percent change at each timepoint. The number of missing observations at day 84 were as follows: 3 in the FDC group, 6 in the obicetrapib monotherapy group, 5 in the ezetimibe monotherapy group, and 4 in the placebo group. In all panels, the error bars represent the 95% CIs. FDC=fixed-dose combination of obicetrapib and ezetimibe.

	Obicetrapib plus ezetimibe FDC (n=102)	Obicetrapib monotherapy (n=102)	Ezetimibe monotherapy (n=101)	Placebo (n=102)
Primary endpoint: least-squares mean percent difference in LDL cholesterol reduction (95% CI)				
Obicetrapib plus ezetimibe FDC	NA	-16.8 (-26.4 to -7.1)	-27.9 (-37.5 to -18.4)	-48.6 (-58.3 to -38.9)
Obicetrapib monotherapy	NA	NA	NA	-31.9 (-41.6 to -22.1)
Secondary endpoints				
Least-squares mean percent difference in non-HDL cholesterol reduction (95% CI)				
Obicetrapib plus ezetimibe FDC	NA	-15.2 (-23.5 to -6.9)	-25.4 (-33.7 to -17.2)	-45.1 (-53.4 to -36.8)
Obicetrapib monotherapy	NA	NA	NA	-29.9 (-38.3 to -21.5)
Least-squares mean percent difference in apolipoprotein B reduction (95% CI)				
Obicetrapib plus ezetimibe FDC	NA	-9.4 (-16.3 to -2.6)	-14.2 (-21.1 to -7.4)	-29.2 (-36.0 to -22.4)
Obicetrapib monotherapy	NA	NA	NA	-19.8 (-26.7 to -12.8)
Observed values for LDL cholesterol, mean (95% CI), mmol/L				
Baseline	2.5 (2.3 to 2.6)	2.6 (2.4 to 2.8)	2.5 (2.4 to 2.7)	2.4 (2.2 to 2.5)
Day 84*	1.3 (1.1 to 1.5)	1.7 (1.5 to 1.9)	2.0 (1.8 to 2.2)	2.5 (2.3 to 2.6)
Observed difference at day 84*	-1.2 (-1.3 to -1.0)	-0.9 (-1.0 to -0.7)	-0.5 (-0.7 to -0.3)	0.05 (-0.1 to 0.2)
FDC=fixed-dose combination. NA=not applicable. The conversion factor between conventional units and SI units for LDL is 38.67 mg/dL = 1 mmol/L. *Day 84 values and observed differences were calculated among patients with non-missing LDL cholesterol data at baseline and day 84, namely 99 patients in the obicetrapib plus ezetimibe FDC group, 97 patients in the obicetrapib monotherapy group, 96 patients in the ezetimibe monotherapy group, and 96 patients in the placebo group.				
Table 2: Efficacy endpoints in the intention-to-treat population				

Figure 3: Waterfall plots showing the distribution of individual LDL cholesterol responses in the treatment groups
Each vertical bar represents the percent change in LDL cholesterol measured by preparative ultracentrifugation for an individual patient in the treatment group from baseline to day 84 following randomisation in the intention-to-treat population. FDC=fixed-dose combination of obicetrapib and ezetimibe.



	Obicetrapib plus ezetimibe FDC (n=102)	Obicetrapib monotherapy (n=102)	Ezetimibe monotherapy (n=101)	Placebo (n=102)
Any adverse event	52 (51%)	55 (54%)	54 (53%)	38 (37%)
Trial agent-related adverse event	3 (3%)	7 (7%)	3 (3%)	4 (4%)
Adverse event leading to discontinuation of trial agent	5 (5%)	9 (9%)	7 (7%)	4 (4%)
Death	1 (1%)	1 (1%)	1 (1%)	0
Cardiogenic and septic shock	0	0	1 (1%)	0
Metastatic cancer	0	1 (1%)	0	0
Shock	1 (1%)	0	0	0
Serious adverse event	3 (3%)	6 (6%)	7 (7%)	4 (4%)
Cardiac disorders*	1 (1%)	1 (1%)	3 (3%)	1 (1%)
Infections†	0	2 (2%)	2 (2%)	0
Nervous system disorders‡	0	3 (3%)	1 (1%)	0
Respiratory, thoracic, and mediastinal disorders§	1 (1%)	1 (1%)	2 (2%)	0
Gastrointestinal disorders	0	0	3 (3%)	0
Hepatobiliary disorders	0	1 (1%)	1 (1%)	0
Neoplasms	0	1 (1%)	0	1 (1%)
Vascular disorders¶	1 (1%)	0	0	1 (1%)
Thrombocytopenia	0	1 (1%)	0	0
Chest pain	1 (1%)	0	0	0
Dehydration	0	1 (1%)	0	0
Accidents	0	0	0	1 (1%)
Osteoarthritis	1 (1%)	0	0	0
Acute kidney injury	1 (1%)	0	0	0
Prespecified events or laboratory findings of special interest				
AST or ALT >3 × ULN	0	2 (2%)	1 (1%)	0
Total bilirubin >2 × ULN	0	0	0	0
Creatine kinase >5 × ULN	1 (1%)	1 (1%)	0	0
New-onset diabetes or worsening of glycaemic control	31 (30%)	28 (27%)	42 (42%)	31 (30%)
Changes to or initiation of antihypertensive medications due to changes in blood pressure**	5 (5%)	4 (4%)	0	2 (2%)
Decrease of renal function from baseline††	7 (7%)	5 (5%)	6 (6%)	5 (5%)
Macular degeneration	0	0	0	0
Other adverse events and changes in vital signs				
Arthralgia	2 (2%)	7 (7%)	5 (5%)	3 (3%)
Upper respiratory tract infection	4 (4%)	4 (4%)	3 (3%)	3 (3%)
Diarrhoea	5 (5%)	3 (3%)	2 (2%)	0
Fatigue	4 (4%)	5 (5%)	0	1 (1%)
Headache	1 (1%)	6 (6%)	1 (1%)	2 (2%)
Hypokalaemia	0	0	4 (4%)	1 (1%)
Change in systolic blood pressure from baseline to day 84, mm Hg	-0.8 (13.2)	1.8 (12.7)	0.7 (12.6)	0 (13.6)
Change in diastolic blood pressure from baseline to day 84, mm Hg	-1.4 (7.6)	0.2 (7.2)	-0.9 (6.9)	0.2 (7.5)
Increase in blood pressure‡‡	2 (2%)	0	1 (1%)	0

Data are n (%) or mean (SD). ALT=alanine aminotransferase. AST=aspartate aminotransferase. FDC=fixed-dose combination. ULN=upper limit of normal. *Includes reported events of angina, acute myocardial infarction, atrial fibrillation, cardiomyopathy, congestive heart failure, and cardiogenic shock. †Includes reported events of appendicitis, pneumonia, urinary tract infection, and septic shock. ‡Includes reported events of stroke, cerebrovascular accident, transient ischaemic attack, and metabolic encephalopathy. §Includes reported events of acute respiratory failure, chronic obstructive pulmonary disease, and hypoxia. ¶Includes reported events of arterial haemorrhage, hypertension, and shock. ||Defined as one or more of the following criteria: adverse events indicating new type 1 or type 2 diabetes, initiation of anti-diabetes medication with confirmation of the diagnosis of diabetes by blinded external review, HbA_{1c} ≥6.5%, or two consecutive values of fasting plasma glucose ≥7.0 mmol/L (≥126 mg/dL). **Defined as changes in antihypertensive medications due to changes in blood pressure in participants receiving antihypertensive medication(s) at baseline, and new antihypertensive medication prescriptions in participants not previously treated for hypertension. ††Defined as a >25% decrease in estimated glomerular filtration rate (eGFR) from baseline, or an eGFR <30 mL/min/1.73 m² calculated using the Chronic Kidney Disease Epidemiology Collaboration equation, or an increase in serum creatinine of ≥0.3 mg/dL (≥26.5 μmol/L) from baseline. ‡‡Investigator-reported.

Table 3: Adverse events and safety-related laboratory findings in the safety population

Research in context

Evidence before this study

A PubMed search for all articles with the keywords “obicetrapib” and “ezetimibe” published from database inception to March 2, 2025 yielded two results of original research manuscripts. Of these, only one study, namely the ROSE2 trial, studied the combination of obicetrapib and ezetimibe. ROSE2 was a randomised phase 2 trial of obicetrapib plus ezetimibe for LDL cholesterol reduction, and provided initial data regarding the LDL cholesterol-lowering efficacy of obicetrapib plus ezetimibe in 97 patients with dyslipidaemia.

Added value of this study

The TANDEM study provides randomised phase 3 trial evidence, for the first time, regarding the LDL cholesterol-lowering efficacy, safety, and tolerability of an orally administered,

single-pill, fixed-dose combination (FDC) of obicetrapib 10 mg and ezetimibe 10 mg in patients with high risk for or pre-existing atherosclerotic cardiovascular disease (ASCVD). The FDC of obicetrapib and ezetimibe provided nearly 50% LDL cholesterol lowering compared with placebo and was generally well tolerated across 84 days.

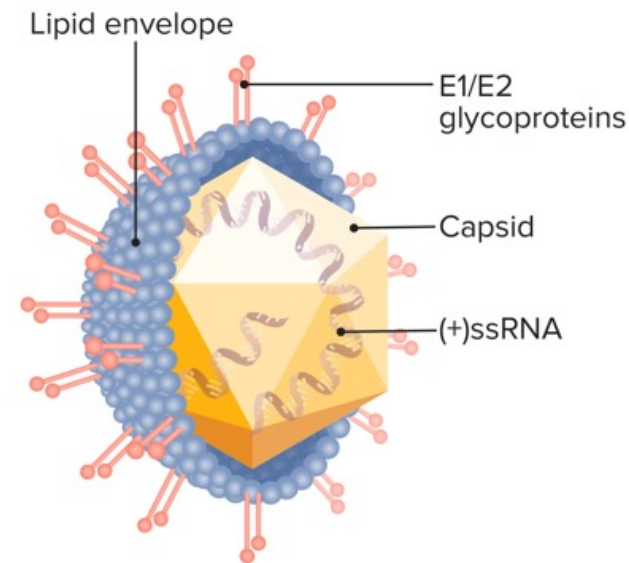
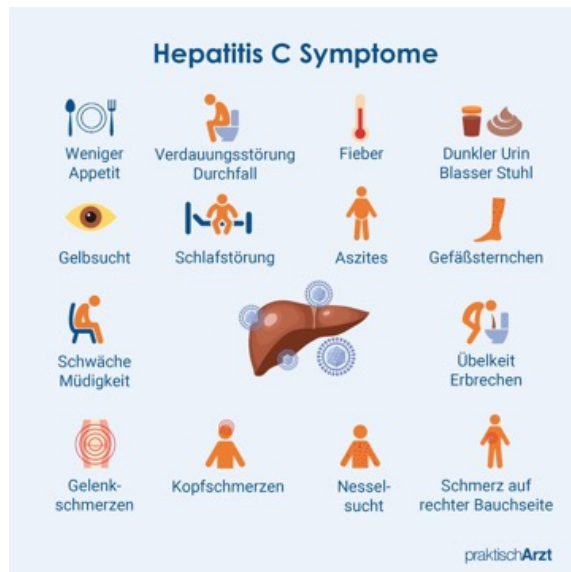
Implications of all the available evidence

Many patients with high risk for or pre-existing ASCVD do not meet LDL cholesterol treatment goals despite the use of intensive statin therapy and the availability of multiple classes of LDL cholesterol-lowering drugs. The FDC of obicetrapib and ezetimibe could offer an orally administered, tolerable, single-pill therapy to improve LDL cholesterol management in these high-risk patients who can be challenging to treat.

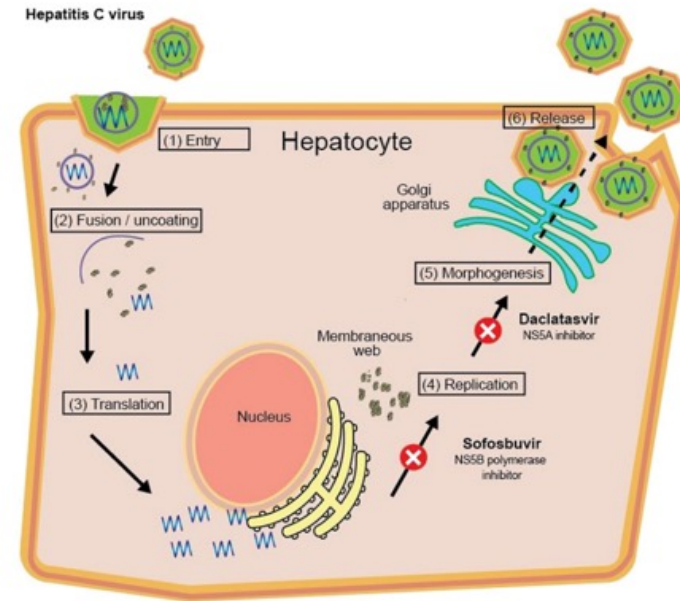
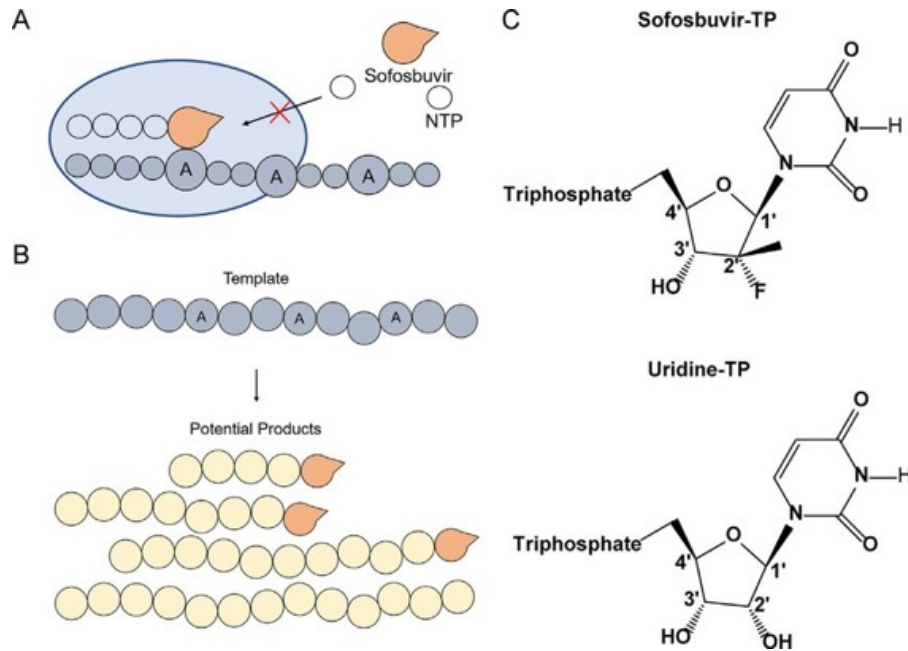
Die Hepatitis C ist eine Virushepatitis, welche meistens chronisch verläuft. Sie war vor Entdeckung ihres Erregers im Jahr 1990 für eine Vielzahl von transfusionsbedingten Hepatitiden verantwortlich, da sie mit Blutprodukten übertragen wurde (sog. Posttransfusionshepatitis).

Erreger der Hepatitis C ist das Hepatitis-C-Virus (HCV). Es ist ein einzelsträngiges RNA-Virus (ssRNA(+)) aus der Gruppe IV der Baltimore-Klassifikation und gehört zur Familie der Flaviviridae. Beim Hepatitis-C-Virus sind 7 Genotypen und über 100 verschiedene Subtypen mit modifizierten Eigenschaften bekannt. Eine Mehrfachinfektion mit verschiedenen Subtypen ist möglich, eine einmalige Infektion schützt daher nicht vor erneuter Infektion.

Durch die immunologischen Besonderheiten eines RNA-Virus bedingt ist die Entwicklung einer wirksamen Impfung gegen Hepatitis C bisher nicht gelungen. Es befinden sich aber einige vielversprechende Impfstoffe in der Entwicklung.



Sofosbuvir ist ein antivirales Medikament, das in der Behandlung der chronischen Hepatitis C eingesetzt wird. Es fungiert als Prodrug, das im Körper zu einem aktiven Uracil-Nukleotid-Analogon umgewandelt wird und selektiv die RNA-abhängige RNA-Polymerase (NS5B) des Hepatitis-C-Virus hemmt.



Daclatasvir ist ein antiviraler Wirkstoff, der selektiv die NS5A-Proteinfunktion des Hepatitis C-Virus inhibiert und so die virale RNA-Replikation und Virionenmontage blockiert. Es wird hauptsächlich in Kombinationstherapien zur Behandlung von chronischer Hepatitis C verschiedener Genotypen eingesetzt.

Treatment options to support the elimination of hepatitis C: an open-label, factorial, randomised controlled non- inferiority trial

Summary

Background WHO recommends treating hepatitis C infection with one of three antiviral combinations for 8–12 weeks. No randomised trials have compared these regimens, and high cure rates might be achievable with shorter durations of therapy. We aimed to compare sofosbuvir–daclatasvir with sofosbuvir–velpatasvir, and to evaluate potential novel treatment strategies.

Methods We conducted a multi-arm, open-label, randomised controlled non-inferiority trial in two public hospitals in Viet Nam. Adults (aged ≥ 18 years) with chronic hepatitis C infection and mild-to-moderate liver fibrosis were eligible. Recruitment was stratified by centre and viral genotype (1–5 vs 6) with 1:1 random allocation to an oral fixed-dose combination of sofosbuvir 400 mg plus daclatasvir 60 mg (sofosbuvir–daclatasvir) or sofosbuvir 400 mg plus velpatasvir 100 mg (sofosbuvir–velpatasvir). Participants were simultaneously factorially randomly assigned to one of four treatment strategies: 12 weeks' standard of care (SOC); 4 weeks' therapy with four weekly PEGylated interferon alfa-2a subcutaneous injections; induction and maintenance therapy with 2 weeks' standard therapy followed by 10 weeks' therapy 5 days a week; and response-guided therapy (RGT) for 4, 8, or 12 weeks determined by viral load on day 7. The primary outcome was sustained virological response (SVR) 12 weeks after treatment completion, analysed in all evaluable participants regardless of actual treatment received. We chose a 5% non-inferiority margin for the drug comparison, and a 10% non-inferiority margin for the treatment strategy comparisons. Safety was assessed in all randomised participants. This trial is registered with ISRCTN, 61522291, and is completed.

Findings Between June 19, 2020, and May 10, 2023, 624 participants were randomised (470 [75%] were male and 154 [25%] were female). 296 (47%) had genotype 6 and 328 (53%) had genotypes 1–5. The primary outcome was assessable in 609 (98%) participants. SVR occurred in 294 (97%) of 302 participants in the sofosbuvir–daclatasvir group and 292 (95%) of 307 participants in the sofosbuvir–velpatasvir group (risk difference 2.2%, 90% credible interval [CrI] –0.2 to 4.8, within the 5% non-inferiority margin; 93% probability that sofosbuvir–daclatasvir is superior to sofosbuvir–velpatasvir). SVR occurred in 148 (99%) of 150 in the SOC group, 143 (94%) of 152 in the 4-week antiviral plus interferon group (–4.5%, 90% CrI –8.3 to –1.3), 151 (99%) of 152 in the induction–maintenance group (0.6%, –1.1 to 2.7), and 144 (93%) of 155 in the RGT group (–5.7%, –9.6 to –2.3); all risk differences were within the 10% non-inferiority margin. Serious adverse events were rare (11 [4%] of 313 participants in the sofosbuvir–velpatasvir group *vs* six [2%] of 311 in the sofosbuvir–daclatasvir group; risk difference –1.6% [95% CrI –4.2 to 0.8]) with no evidence of differences between regimens or strategies, but adverse reactions were very common in the 4-week antiviral plus interferon group compared with the other treatment strategies (risk difference *vs* SOC group, 66.8% [59.2 to 74.0]; $p < 0.0001$).

Interpretation Sofosbuvir–daclatasvir was non-inferior to sofosbuvir–velpatasvir. High efficacy was seen with novel strategies, which might help to inform approaches to treatment for harder-to-reach populations.

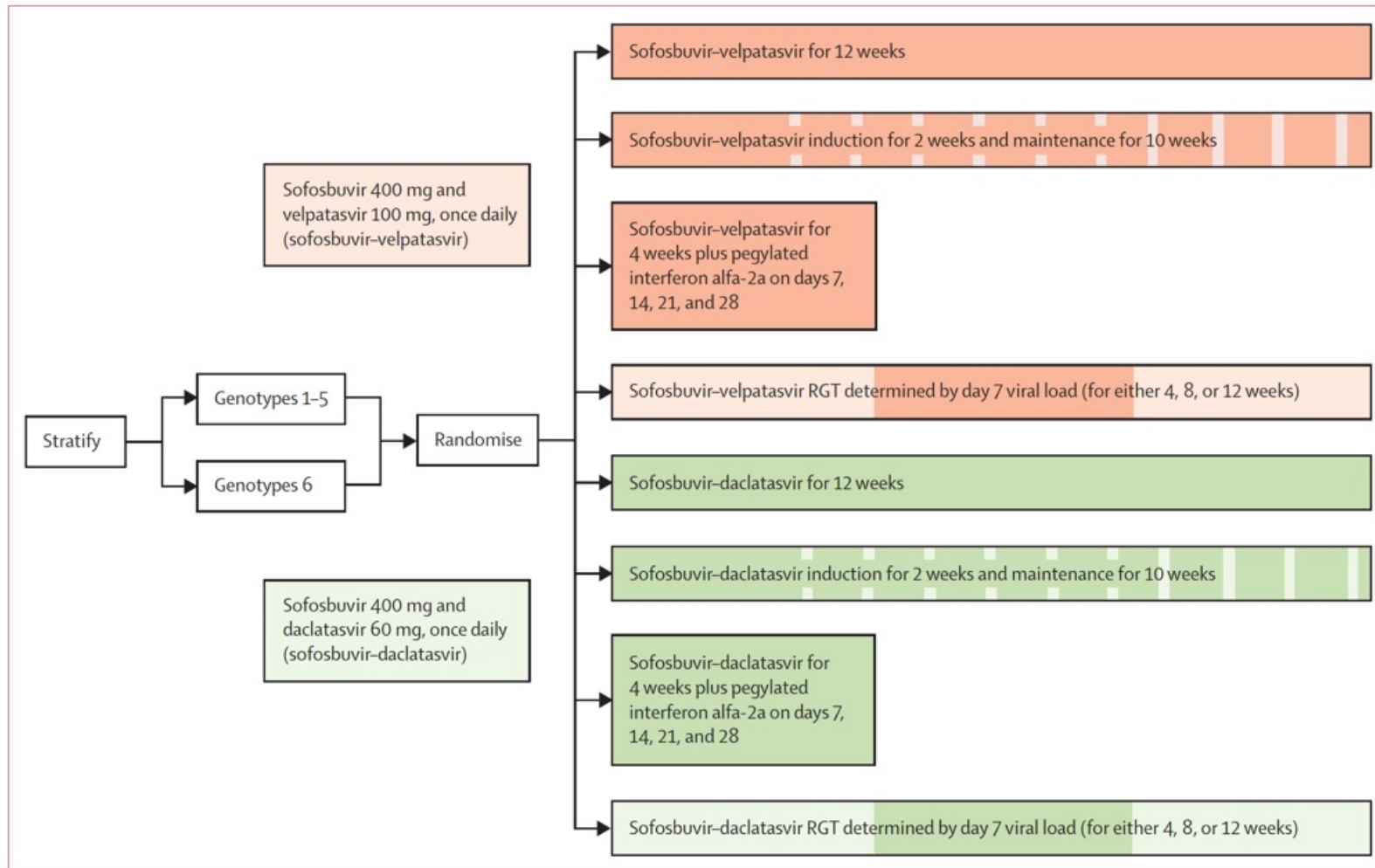


Figure 1: Trial design

Random assignment was stratified by centre and viral genotype. RGT=response guided therapy.

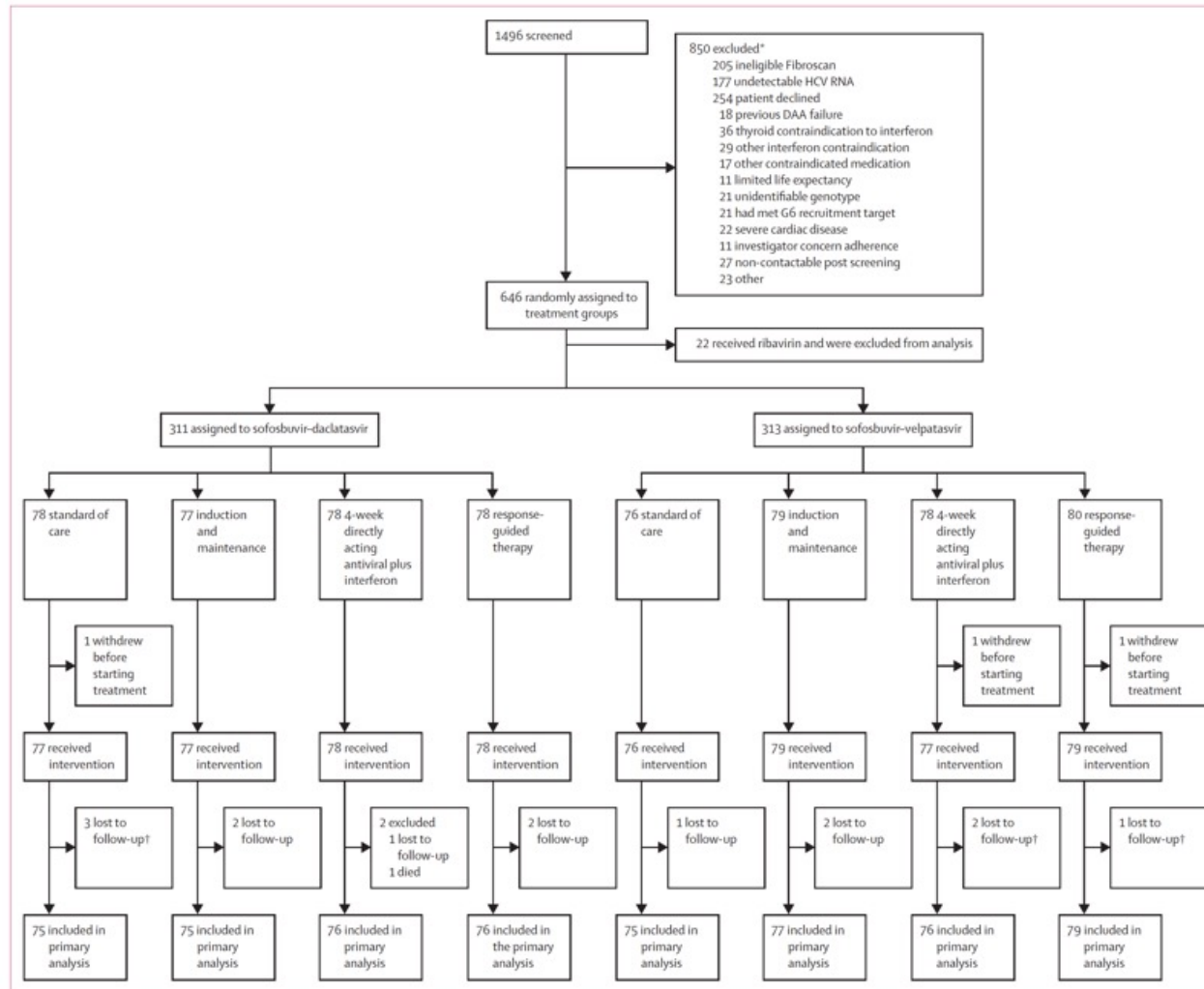


Figure 2: CONSORT diagram

Three participants withdrew immediately after random assignment without starting treatment so could not be evaluated for the primary endpoint. DAA=direct-acting antiviral. HCV=hepatitis C virus. SOC=standard of care. *Individuals might have had more than one reason for exclusion. †One patient lost to follow-up in this group was still eligible for inclusion in the primary analysis as they had provided data for viral load at 12 weeks after end of treatment (appendix p 5).

	Treatment combination		Treatment strategy			
	Sofosbuvir-velpatasvir (n=313)	Sofosbuvir-daclatasvir (n=311)	Standard of care (n=154)	Induction and maintenance (n=156)	4-week antiviral plus interferon (n=156)	Response-guided therapy (n=158)
Age, years	42 (37-50)	42 (37-51)	43 (37-50)	42 (36-49)	43 (39-52)	42 (36-53)
Sex						
Female	80 (26%)	74 (24%)	40 (26%)	36 (23%)	38 (24%)	40 (25%)
Male	233 (74%)	237 (76%)	114 (74%)	120 (77%)	118 (76%)	118 (75%)
BMI, kg/m ²	22.0 (20.3-24.5)	22.3 (20.3-24.4)	21.9 (20.3-24.9)	22.4 (20.4-24.5)	22.5 (20.7-24.6)	21.9 (19.8-24.0)
HCV viral load, log ₁₀ IU/mL	6.1 (1.1)	6.1 (1.0)	6.0 (1.0)	6.2 (1.1)	6.1 (1.0)	6.1 (1.1)
HCV genotype						
1	131 (42%)	126 (41%)	61 (40%)	62 (40%)	66 (42%)	68 (43%)
2	21 (7%)	28 (9%)	11 (7%)	14 (9%)	13 (8%)	11 (7%)
3	13 (4%)	9 (3%)	8 (5%)	6 (4%)	4 (3%)	4 (3%)
6	148 (47%)	148 (48%)	74 (48%)	74 (47%)	73 (47%)	75 (48%)
Fibroscan result, kPa	6.2 (5.1-7.4)	6.1 (5.0-7.1)	6.2 (5.3-7.2)	6.2 (5.0-7.4)	6.0 (5.0-7.0)	6.1 (4.9-7.6)
Missing data	4	5	6	0	2	1
HIV positive	41 (13%)	42 (14%)	21 (14%)	22 (14%)	18 (12%)	22 (14%)
HBsAg positive	16/312 (5%)	23/311 (7%)	8/154 (5%)	9/156 (6%)	14/152 (9%)	8/157 (5%)
IFNL4 genotype						
CC	270/312 (87%)	263/310 (85%)	137/153 (90%)	128/156 (82%)	132/155 (85%)	136/158 (86%)
CT	17/312 (5%)	22/310 (7%)	6/153 (4%)	11/156 (7%)	13/155 (8%)	9/158 (6%)
TT	25/312 (8%)	25/310 (8%)	10/153 (7%)	17/156 (11%)	10/155 (6%)	13/158 (8%)

Data are median (IQR), n (%), or n/N (%) when the denominator differs from that in the column heading. All standardised mean differences (data not shown) are <0.2 suggesting small differences.¹²

Table 1: Baseline characteristics by treatment combination and treatment strategy

	Treatment combination		Treatment strategy			
	Sofosbuvir-velpatasvir (n=313)	Sofosbuvir-daclatasvir (n=311)	Standard of care (n=154)	Induction and maintenance (n=156)	4-week acting plus interferon (n=156)	Response-guided therapy (n=158)
Primary outcome						
Number assessable	307 (98.1%)	302 (97.1%)	150 (97.4%)	152 (97.4%)	152 (97.4%)	155 (98.1%)
SVR 12 weeks after end of first-line treatment	292/307 (95.1%)	294/302 (97.4%)	148/150 (98.7%)	151/152 (98.7%)	143/152 (94.1%)	144/155 (92.9%)
Primary efficacy comparison (90% CrI)	1 (ref)	2.2% (-0.2 to 4.8); P=0.069	1 (ref)	0.6% (-1.1 to 2.7); P=0.26	-4.5% (-8.3 to -1.3); P=0.99	-5.7% (-9.6 to -2.3); P=1.00
Stratification subgroup						
Genotypes 1-5	152/162 (93.8%)	153/159 (96.2%)	78/78 (100.0%)	79/80 (98.8%)	73/82 (89.0%)	75/81 (92.6%)
Genotype 6	140/145 (96.6%)	141/143 (98.6%)	70/72 (97.2%)	72/72 (100.0%)	70/70 (100.0%)	69/74 (93.2%)
Secondary outcomes						
SVR 12 weeks after first-line and any re-treatment	305/307 (99.3%)	302/302 (100.0%)	150/150 (100.0%)	151/152 (99.3%)	151/152 (99.3%)	155/155 (100.0%)
No initial virological response*	3/311 (1.0%)	1/310 (0.3%)	0/153	2/156 (1.3%)	0/155	2/157 (1.3%)
Data are n (%) or n/N (%), unless otherwise specified. P indicates the one-sided probability that the difference versus the reference is less than zero from the Bayesian model and is not a frequentist p value. CrI=credible interval. SVR=sustained virological response. *Not possible to calculate 90% CrI or P for the strategy comparisons due to zeros in the reference and other groups.						
Table 2: Efficacy outcomes						

	Treatment combination		Treatment strategy			
	Sofosbuvir–velpatasvir (n=313)	Sofosbuvir–daclatasvir (n=311)	Standard of care (n=154)	Induction and maintenance (n=156)	4-week antiviral plus interferon (n=156)	Response-guided therapy (n=158)
Serious adverse events	11 (3.5%); 13 events	6 (1.9%); 6 events	4 (2.6%); 4 events	3 (1.9%); 3 events	4 (2.6%); 5 events	6 (3.8%); 7 events
Prolonged hospitalisation	11 events	5 events	4 events	3 events	3 events	6 events
Died	0	1 event	0	0	1 event	0
Other important medical condition	2 events	0	0	0	1 event	1 event
Risk difference in serious adverse events (95% CrI)	1 (ref)	-1.6% (-4.2 to 0.8); P=0.90	1 (ref)	-0.6% (-4.1 to 2.6); P=0.66	0.0% (-3.6 to 3.5); P=0.51	1.2% (-2.7 to 5.2); P=0.26
Adverse reactions	59 (18.8%); 89 events	66 (21.2%); 88 events	5 (3.2%); 5 events	6 (3.8%); 7 events	109 (69.9%); 160 events	5 (3.2%); 5 events
Risk difference in adverse reactions (95% CrI)	1 (ref)	2.3% (-1.9 to 6.3); P=0.14	1 (ref)	0.6% (-3.4 to 4.8); P=0.38	66.8% (59.2 to 74.0); P<0.0001	-0.1% (-3.9 to 3.9); P=0.51
Changed study drugs due to adverse event	4 (0.6%); 5 events	0	0	0	4 (2.6%); 5 events	0
Grade 3 or 4 adverse events	5 (0.8%); 5 events	0	0	1 (0.6%); 1 event	3 (1.9%); 3 events	1 (0.6%); 1 event
3	5 events	0	0	1 event	3 events	1 event
4	0	0	0	0	0	0

Data are number (%) of participants who had that event, number of events, or both, unless otherwise indicated. P indicates the one-sided probability that the difference versus reference is less than zero from the Bayesian model and is not a frequentist p value. CrI=credible interval.

Table 3: Safety outcomes

Research in context

Evidence before this study

WHO recommends three alternative first-line treatments for treatment of chronic hepatitis C; sofosbuvir–daclatasvir, sofosbuvir–velpatasvir, and glecaprevir–pibrentasvir. Sofosbuvir–daclatasvir and sofosbuvir–velpatasvir are widely available in low-income countries through generic suppliers and countries vary in their preference for first-line therapy. However, prices vary widely and remain a barrier to access to care in many settings. We searched PubMed and Embase for articles published between Jan 1, 2010, and Dec 31, 2024, using the terms “hepatitis”, “sofosbuvir”, “daclatasvir”, “velpatasvir”, “glecaprevir/pibrentasvir”, “trials”, and “RCT”. We found that there have been no previous head-to-head studies to compare the efficacy of these first-line treatments. As national efforts make progress in scaling treatment, elimination of hepatitis C will be challenged by a small but substantial proportion of patients who require shorter or supervised therapy to be cured. There is a limited evidence base to inform treatment in these groups, a gap highlighted in previous WHO guidelines.

Added value of this study

This study is the first head-to-head study of WHO recommended hepatitis C therapy, comparing two options widely available in low-income settings. We found that

sofosbuvir–daclatasvir was non-inferior to sofosbuvir–velpatasvir. We demonstrate the high efficacy of the treatment combinations studied and, contrary to expectation, a 93% probability that sofosbuvir–daclatasvir was superior to sofosbuvir–velpatasvir in this trial. In addition to the primary comparison of sofosbuvir–velpatasvir and sofosbuvir–daclatasvir, the factorial design allowed exploration of possible strategies that might be suitable for individuals who find 12-week therapy challenging because of either lifestyle or cost. This study found high efficacy (>90%) with three novel potential treatment strategies, all of which were non-inferior to standard of care.

Implications of all the available evidence

This study finds evidence to support the use of sofosbuvir–daclatasvir and sofosbuvir–velpatasvir in first-line treatment options. These data will be valuable to national programmes procuring treatment. For most countries scaling treatment, simplicity and standardised treatment is key. For settings with more advanced elimination programmes, the alternative strategies explored in this study can inform more individualised therapeutic decisions for those struggling to access care (eg, through supervised therapy).

Opportunities for chronic pain self-management: core psychological principles and neurobiological underpinnings

One in five of the population lives with chronic pain. Psychological interventions for pain reveal core principles that can be used to create opportunities for chronic pain self-management in primary practice, across health-care settings, and at home. We highlight the different types of chronic pain and illustrate the psychoneurobiological mechanisms involved. We review core principles for psychological pain management, evaluate the evidence, and illustrate the underlying neurobiology involved. We provide practical advice for how to facilitate pain self-management in clinical practice. Finally, we discuss scientific caveats and practical obstacles to improvement, suggesting possible pathways to implementation.

Panel: Definitions and classifications of pain

The International Association for the Study of Pain (IASP) definition of pain^{6,7}

Pain:

An unpleasant sensory and emotional experience associated with, or resembling that associated with, actual or potential tissue injury.

Notes:

- Pain is always a personal experience that is influenced to varying degrees by biological, psychological, and social factors
- Pain and nociception are different phenomena: the experience of pain cannot be reduced to activity in sensory pathways
- Through their life experiences, individuals learn the concept of pain and its application
- A person's report of an experience as pain should be accepted as such and respected*
- Although pain usually serves an adaptive role, it may have adverse effects on function and social and psychological wellbeing
- Verbal description is only one of several behaviours to express pain; inability to communicate does not negate the possibility that a human or a non-human animal experiences pain

Etymology

Middle English, from Anglo-French *peine*, from Latin *poena* (penalty, punishment), in turn from Greek *poin* (payment, penalty, recompense).

ICD-11 classification of chronic primary pain and secondary pain syndromes

Chronic primary pain⁸

Defined as pain in one or more anatomical regions that:

- Persists or recurs for longer than 3 months;
- Is associated with significant emotional distress (eg, anxiety, anger, frustration, or depressed mood) or significant functional disability (interference in activities of daily life and participation in social roles), or both;
- Has symptoms not better accounted for by another diagnosis

Examples of diagnostic entities within this category are widespread pain (eg, fibromyalgia) and complex regional syndromes.

Chronic secondary pain⁹

Defined as syndromes that are linked to other diseases as the underlying cause for which pain may initially be regarded as a symptom. Examples of diagnostic entities within this category are chronic cancer-related pain and chronic postsurgical or post-traumatic pain.

Three main categories of chronic pain⁷

- Nociceptive pain arises from actual or threatened damage to non-neural tissue and is due to the activation of nociceptors
- Neuropathic pain is caused by a lesion or disease of the somatosensory nervous system
- Nociplastic pain arises from altered nociception despite no clear evidence of actual or threatened tissue damage causing the activation of peripheral nociceptors or evidence for disease or lesion of the somatosensory system causing the pain

	Description	Example
Education	Learning that pain is not always due to illness, injury, or disease; learning how pain behaviour might lead to undesired outcomes; learning the role emotion can play in pain severity	Responding to chronic pain as if it was acute pain might lead to dysfunctional avoidance, withdrawal, and substantial personal loss; what appears defensive and protective can actually be harmful
Problem framing	Identifying problem frames and how to define solutions; learning to experiment with alternative problem definitions and experiment with different solutions	Persevering or perseverating with any behaviour (eg, fixating on losses, taking medication, and sleeping in the daytime), even though they have not worked in the past
Values determination	Identifying what is important to oneself in life; recognising how much of life is not often in the service of these values; recognising how pain changes the focus away from what one values	Pain can distract one into working hard to do the wrong things; identifying what one values most in life can be powerful because it is rarely something we allow ourselves to do; identifying how pain and our response to pain frustrate our attempts to do what is important to us can be a valuable insight for change
Goal setting	Identifying goals and tasks that can help one reach those values; learning to break down tasks into manageable and achievable activities; pacing our attempts to meet those goals, which can take time and effort; establishing goal-contingent behaviour, not pain-contingent behaviour	Identifying a goal and the substeps to reach that goal; for example, if the value is independence and the goal is to wash one's own hair, then breaking down the goal into tasks and subtasks (eg, collecting necessary products, creating time, and working on physical mobility to raise arms above head)
Relaxation training	Identifying the role of physiological arousal and its effects on pain by bringing attention to the body; identifying how much of life is focused on the future and the past and bringing attention to the now; attempting different relaxation techniques for these purposes, such as mindfulness meditation, biofeedback, and yoga	Use a relaxation protocol or mindfulness meditation technique
Automatic thought detection and defusion	Recognising the automaticity of thoughts about pain and its feared consequences, and the strong and fixed belief in the reality of those thoughts, as if they must have intrinsic truth value; challenging their veracity and replacing them or observing them as separate from self; identifying core beliefs that underpin automatic thought and exploring how those beliefs shape outcomes	Common unhelpful thoughts: pain must be a signal of damage, something must have been missed, I cannot move because I have a damaged body, I am going to be overwhelmed by this pain and everything will go horribly wrong, or I will never be able to cope with this; core beliefs that underpin these automatic thoughts could be related to pain, body, or self: pain is always a sign of damage, pain is something my body is too fragile to cope with, or pain is something I cannot and should not bear
Exposure	Identifying a feared object or setting; graded exposure to the characteristics of the feared object; learning that one can survive exposure to the feared object; challenging safety behaviours	Fear of entering a busy or crowded room because of being bumped into, which will make my pain so much worse; working slowly on doing what one least wants to do because it hurts, but recognising that doing it will be better in the long term; doing what one most fears and finding that it does not lead to the feared outcome (finding non-confirmatory evidence of fears)

Psychological therapy for pain self-management involves a range of interventions. Classic interventions, such as cognitive behavioural therapy, involve combinations of the specific factors listed. All psychological interventions for pain self-management are delivered with a focus on many of the central non-specific factors.

Table 1: Specific elements of psychological interventions for pain self-management

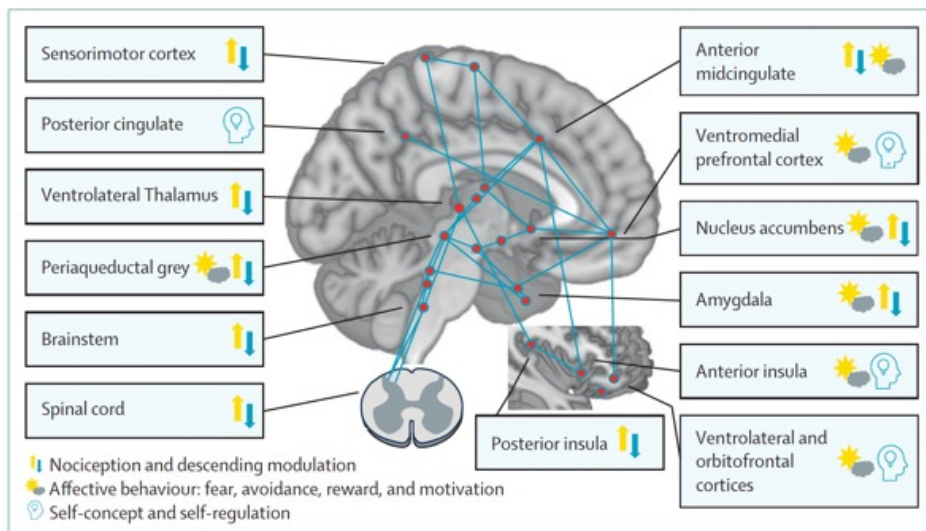


Figure 1: Psychoneurobiological underpinnings of the experience of chronic pain

The experience of pain encompasses sensory-discriminative, motivational-affective, and cognitive-evaluative characteristics. The neurobiological underpinnings of the pain experience are emerging and changes in multiple systems appear, including ascending pathways carrying pain-related information to the brain and descending modulation of nociceptive input; affective behaviours such as fear, avoidance, reward, and exploration; and in humans, some of these systems are also integral to our self-concept and self-regulation. The icons suggest some of the primary functions played by the key regions. Each region has multiple functions, in keeping with the interlinked nature of pain, motivation, and cognition. The information has been obtained from human neuroimaging and electrophysiological studies and the neuroplastic alterations in pathways and circuits that appear to contribute to pain behaviours are being elicited by mechanistic studies in non-human animals. The pink circles suggest brain regions that are altered in animal models of persistent pain, such as partial nerve injury, and the blue lines suggest anatomical connections that group them into pathways and systems. For further information on the emerging neurocircuitry underlying chronic pain, please see the appendix.

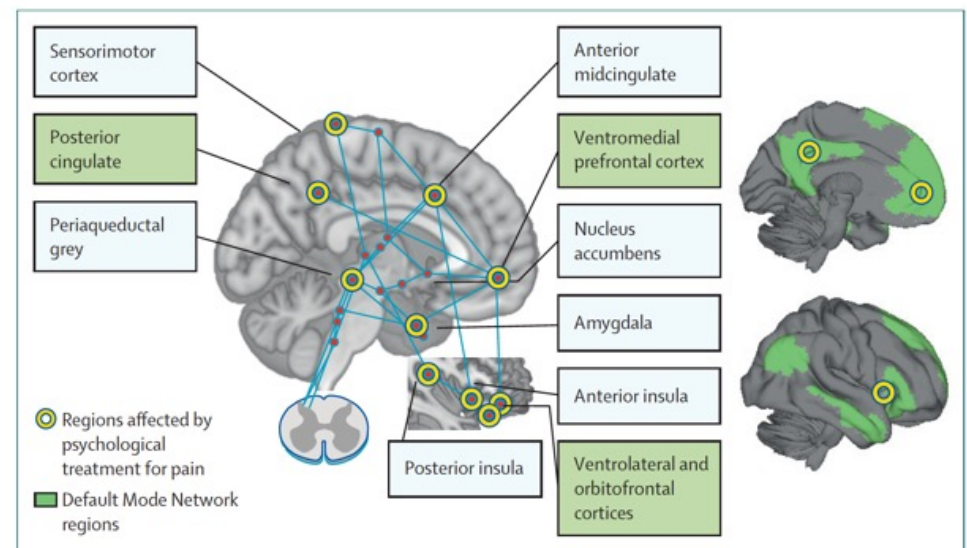


Figure 2: Psychological interventions for chronic pain and alterations in neurobiological underpinnings

Brain imaging studies suggest that psychological interventions for chronic pain could induce alterations in a subset of the regions (yellow circles) known to be involved in chronic pain in mechanisms studies (red dots; figure 1). The evidence base to date is small and immature, but the alterations appear to include reduced activity, connectivity, or both in regions associated with nociceptive processing and descending modulation (eg, sensorimotor cortices, periaqueductal grey, and posterior and mid-insula). The alterations also seem to involve changes in areas, highlighted in green, that are part of the Default Mode Network; a network of regions associated with the sense of self, self-regulation, and emotional experiences that has been suggested to help shape motivated behaviour and the bodily physiological processes. This emerging picture is incomplete, and further large-scale, well-controlled neuroimaging studies of psychological pain treatments are needed.

	Description
Working alliance	Creating and maintaining a shared investment and commitment to the patient's desire for self-management; fostering mutual respect; finding opportunities for challenge while in alliance
Validation	Recognising and affirming the emotional validity of suffering; non-judgmental, non-reactive listening; resisting problem solving; promoting empathic witnessing
Behavioural activation	Moving in pain; moving in and upon the world; acting counter to pain
Practice	Homework tasks; planning and reward for practice of new skills
Reinforcement scheduling	Identifying the antecedents of problem behaviours; reinforcing alternate behaviours; scheduling the reinforcement to best fit the context

Psychological therapy for pain self-management involves a range of interventions. Classic interventions, such as cognitive behavioural therapy, involve combinations of the specific factors listed. All psychological interventions for pain self-management are delivered with a focus on many of the central non-specific factors.

Table 2: Non-specific elements of psychological interventions for pain self-management

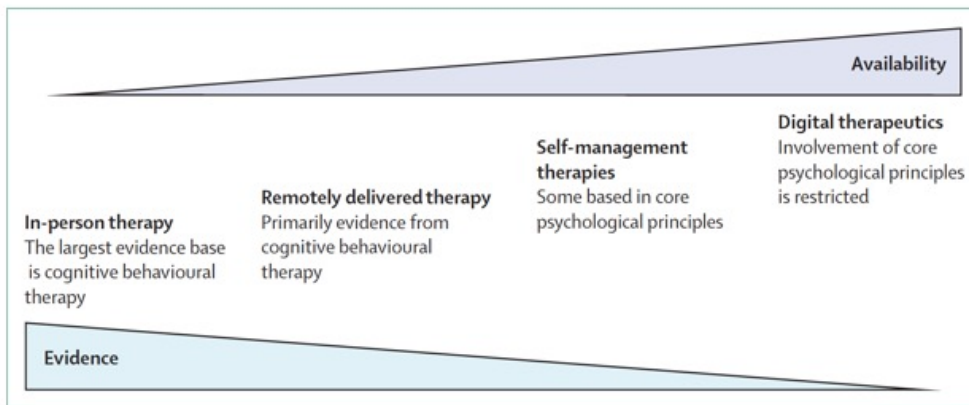


Figure 3: Development in psychological-based interventions for chronic pain self-management

Psychological interventions have developed from in-person therapy to internet-based and digital therapies and apps. In this process, therapies have become broadly available, although evidence is still scarce. To date, cognitive behavioural therapy trials provide the largest base of evidence. In large Cochrane reviews, in-person cognitive behavioural therapy interventions have shown effect compared with active control interventions,³⁹ and remotely delivered cognitive behavioural therapy interventions have shown effect compared with treatment as usual.⁶⁴ A variety of protocols to assist pain self-management have developed; some are based in core psychological principles and most are tested primarily in comparison to treatment as usual, so replication and carefully matched control conditions are needed.⁶⁵ The rapid development in digital therapeutics has insufficient evidence to date.

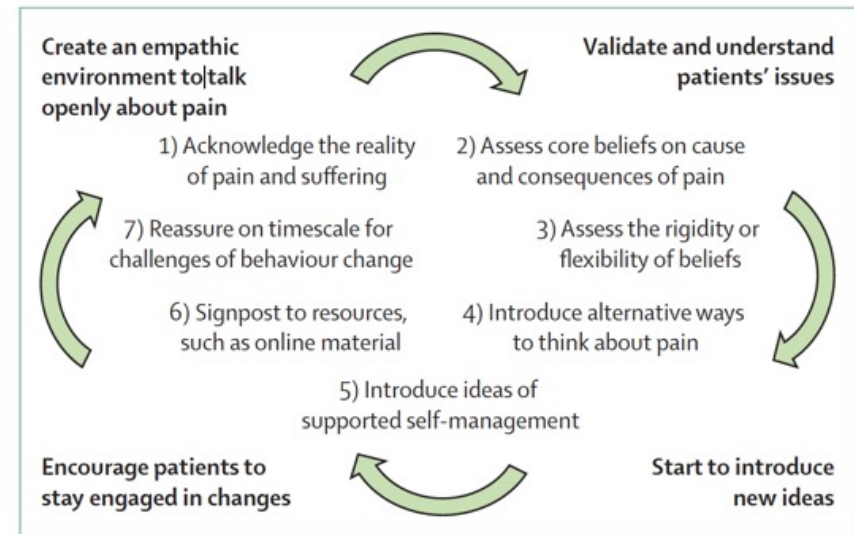


Figure 4: Opportunities for promoting self-management in health-care consultations

Both specific and non-specific content and approach should be planned and managed. Non-specific influences include courageously challenging fear and safety signals, setting realistic expectations, validating experiences, and delivering all with empathy and openness. Specific components include addressing the repetitive rigidity of thoughts and behaviours that do not serve positive outcomes. The emphasis is on function: how far beliefs bring about desired change or how far they promote the unwanted status quo. All behaviour happens in social contexts in which change requires opportunity, support, resources, and attention to maintenance, including managing inevitable setbacks.

Future directions

We have argued that the principles of evidence-based psychological interventions can and should be applied more generally, not only in specialised pain care services, but also in health care more broadly. However, these principles emerge from the successful treatment of those with high-impact chronic pain, delivered by psychologists trained in pain management. However, some studies of attempts to broaden awareness to the community have been negative^{90,91} and although we have argued for an emphasis on all clinical interactions being therapeutic opportunities, it remains unclear how far these low-intensity interventions can be delivered by non-psychologists, or exactly which content they should focus on. There is also need for a classification of intervention content and a standardisation of language of intervention to help innovation and evidence generation. Clarity over common features and components of intervention is needed. The specific and non-specific content and understanding dose, timing, order, and any interactive effects will also help guide the design of the placebo comparators necessary for establishing efficacy and safety.

Furthermore, greater investment in mechanistic studies is needed. The challenge is to bring together different levels of explanation. It could be possible to identify neurobiological changes associated with psychological interventions, but these only make sense in the context of well-defined cognitive or learning mechanisms. Furthermore, this mechanistic view is not just about change, but failure to change. A focus on treatment resistance, on how both pain and disabling pain behaviour can become stuck, is a priority for mechanistic studies to help overcome it.⁹²

Finally, our shift from specialised health-care intervention to the community focuses on primary care and health-care consultations. We recognise that these clinical encounters are only one place in which beliefs about pain and pain behaviour are formed and reformed. A more systemic approach would include opportunities to apply these principles in the workplace^{93,94} using social media,⁹⁵ in public health campaigns,⁹⁶ and ideally in a developmentally sensitive approach.^{97,98} Ultimately, there is a need to incorporate a more sociocultural understanding of how to change the experience of pain.⁸⁸

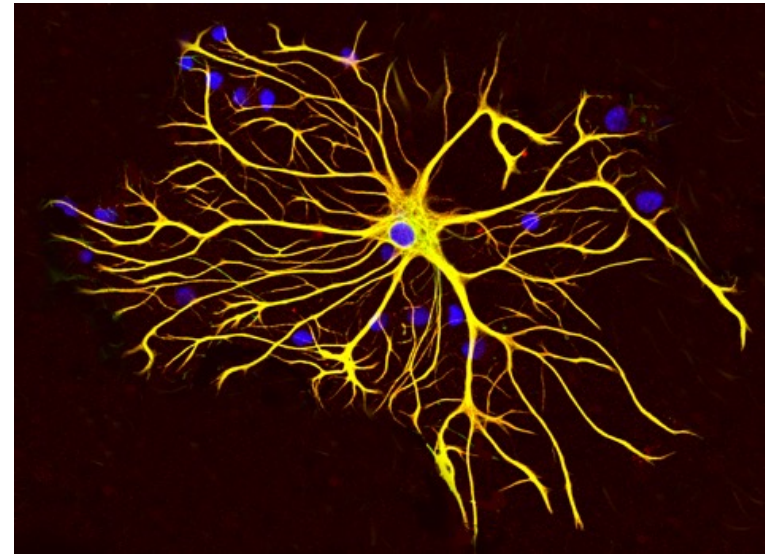
Astrozyten sind Gliazellen, die den Großteil der Zellen im Zentralnervensystem (ZNS) ausmachen. Sie haben vielfältige Funktionen, darunter metabolische, strukturelle, homöostatische und neuroprotektive Aufgaben. Es sind stern- bzw. spinnenförmig verzweigte Zellen, deren Fortsätze Grenzmembranen zur Gehirnoberfläche (bzw. zur Pia mater) und zu den Blutgefäßen bilden. Mit ihren zahlreichen Zellausläufern bilden die Astrozyten ein stabiles Grundgerüst zwischen den Nervenzellen.

•Metabolische Funktionen:

•Astrozyten spielen eine wichtige Rolle im Energiestoffwechsel des Gehirns, indem sie Glucose aufnehmen, in Laktat umwandeln und dieses an Neurone abgeben. Sie speichern auch Glykogen und können bei Bedarf Glucose für die Neurone zur Verfügung stellen.

Homöostatische Funktionen:

Astrozyten regulieren die Konzentration von Neurotransmittern, Kalium und anderen Ionen im Gehirn, um die neuronale Aktivität zu stabilisieren und die Homöostase aufrechtzuerhalten.



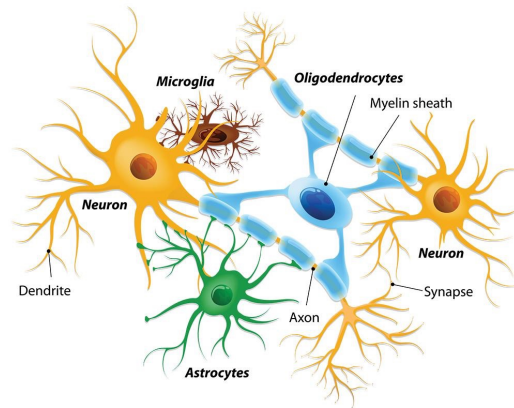
Astrocytes, a type of glial cell, originate from radial glial cells located in the ventricular zone of the developing brain. These radial glial cells act as a source of both neurons and astrocytes during development. In addition to radial glial cells, astrocytes can also be generated from progenitor cells in the subventricular zone (SVZ) and from locally proliferating glia within the cortex.



Astrocytes, hidden puppet masters of the brain

Astrocyte signaling pathways influence neuronal networks and behavioral responses to neuromodulators

It is accepted that neuromodulators such as norepinephrine and dopamine bind to and activate receptors on neurons to influence the activity of neuronal circuits and plasticity (changes in strength or wiring patterns) of synaptic connections, thus shaping the behavior of the organism. Unlike classical neurotransmitters (e.g., glutamate), which typically mediate fast, point-to-point synaptic communication, neuromodulators diffuse broadly through neural tissue to regulate the strength, duration, and plasticity of neuronal signaling. Emerging evidence now implicates astrocytes—traditionally seen as passive support cells—as active players in neuromodulation.- However, whether astrocytes are necessary intermediaries in neuromodulation or represent regulatory adjuncts to neuronal actions is unclear. On pages 763, 769, and 776 of this issue, Guttenplan *et al.*, Chen *et al.*, and Lefton *et al.*, respectively, address these gaps in knowledge by reporting that astrocytes are indispensable for neuromodulatory signaling across diverse neural circuits, behavioral contexts, and species.



The studies by Guttenplan *et al.*, Chen *et al.*, and Lefton *et al.* establish astrocytes as active intermediaries linking neuromodulators directly to neuronal activity and behavior. Together, these findings position astrocytes as essential nodes in neural signaling networks. Several key questions remain, such as why did astrocytes evolve to serve as intermediaries in neuromodulation? Furthermore, the roles of astrocytic neuromodulation in higher brain functions such as decision-making, sensory perception, and learning and memory remain largely unexplored. A study using live imaging in awake mice found that hippocampal astrocytes actively encode spatial information about reward locations, suggesting that astrocytes may directly contribute to cognitive functions traditionally attributed solely to neurons.

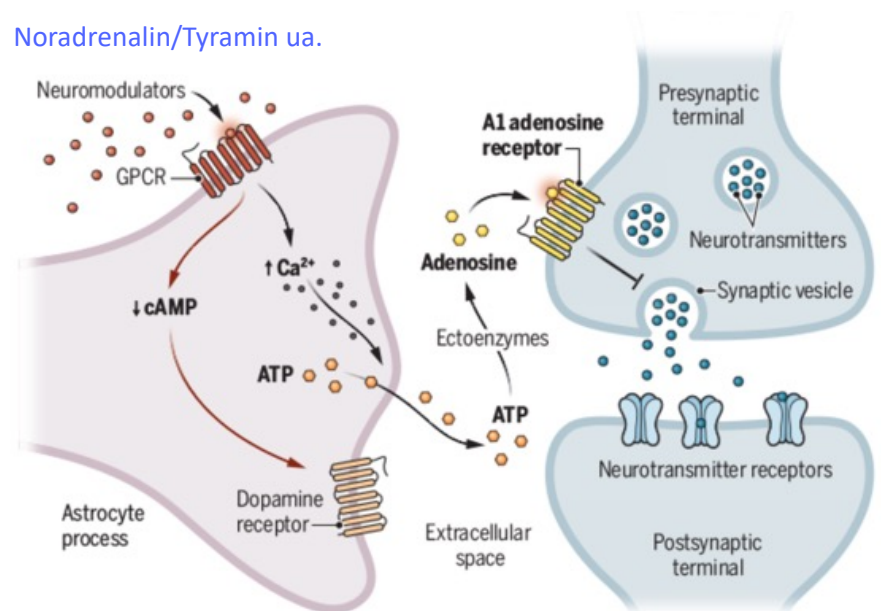
Future work would benefit from examining astrocytic neuromodulation in other mammalian brain regions, such as the cortex, amygdala, basal ganglia, and thalamus, and in behaviors related to higher brain functions. Some technical issues, particularly regarding cell-type specificity and efficiency of genetic manipulations, also need to be addressed. Advances in genetic tools have enabled the selective attenuation of **Gq GPCR signaling** in astrocytes. This attenuation resulted in specific behavioral deficits in mice, underscoring the necessity of precise genetic approaches to dissect astrocytic functions and their effects on behavior.

The findings of Guttenplan *et al.*, Chen *et al.*, and Lefton *et al.* signify the importance of expanding the conceptual framework for investigating neurological and psychiatric disorders that involve dysregulation of neuromodulation. **For instance, disorders such as depression, anxiety, and schizophrenia**, which are traditionally attributed to neuronal neuromodulatory receptor dysfunction, may stem from disrupted astrocyte signaling. Exploring the potential clinical applications of astrocyte-targeted interventions may unveil new therapeutic avenues for these disorders.

Astrocytes take center stage in neuromodulation

Neuromodulators (specifically norepinephrine in mammals and fish, and tyramine in fruit flies) bind to G protein-coupled receptors (GPCRs) on the surface of astrocytes, initiating an increase in intracellular calcium (Ca^{2+}) concentrations and a decrease in cyclic adenosine monophosphate (cAMP) signaling. Increased calcium triggers the release of adenosine triphosphate (ATP), which is converted to adenosine in the extracellular space. Adenosine binds to receptors on the presynaptic terminal to inhibit the release of neurotransmitter from synaptic vesicles, thus modulating neuronal circuit activity. The decrease in cAMP signaling results in increased trafficking of dopamine receptors to the surface of the astrocyte, thus gating astrocytic responsiveness to dopamine.

Noradrenalin/Tyramin ua.



Genetics of Korea's extreme divers could unlock chronic disease treatments



60 ft = 20 m, = 3 BAR; = 2300 mm Hg pressure

The secret to tackling one of the United States' most deadly chronic diseases may reside thousands of miles away in the chilly waters separating the Korean Peninsula and Japan, where generations of Jeju Island women have been diving to gather food from depths of up to 60 feet using only the bodies that genes and conditioning have given them.

They are known as the Haenyeo, or “sea women,” and when younger, many of them dove throughout pregnancy and resumed their gathering of seaweed, abalone and other food only a few days after giving birth. The practice is dying out, and most of those diving in the 50-degree waters today are in their 60s, 70s and 80s.

Now, an international team of researchers has found evidence of natural selection at work: a genetic variation found in Jeju Islanders that helps to keep their blood pressure from rising as much when diving, according to a paper published in the journal [Cell Reports](#).

Researchers measured physiological characteristics, such as blood pressure and heart rate, then sequenced the DNA of participants to look for genetic differences.

In a simulated dive, ordinary Jeju Islanders' heartbeats slowed by about 20 beats per minute, researchers found, about the same amount as women on the South Korean mainland. In the same circumstances, the Haenyeo, who have been diving their whole lives, slow their heartbeats by up to twice that number.

In simulated dives, participants held their breath and submerged their faces in a basin of cold water, which triggers the same response in the body as diving. The simulation allowed the researchers to carry out the study without having untrained, and possibly non-swimming, older women try to dive in the open ocean.



Der Tauchreflex (auch "diving reflex" genannt) ist eine physiologische Reaktion, die bei lungenatmenden Tieren (einschließlich Menschen) beim Eintauchen in Wasser auftritt. Er hilft, die Sauerstoffversorgung während des Tauchens zu optimieren und kann auch helfen, Stress und Angst zu reduzieren.

Bradykardie: Die Herzfrequenz sinkt, um den Sauerstoffverbrauch zu reduzieren.

Apnoe: Die Atmung wird gehemmt.

Vasokonstriktion: Die Blutgefäße in den Extremitäten verengen sich, um das Blut zu den lebenswichtigen Organen zu leiten

Genetic and training adaptations in the Haenyeo divers of Jeju, Korea

Highlights

- Evidence of selection that may increase the safety of diving during pregnancy
- Regular diving increases the magnitude of bradycardia in response to dive stimulus
- The Haenyeo may represent the second known population evolved for diving

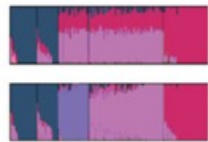
Summary

Natural selection and relative isolation have shaped the genetics and physiology of unique human populations from Greenland to Tibet. Another such population is the Haenyeo, the all-female Korean divers renowned for their remarkable diving abilities in frigid waters. Apnea diving induces considerable physiological strain, particularly in females diving throughout pregnancy. In this study, we explore the hypothesis that breath-hold diving has shaped physiological and genetic traits in the Haenyeo. **We identified pronounced bradycardia during diving, a likely training effect.** We paired natural selection and genetic association analyses to investigate adaptive genetic variation that may mitigate the effects of diving on pregnancy through an associated reduction of diastolic blood pressure. **Finally, we identified positively selected variation in a gene previously associated with cold water tolerance, which may contribute to reduced hypothermia susceptibility.** These findings highlight the importance of traditional diving populations for understanding genetic and physiological adaptation.

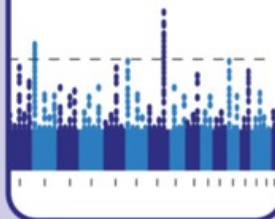
Haenyeo: all-female Korean breath-hold divers



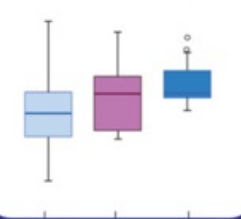
population structure



selection scan



adaptive phenotypes



- A variant in the sarcoglycan zeta gene is linked to cold tolerance, helping the Haenyeo withstand the cold waters.